OUKA
The University of Osaka
Institutional Knowledge Archive

Title	Interactions between water and biomaterials by infrared (IR) spectroscopy with a relative humidity control system
Author(s)	工藤, 幸会
Citation	大阪大学, 2019, 博士論文
Version Type	VoR
URL	https://doi.org/10.18910/72681
rights	
Note	

The University of Osaka Institutional Knowledge Archive : OUKA

https://ir.library.osaka-u.ac.jp/

The University of Osaka

Doctoral Thesis

博士論文

Interactions between water and biomaterials by infrared (IR) spectroscopy with a relative humidity control system

相対湿度制御付き赤外分光法による
生体物質と水の相互作用

Department of Earth and Space Science,
Graduate School of Science, Osaka University
Sachie Kudo

大阪大学大学院　理学研究科　宇宙地球科学専攻
工藤　幸会

February 2019

Acknowledgments

I would like to thank first Professor Satoru Nakashima, at the Laboratory of Physical Geochemistry, for all his technical, scientific and moral supports.

I am grateful to Associate Professor Osamu Hisatomi and Assistant Professors Makoto Katsura and Noriko Nakayama for their valuable discussions and comments during my studies at Osaka University.

I would like to thank the friendship and cooperation of all the members of Nakashima group, especially Ms. Hiromi Ogawa, Ms. Eri Yamakita, Mr. Yudai Ikuno, Mr. Ryosuke Umezawa and Mr. Yuki Nakaya.

I thank technical supports of Mr. Shio Watanabe of Thermo Fisher Scientific for mass spectrometry of collagen and Dr. Toshiyuki Suzuki of Perkin Elmer, Japan for differential thermal analyses of collagen.

I wish to express my gratitude to my colleagues at Taki Chemical Corporation Limited, Dr. Isamu Yamaguchi, Mr. Toshihiko Kakio and Mr. Hiroshi Nishikura for their scientific and administrative supports.

Abstract

Infrared (IR) microspectroscopy combined with a quartz crystal microbalance (QCM) together with an original relative humidity (RH) control system has been developed to study water adsorption on four biomaterials: collagen, keratin, lecithin and ceramide.

The adsorbed water weights measured by QCM indicate that the collagen film was close to the water adsorption / desorption equilibria. A broad OH + NH stretching band area (3700 − 3000 cm^{-1}) in the IR spectra of the collagen increased with the adsorbed weight. The OH + NH band could be simulated by four Gaussian components at 3440 (free water with longer H bonds), 3330 (amide A (NH)), 3210 (bound water with shorter H bonds), and 3070 (amide B (NH)) cm^{-1} with the relatively constant band areas of amide A and B for increasing and decreasing RH. Bound water is major in the total water (3440 + 3210 cm^{-1} band areas) at low RHs but decreases at high RHs, where free water become dominant. The peak shifts of C=O stretching (amide I) and N−H bending (amide II) can be understood by increasing hydrogen bonding of water molecules (bound water) bound to peptides at lower RH. The higher wavenumber shifts of CH stretching can be due to the loose binding of water molecules (free water) to aliphatic chains on the collagen surface, especially at higher RH.

Keratin is the main component of human hair, nail and skin surface. Water contents increased with RH up to about 19 wt% and were correlated linearly with the OH + NH band areas in IR spectra of the keratin. The OH + NH band areas for the triple helix collagen are about twice as large as those for the keratin (double helix). The free water component increased with RH by keeping the bound water component minor for the keratin. About twice of water retention capacity of the collagen can be due to increasing adsorption of free water, interacting possibly with hydrophobic aliphatic CH surfaces.

Soybean lecithin, one of phospholipids, were selected as a representative cellular membrane. The water weight ratio increased gradually from nearly 0 wt% at RH = 4.3 % until 19.6 wt% at RH = 91.5 %. The 1230 cm^{-1} band due to PO_2^- and the 1735 cm^{-1} band due to C=O shifted to lower wavenumbers (red shift), while the 1060 cm^{-1} band due to PO_2^- and P−O−C shifted to higher wavenumber (blue shift) with increasing RH. This can be explained

by increasing hydrogen bonding by water molecules to phosphates and carboxylic acids and/or esters. Band areas of 1230 and 1060 cm^{-1} bands of phosphates increase with increasing RH. The band areas of phosphates correlate positively with the band area of bound water. Bound water molecules might be bound to these phosphate groups. Band areas of aliphatic CH stretching bands decrease throughout the RH increase and are negatively correlated to the increasing adsorption of free water. Free water molecules might interact loosely with aliphatic chains of the lecithin.

Ceramide is a representative inter-cellular lipid. The water weight ratio increased quasi-linearly from nearly 0 wt% at RH = 2.0 % to 1.2 wt% at RH = 84.8 %. No significant peak shifts were observed for aliphatic CHs and amides. The 1045 cm^{-1} band due to C−O stretching shifted from 1046 to 1042 cm^{-1} with increasing RH. The free water component increases only slightly with RH, while the bound water component increases slightly at low RHs and more from about RH = 60 %. Since the peak shift of C−O was observed at higher RHs than 60 %, bound water is considered to be adsorbed to C−O bonds. These are significantly different from lecithin with phosphate groups adsorbing bound water and aliphatic chains interacting with free water molecules.

The present IR microspectroscopy combined with quartz crystal microbalance (QCM) and the relative humidity control system developed in this study can provide quantitative bases for amounts (wt%) and species (free and bound water) of water interacting with several functional groups (amides, phosphates, carbonyls, alcohols, aliphatic CHs) of biomaterials.

要旨

生命にとって水は必要不可欠のものであり，生体内の様々な生体物質が水と相互作用していると考えられるが，生体物質のどのような部分にどのような水がどのくらい吸着しているのかは良くわかっていない．本研究では，顕微赤外分光器に相対湿度制御セルを設置し，水晶振動子微小重量天秤(QCM)を組み込んだ新しい手法を開発し，水晶振動子の金電極上に膜状生体物質を作成し，相対湿度 RH を約 0 − 95 %の範囲で段階的に増加・減少させ，周波数変化量から吸着・脱着した水分量を求めた．同時に，赤外透過反射測定を行い，OH 吸収帯や各官能基の吸収帯のシフトや面積の変化を解析した．

最初に，皮膚等の生体組織中に存在するコラーゲン（3 重らせん構造）への水の吸着・脱着過程を調べた．相対湿度増加・減少に伴い，QCM より求めた吸着水量は増加・減少し，水の吸着脱着が確認できた．一方，OH + NH 吸収帯(3700 − 3000 cm^{-1})をガウス型 4 成分で近似すると，アミド（NH）吸収帯面積はほぼ一定だが，自由水（3440 cm^{-1} 付近）及び結合水（3210 cm^{-1} 付近）が増加・減少した．低湿度では結合水が卓越し，ペプチド結合に吸着していると考えられたが，高湿度では自由水が増加し，脂肪族 CH のピークシフトから，コラーゲン分子の表面に露出するアミノ酸疎水部と水分子の相互作用が示唆された．

ケラチンは皮膚や髪の毛，爪などを構成するタンパク質であり，2 重らせん構造を取っている．QCM による水の吸着量は，RH 約 80 %でケラチンへは 17.0 wt%であり，コラーゲンの 24.6 wt%よりも少なかった．OH + NH 吸収帯面積は，コラーゲンの方が約 2 倍程度大きかった．ケラチンでは，結合水の吸着は少なく，自由水の吸着が卓越した．脂肪族 CH_3 のピークシフトから，ケラチン分子の表面に露出する疎水部先端と水分子の相互作用が示唆された．

細胞膜リン脂質の代表としてレシチンを，細胞間脂質としてセラミドを取り上げ，水の吸着を評価し比較した．水吸着量は RH 約 80 %で，レシチンへは 12.2 wt%，セラミドへは 1.2 wt%となった．レシチンでは，P−O, P−O−C 及び C=O 吸収帯がシフトし，一方セラミドでは，C−O 吸収帯がシフトしたことから，これらの極性官能基に水が吸着したと考えられる．これらの吸収帯の面積と結合水・自由水のそれらとを比較すると，結合水が低湿度で上記の極性官能基に吸着し，自由水の一部がこれにさらに吸着したと考えられる．脂肪族 CH の吸収帯面積は自由水と相関し，特にレシチンでは直線的な相関を示した．従って，疎水的な脂肪族炭素鎖に自由水が緩く相互作用していると考えられた．

これらの結果から，代表的な生体物質 4 つについて，水の吸着量，水と相互作用する官能基の種類，相互作用する水の種類（自由水，結合水）を定量的に評価することが出来た．本研究で開発した水晶振動子微小重量天秤(QCM)を組み込んだ相対湿度制御顕微赤外分光法は，生体物質と水の相互作用を調べる有力な方法と期待される．

Table of Contents

Chapter 1. General Introduction

Interactions of water with biomolecules have been extensively studied (Frank, 2000; Marechal, 2007; Cameron et al., 2011; Cameron et al., 2013). However, the nature of water adsorbing to biomolecules still remains unclear.

For example, water contents at the stratum corneum (SC) of human skins are considered to affect skin health (Tanaka et al., 1998; Edwards and Marks, 2005; Serup, 2005) and penetration of several chemical components (Raut et al., 2014; Li et al, 2016). Water contents of human SC have been evaluated mostly by relative values using electrical methods (Khazaka, 2005; Barel and Clarys, 2014; Tagami, 2014), which correspond to water contents throughout the whole SC layers. Except for some studies using confocal Raman microscopy determining depth profiles of water contents from about 70 to 20 wt% over the SC (Caspers et al., 2000; Sieg, 2014), few quantitative estimates of water contents are available for individual constituents of human skins.

Collagen is one of the representative biomolecules present in biological tissues such as animal skins and bones. Natural collagens are considered to be in the triple helix form bound by hydrogen bonding, mainly between peptide bonds (Shoulders and Raines, 2009) with some contribution of water to peptide bonding (Boryskina et al., 2007). However, only limited literature is available for water adsorption to collagens. Boryskina et al. (2007) studied the structural stability of type I collagen and its model tripeptide (Gly−Pro−Pro) by using infrared (IR) spectroscopy and piezo gravimetry separately under controlled relative humidity (RH). They observed adsorption of three to four water molecules to peptide bonds up to RH = 60 %, which stabilizes the internal structure of collagen. However, interactions of water with native fibril structures of collagen, including both internal and external helix structures, remain unknown. Zhang et al. (2011) studied hydration of collagens by Raman spectroscopy and dynamic vapor sorption under varying RH and $H_2O - D_2O$ exchange and found that the 938 cm^{-1} Raman band (C−C stretching of protein backbone) was a good indicator of collagen-bound water. However, adsorbed water molecules and their interactions with other structures than peptide bonds were not studied.

α-Keratin is the main constituent of hair, nail, and skin surface (stratum corneum) (Leveque, 2005; Wang et al., 2016). Its structure is mainly in the form of α helix by hydrogen bonding among peptide bonds. Two α helices forms double helix chains of about 45 nm long and 2 nm in width. The double helix chains are assembled into protofilament groups called protofibril with a diameter of about 7 nm (Wang et al., 2016). The double helices are forming crystalline phases, while others are in amorphous states bound either by strong S−S bonds or by weak H bonds among peptides (Xiao and Hu, 2016). Water sorption properties of α-keratin have been studied by sorption isotherms, thermal analyses, Raman and IR spectroscopy (Leveque, 2005; Barba et al., 2011; Xiao and Hu, 2016). Although different natures of water (bound water and free water) adsorbed to α-keratin have been proposed mainly by thermal analyses (Leveque, 2005), detailed natures of water molecules and their interactions with keratin functional groups still remain unclear.

Soybean lecithin, one of phospholipids, is also selected as a representative cellular membrane. There are some studies about interactions between water molecules and lecithin. Pohle et al. (2001) compared the behavior of water molecules bound to lecithins and cephalins, and they suggested that lecithins take up more water than cephalins, independently of the nature of their acyl chains. Shchipunov and Shumilina (1995) studied how polar solvents such as water, glycerol and formamide bound to the lecithin, and they indicated that polar solvents are hydrogen-bonded with the phosphate group. However, quantities of water molecules bound to the phospholipid and their sorption-desorption behaviors are not known.

Other types of lipids are present in biological systems such as inter-cellular lipids (Jung et al., 2015). For example, different types of ceramides are present in inter-cellular spaces in animal skins (Jung et al., 2015; Masukawa et al., 2008). Among them, ceramide 3 has been selected in this study. It is composed of phytosphingosine [P] unit and non-hydroxyl fatty acid [N] unit, which are bound by an amide bond (Masukawa et al., 2008). The non-hydroxyl fatty acid is generally stearic acid ($CH_3(CH_2)_{16}COOH$) which can contain a few double bonds (unsaturated parts). The phytosphingosine unit is originally a long aliphatic chain (around C_{18}) amino alcohol having three hydroxyls (OH). There are some studies about interactions between water molecules and ceramide (Adhikari et al., 2016). They used vibrational sum

frequency generation spectroscopy and molecular dynamic simulation for studying orientation of water molecules on ceramide. Based on these, they proposed both H up and H down orientations of water molecules facing to polar C−OH head groups of ceramide. However, quantities of water molecules bound to ceramide and their sorption-desorption behaviors are not known.

Although infrared (IR) spectroscopy has been used for studying amide structures of collagens and keratins and their denatured forms (Doyle et al., 1975; Payne and Veis, 1988; Boryskina et al., 2007; Xiao and Hu, 2016), it has not been employed extensively for studying water bound to biomaterials except for some limited studies mentioned above.

For investigating water molecules bound to biomaterials, IR microspectroscopy equipped with a humidity control system has been developed in this study. Although IR band areas can correspond to quantities of water and other species through the Beer-Lambert law, information about absorption coefficients and sample thicknesses are necessary for quantitative evaluation. However, these are often unknown on practical samples.

For measuring amounts of water adsorbed on materials, water vapor pressure measurements are conventionally performed (Zhang et al., 2011; Hatch et al., 2012). However, several tens of mg of powder samples should be used in these measurements. Only the total water weights adsorbed on materials can be measured on a bulk material. On the other hand, quartz crystal microbalance (QCM) has been employed to measure small weight changes during adsorption / desorption processes (Schuttlefield et al., 2007). The QCM is capable of measuring mass change in the nano gram range from a shift of the resonant frequency of the quartz crystal (Sauerbrey, 1959).

Although some studies conducted the QCM and IR measurement simultaneously for adsorption / desorption behavior using the same relative humidity or gas flow unit, the QCM and IR units are separately measured (Boryskina et al., 2007). In this study, we have developed a new measurement system where IR microspectroscopy and QCM measurement can be conducted at the same time on the same sample for studying water adsorption / desorption.

The OH stretching band around 3400 cm^{-1} in the IR spectra for liquid water is broad and has been reported to be composed of two to four components (Masuda et al., 2003; Kitadai et al., 2014; Hamamoto et al., 2015). The OH stretching frequency was reported to decrease with decreasing hydrogen bond distance among water molecules (Nakamoto et al., 1955). Therefore, higher and lower wavenumber components in the OH band correspond to longer and shorter hydrogen bond components, respectively. The longer H bond component is often called ‘‘free water,’’ while the shorter H bond component is known as ‘‘bound water’’ (Einhorn-Stoll et al., 2012). Water adsorbed on the above biomaterials measured by IR microspectroscopy with changing relative humidity (RH) is analyzed here based on these different H bond components. Moreover, interactions of water molecules were studied not only for internal peptide bonds (amides I, II, III) but also for aliphatic CH species on external surfaces of collagen triple helices and keratin double helices. Therefore, in this study, natures and amounts of water molecules adsorbed on biomaterials are compared for keratins with double helices and collagens with triple helices both forming fibril structures together with a phospholipid (lecithin) and a ceramide.

Chapter 2. Development of Evaluation Methods for Water Adsorption to Biomaterials

This chapter has been published as the following paper:
"Adsorption of Water to Collagen as Studied Using Infrared (IR) Microspectroscopy Combined with Relative Humidity Control System and Quartz Crystal Microbalance"
Sachie Kudo, Hiromi Ogawa, Eri Yamakita, Shio Watanabe, Toshiyuki Suzuki and Satoru Nakashima
Applied Spectroscopy, Vol. 71 (7), 1621-1632, 2017.
Society for Applied Spectroscopy, SAGE publications.

2.1. Abstract

Infrared (IR) microspectroscopy combined with a quartz crystal microbalance (QCM) together with an original relative humidity (RH) control system has been developed for studying water adsorption on a collagen film. The adsorbed water weights measured by QCM were almost similar for wetting and drying processes at 28 °C, indicating that the collagen film was close to the water adsorption / desorption equilibria. A broad OH + NH stretching band area (37000 − 3000 cm^{-1}) in the IR spectra of the collagen film increased linearly with the adsorbed weight until about 1.2 μg / 8.0 μg dry collagen film at RH = 40 %, while at higher RH (60 %, 80 %), the band area deviated from the linear trend to the lower side, due to viscoelasticity and others. The OH + NH band could be simulated by four Gaussian components at 3440, 3330, 3210 and 3070 cm^{-1} with the relatively constant band areas of 3330 and 3070 cm^{-1} components due to amide A and B (NH) for increasing and decreasing RH. Bound water (3210 cm^{-1} component: short H bond) constitutes around 70 % of total water (3440 + 3210 cm^{-1} band areas) at RH = 4.9 % but decreases to 23 % at RH = 80.3 %, where free water (3440 cm^{-1} component: long H bond) becomes dominant over 70 %. The peak shifts of C=O stretching (Amide I) and N−H bending (Amide II) can be understood by increasing hydrogen bonding of water molecules (bound water) bound to peptides at lower

RH. The higher wavenumber shifts of CH stretching can be due to the loose binding of water molecules (free water) to aliphatic chains on the collagen surface, especially at higher RH. The present combined QCM-IR method is useful for studying amounts and natures of water adsorbing on biomolecules.

2.2. Introduction

Extensive studies have been conducted on the interactions of water with biomolecules (Frank, 2000; Marechal, 2007; Cameron et al., 2011; Cameron et al., 2013). However, the nature of water adsorbing to biomolecules still remains unclear.

Collagen is one of the representative biomolecules present in biological tissues such as animal skins and bones. Natural collagens are considered to be in the triple helix form bound by hydrogen bonding, mainly between peptide bonds (Shoulders and Raines, 2009) with some contribution of water to peptide bonding (Boryskina et al., 2007). However, only limited literature is available for water adsorption to collagens. Boryskina et al. (2007) studied the structural stability of type I collagen and its model tripeptide (Gly−Pro−Pro) by using infrared (IR) spectroscopy and piezo gravimetry separately under controlled relative humidity (RH). They observed adsorption of three to four water molecules to peptide bonds up to RH = 60 %, which stabilizes the internal structure of collagen. However, interactions of water with native fibril structures of collagen, including both internal and external helix structures, remain unknown. Zhang et al. (2011) studied hydration of collagens by Raman spectroscopy and dynamic vapor sorption under varying RH and $H_2O - D_2O$ exchange and found that the 938 cm^{-1} Raman band (C−C stretching of protein backbone) was a good indicator of collagen-bound water. However, adsorbed water molecules and their interactions with other structures than peptide bonds were not studied.

Although IR spectroscopy has often been used to study amide structures of collagens and their thermally denatured forms (Doyle et al., 1975; Payne and Veis, 1988; Boryskina et al., 2007), it has not been employed extensively for studying water bound to collagens except for some limited studies mentioned above. For investigating water molecules bound to biomaterials, IR microspectroscopy equipped with a humidity control system has been

developed in this study. Although IR band areas can correspond to quantities of water and other species through the Beer-Lambert law, information about absorption coefficients and sample thicknesses are necessary for quantitative evaluation. However, these are often unknown on practical samples.

For measuring amounts of water adsorbed on materials, water vapor pressure measurements are conventionally performed (Zhang et al., 2011; Hatch et al., 2012). However, several tens of mg of powder samples should be used in these measurements. Only the total water weights adsorbed on materials can be measured on a bulk material. On the other hand, quartz crystal microbalance (QCM) has been employed to measure small weight changes during adsorption / desorption processes (Schuttlefield et al., 2007). The QCM is capable of measuring mass change in the nano gram range from a shift of the resonant frequency of the quartz crystal (Sauerbrey, 1959).

Although some studies conducted the QCM and IR measurement simultaneously for adsorption / desorption behavior using the same relative humidity or gas flow unit, the QCM and IR units are separately measured (Boryskina et al., 2007). In this study, we have developed a new measurement system where IR microspectroscopy and QCM measurement can be conducted at the same time on the same sample to study water adsorption / desorption.

The OH stretching band around 3400 cm^{-1} in the IR spectra for liquid water is broad and has been reported to be composed of two to four components (Masuda et al., 2003; Kitadai et al., 2014; Hamamoto et al., 2015). The OH stretching frequency was reported to decrease with decreasing hydrogen bond distance among water molecules (Nakamoto et al., 1955). Therefore, higher and lower wavenumber components in the OH band correspond to longer and shorter hydrogen bond components, respectively. The longer H bond component is often called ‘‘free water,’’ while the shorter H bond component is known as ‘‘bound water’’ (Einhorn-Stoll et al., 2012). Water adsorbed on the above biomaterials measured by IR microspectroscopy combined with a QCM and RH control system is analyzed here based on these different H bond components. Moreover, interactions of water molecules were studied not only for internal peptide bonds (amide I, II) but also for aliphatic CH species on external surfaces of collagen triple helices.

2.3. Materials and Methods

2.3.1. Collagen Extraction Procedure

Triple Helix Collagen (Ti-03SP) from a fish (Tilapia) scale was prepared by Taki Chemical Co., Ltd., Japan (lot. no. 160112). First, demineralized fish scales of Tilapia were washed in 0.1 mol L^{-1} NaOH solution and then soaked in phosphoric acid solution. The swelled fish scales were crashed with a grinder mill. Solubilized atelocollagen was extracted with 0.25 wt% pepsin solution at pH 2.0 − 2.5 for 48 h. Insoluble collagen was separated with a centrifuge at 11120 × g. The solubilized atelocollagen solution was purified by salting-out in 1 mol L^{-1} NaCl solution and dialyzed with purified water. The solution was diluted with HCl solution and then sterilized with membrane filter to obtain the transparent pH 3.5 solution containing 0.34 % (wt / wt) solubilized atelocollagen.

2.3.2. Characterization of Collagen Solution Using Liquid Chromatography-Mass Spectrometry, Gel Permeation Chromatography, Sodium Dodecyl Sulfate Poly-Acrylamide Gel Electrophoresis, Optical Rotation, and Differential Scanning Calorimetry

The 0.34 % collagen solution was characterized by high performance liquid chromatography (HPLC: UltiMate3000RSLC, Thermo Fisher Scientific, Column: Acclaim RSLC 120, C18, 2.2 μm Analytical, 2.1 × 150 mm) with a mobile phase (water with 0.1 % formic acid, acetonitrile with 0.1 % formic acid) and analyzed by a mass spectrometer (Q Exactive Plus, Thermo Fisher Scientific). The mass spectra of peptide fragments were analyzed for their amino acid sequences. The 0.34 % collagen solution was freeze-dried and dissolved in 100mM citric acid buffer (pH = 3.5) to obtain a 0.5 wt% collagen solution. Gel permeation chromatography (GPC) analysis with an ultraviolet visible (UV-Vis) detector (SPD-20A; Shimadzu) was conducted on this collagen citric solution. Sodium dodecyl sulfate poly-acrylamide gel electrophoresis (SDS-PAGE) of 0.34 % collagen solution was

performed after being treated with 2-mercaptoethanol to cut S−S bonds and after heating at 45 °C for 3 min. The specific rotation at 589 nm of the 0.34 % collagen solution was measured with the polarimeter. Differential scanning calorimetry (DSC) of the 0.34 % collagen solution was conducted with DSC8500 (PerkinElmer) at 5 °C min^{-1} under nitrogen flow (20 mL min^{-1}).

2.3.3. Relative Humidity Control System

In order to study adsorption behavior of water to collagen, a plastic humidity control cell (36 × 36 × 14 mm) with a CaF_2 window (10 mm diameter) was fabricated (Figure 2.1). The RH of the cell interior was controlled by flowing a mixture of dry air and water-saturated air with varying proportions at a total flow rate of about 1 L min^{-1} (Figure 2.1). The water-saturated air was made by flowing air through two bottles of pure water (Milli-Q, Electrical resistivity > 18.2MΩ cm) by an air pump. The dry air was provided from a dehumidifier (Jasco, AM-12). The humidity and temperature in the cell was monitored every second by a small temperature and humidity sensor (SHT 75, SENSIRION) equipped with a data logger (SHTDL-2-L, SENSIRION) connected to a PC with a USB cable. The humidity was increased from about 5 % to 80 % by changing the flow rates of dry and humid air.

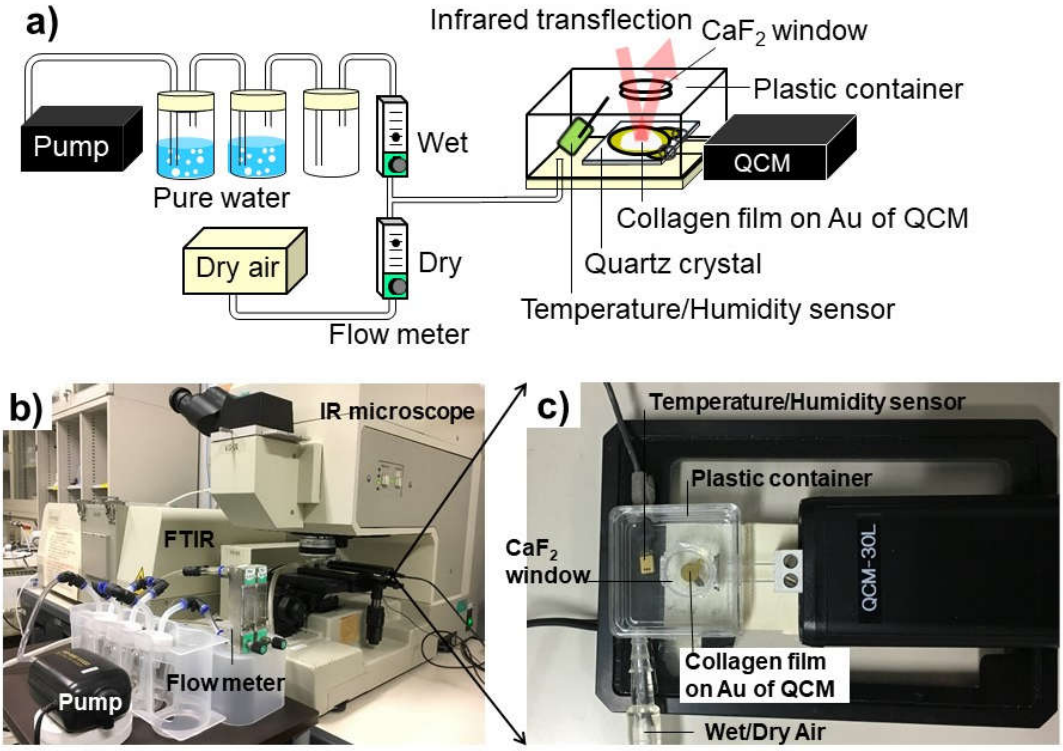

Figure 2.1. Infrared microspectroscopy combined with RH control system and QCM. (a) A schematic image of the system; b) a photograph of the whole system; (c) a close-up photograph of the RH control cell with QCM.

2.3.4. Quartz Crystal Microbalance

A QCM system (SEIKO EG&G, QCM-30L) was used in this study for measuring weights of adsorbed water on a collagen film placed on an a gold (Au) electrode coating on an AT-cut quartz of QCM sensor in a plastic container (Figure 2.1). Changes in resonant frequency of quartz from the initial value (F_0) around 9.0 MHz were monitored at every second when water was adsorbed / desorbed under various relative humidity. These frequency changes can be converted to mass changes by Sauerbrey's equation (Sauerbrey, 1959):

$$\Delta F = -\frac{2F_0^{\,2}}{\sqrt{\rho_Q \mu_Q}} \frac{\Delta m}{A} \qquad (2.1)$$

where ΔF is the change in resonance frequency (Hz), Δm is the mass change (kg), F_0 is the resonant frequency (Hz) at around 9.0MHz, ρ_Q is the density of quartz (2.65×10^3 kg m^{-3}), μ_Q is the shear modulus of quartz (2.95×10^{10} kg m^{-1} s^{-2}) and A is the surface area of the electrode (1.96×10^{-5} m^2) (Lucklum et al., 1997).

2.3.5. Characterization of Collagen Film

One drop of the 0.34 % collagen solution was placed by a micropipette on the Au electrode coating on an AT-cut quartz of the QCM in a plastic container (Figure 2.1). Dried air was flowed in the plastic container with a flow rate of more than 1 L min^{-1} for about 5 min until the stable weight monitored by QCM. The obtained transparent collagen film had a weight of 8.0 μg (at RH = 5.1 %).

The refractive index of a collagen film was measured by an Abbe's refractometer (ER-2S, Atago). A total of 300 μL of the 0.34 % collagen solution was placed on a prism and dried by flowing dried air to the plastic container covering the Abbe's refractometer. The refractive index n of the collagen film was obtained by reading values at the boundary line under the microscope.

The thickness of the collagen film was evaluated by interference fringes measured using visible microspectroscopy. The collagen film dried on the Au electrode on quartz crystal of QCM sensor in the plastic container was placed under the homemade visible microspectrometer (Onga and Nakashima, 2014) connected to the RH control system. Reflectance spectra against the Au electrode reference on a position close to the IR microspectral measurement of the collagen film were measured at RH = 5.7, 20.3, 40.5, 60.5 and 80.4 %. Wavenumber differences ($\nu_2 - \nu_1$, cm^{-1}) of interference fringes for several adjacent fringe pairs were converted to thicknesses of the film L (nm) using the following equation:

$$L = \frac{1}{2(\upsilon_2 - \upsilon_1)\sqrt{n^2 - \sin^2\theta}} \times 10^4 \qquad (2.2)$$

The incident angle θ (= 8.6°) was determined from the numerical aperture (NA) of the 5 x objective lens (NA = n sinθ = 0.15, n = 1.0 for air). Next, 0.65 mL of the 0.34 % collagen solution was dropped on a plastic sheet and dried in a draft chamber for about 24 h. The obtained collagen film was stripped off from the plastic sheet and cut into small pieces of about 1mm^2. Of these collagen film fragments, 0.705 mg was placed in an aluminum container before sealing for DSC.

2.3.6. Infrared Microspectroscopy

In order to evaluate natures of adsorbed water on the collagen film, IR transflection (transmission-reflection) spectra of the collagen film on the Au electrode on QCM quartz crystal were measured under different RH (5 − 80 %). The collagen film on the QCM in the plastic cell with a CaF_2 window was placed under a Fourier transform IR spectroscopy (FT-IR) microscope (Jasco IRT30+FTIR620: a Cassegrain objective mirror with a magnification of 16, MCT detector, ceramic IR source, and KBr beam splitter) (Figure 2.1b). The environment outside the RH cell was the ambient experimental room with normal air conditioning with the temperature around 27 °C and RH of about 60 % (Figure 2.1). No evacuation or gas purging had been conducted on the IR microscope.

A background reflection spectrum was measured on the Au-coated quartz crystal without any sample using an aperture size of 300 × 300 μm^2 and then a sample transflection spectrum was measured on the collagen film with the same aperture. All the spectra were obtained by accumulating 64 scans at a wavenumber resolution of 4 cm^{-1}. The transflection method has been reported to be used quantitatively in IR microspectroscopy (Alipour et al., 2016).

2.4. Results

2.4.1. Characterization of Collagen Solution

Liquid Chromatography-Mass Spectrometry. The mass spectra of peptide fragments of the 0.34 % collagen solution were analyzed for their amino acid sequences. The amino acid

sequences are very similar to those reported for the triple helix collagen from Tilapia (GenBank: BAL40987.1).

Gel Permeation Chromatography. Gel permeation chromatography analysis with a UV-Vis detector on the 0.5 wt% collagen citric acid solution shows a peak around molecular weight of about 300,000.

Sodium Dodecyl Sulfate Poly-Acrylamide Gel Electrophoresis. Sodium dodecyl sulfate poly-acrylamide gel electrophoresis of the 0.34 % collagen solution shows several bands around the molecular weight of 100,000 corresponding to those of separated collagen helices.

Optical Rotation. The specific rotation at 589 nm of the 0.34 % collagen solution was measured with the polarimeter as -380^{o} cm^2 g^{-1}, corresponding to the triple helix structure (Nomura et al., 1995).

Differential Scanning Calorimetry. The DSC curve of the 0.34 % collagen solution during heating shows an endothermic peak at 37.6 ^{o}C corresponding to the denaturation temperature of the triple helix collagen from the Tilapia scale (Ikoma et al., 2003).

2.4.2. Characterization of Collagen Film

By drying one drop of the 0.34 % collagen solution placed on the Au electrode coating on an AT-cut quartz of the QCM, a transparent collagen film was obtained having a weight of 8.0 μg (at RH = 5.1 %) by QCM (Figure 2.1c).

Refractive Index. The refractive index *n* of the collagen film obtained by reading values at the boundary line under the microscope of the Abbe's refractometer under varying relative humidity varied from 1.553 at RH = 2.0 % to 1.531 at RH = 83.2 % (Table 2.1, Figure 2.2). The fitting line of the data is n = 1.554 − 0.0003 RH (%).

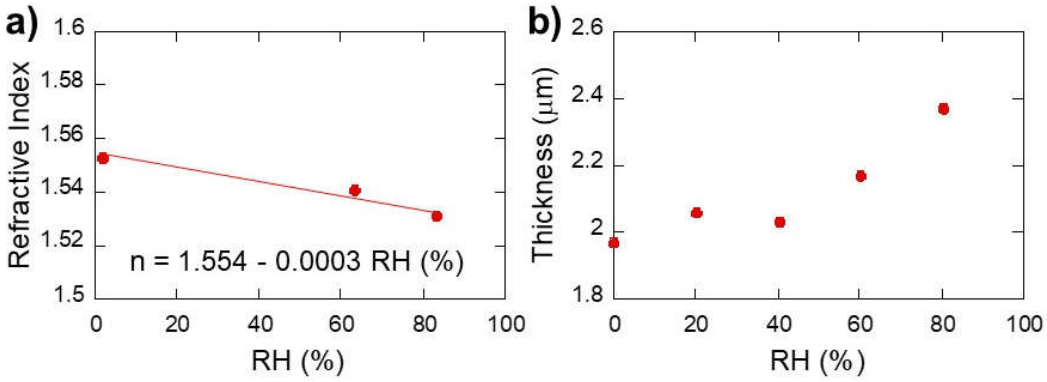

Figure 2.2. Changes with relative humidity (RH) in (a) refractive index (Table 2.1) and (b) thickness of collagen films (Table 2.2). The regression line for refractive index n = 1.554 − 0.0003 RH is also shown.

RH(%)	Refractive Index n
2.0	1.553
63.3	1.541
83.2	1.531 ± 0.005

n = 1.554 - 0.0003 RH (%)

Table 2.1. Changes with relative humidity (RH) in the refractive index n of a collagen film. The regression line for refractive index is n = 1.554 − 0.0003 RH (see Figure 2.2a).

Film Thickness. The thickness of the collagen film was evaluated by interference fringes measured by visible microspectroscopy at RH = 5.7, 20.3, 40.5, 60.5 and 80.4 %. The refractive indices of the collagen film n at each RH were calculated by using the above relation: n = 1.554 − 0.0003 RH (%). The average thickness of the collagen film based on several fringe pairs at each RH slightly increased from 1.97 ± 0.23 μm at RH = 5.7 % to 2.37 ± 0.23 μm at RH = 80.4 % (Table 2.2, Figure 2.2b).

RH (%)	ν_2-ν_1 (cm^{-1})	Thickness (μm)	Average + Error
5.7	1711	1.89	1.97 ± 0.23
	1698	1.91	
	1730	1.87	
	1471	2.20	
20.3	1642	1.98	2.06 ± 0.51
	1571	2.07	
	1762	1.84	
	1262	2.57	
	1748	1.86	
40.5	1486	2.19	2.03 ± 0.16
	1644	1.98	
	1701	1.92	
60.5	1495	2.19	2.17 ± 0.33
	1406	2.33	
	1505	2.17	
	1750	1.87	
	1306	2.50	
	1646	1.99	
80.4	1305	2.52	2.37 ± 0.23
	1467	2.24	
	1292	2.54	
	1533	2.14	
	1301	2.52	
	1443	2.28	

Table 2.2. Changes with relative humidity (RH) in the thickness (μm) of the collagen film (Figure 2.2b) used in the IR / QCM measurements.

Differential Scanning Calorimetry of the Collagen Film. During the first heating at a rate of 5 $^oC\ min^{-1}$ in the DSC, an endothermic peak around 110 ^oC with an onset of 108 ^oC was obtained, corresponding to the thermal denaturation of the collagen film. The second heating at a rate of 20 $^oC\ min^{-1}$ shows a baseline change around 125 ^oC corresponding to the glass transition.

2.4.3. Temperature and Relative Humidity Changes

Temperature in the cell during water adsorption / desorption experiments on the collagen film fluctuated slightly because of air conditioning of the experimental room but was mostly kept constant around 27.7 ± 0.9 ^oC during the increase and decrease of RH from 4.9 % to 81.4 % (Figure 2.3a). The RH value became relatively stable within 5 min with some small

fluctuations at each humidity value with errors of less than 1.4 % (Table 2.3, Figure 2.3a). After keeping the same RH values for about 20 min, the RH values were increased or decreased.

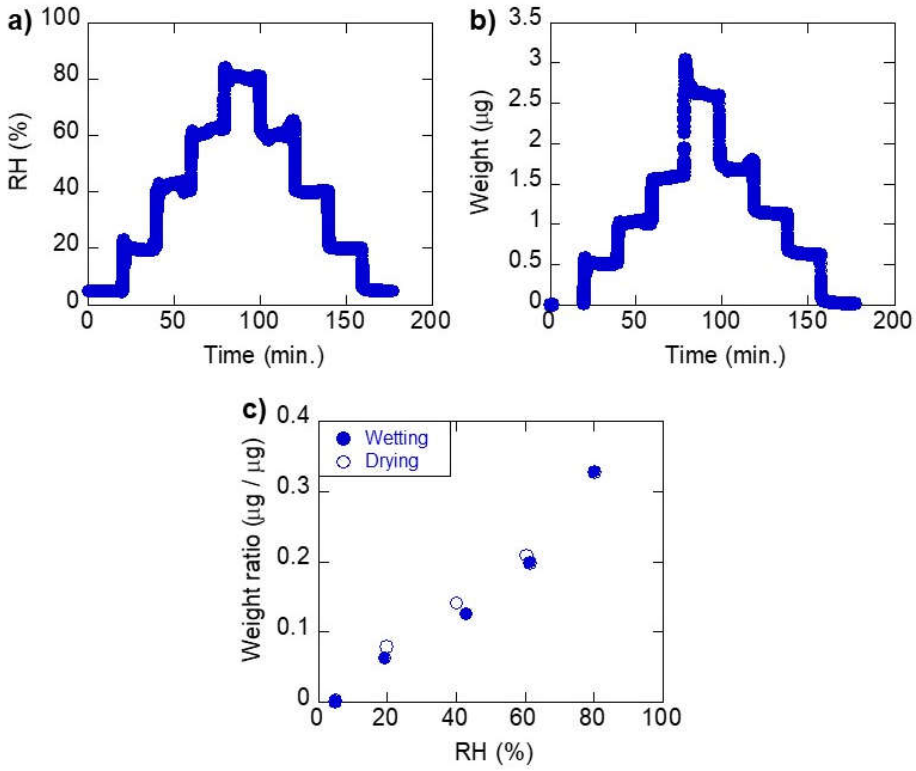

Figure 2.3. (a) Relative humidity (RH) changes; (b) weight changes of the collagen film by QCM; (c) weight ratio of water to dry collagen film plotted against RH, during wetting and drying processes.

Table 2.3 Time, temperature, relative humidity (RH), frequency shift (ΔF), mass changes (Δm), water contents (μg / μg), total OH + NH band area, band areas of free water, amide A, bound water, amide B, band area ratios of free and bound water in the total water band areas and peak positions of amide I, amide II, asymmetric CH_2 and symmetric CH_3 bands during wetting and drying processes of a collagen film.

												Band area			
Time (s)	Time (min)	Temp (℃)	Max error	RH (%)	Max error	ΔF (Hz)	Max error	Δm (μg)	Max error	H_2O μg/μg	Total OH+NH Band area	3440cm^{-1} Free water	3330cm^{-1} Amide A	3210cm^{-1} Bound water	3070cm^{-1} Amide B
0	0	28.1	0.10	4.9	0.04	1	2	0.00	0.002	0.000	39.3	4.3	23.0	10.2	1.4
2040	34	28.3	0.19	19.3	0.03	460	1	0.50	0.001	0.063	62.9	22.3	23.0	14.1	2.3
3000	50	27.5	0.12	42.9	0.09	955	2	1.04	0.002	0.130	81.9	39.2	23.3	17.8	2.9
4200	70	27.8	0.17	61.6	0.28	1458	2	1.58	0.003	0.198	95.6	52.8	23.0	20.0	3.1
5400	90	27.9	0.07	80.3	0.15	2409	3	2.61	0.005	0.326	110.7	72.9	20.7	22.0	2.9
6600	110	27.2	0.13	60.5	0.08	1547	2	1.68	0.002	0.210	97.2	54.7	23.2	19.8	3.1
8040	134	27.8	0.21	40.1	0.15	1044	1	1.13	0.001	0.141	84.5	41.2	24.0	18.1	3.1
9000	150	27.2	0.10	19.9	0.06	579	1	0.63	0.001	0.079	68.2	26.2	24.0	15.5	2.6
10200	170	27.7	0.05	5.0	0.07	16	1	0.02	0.001	0.002	41.0	4.8	23.2	11.0	1.6

			Band area ratio						Peak position			
			(/Total OH band area)				(/Total water)					
Time (s)	Time (min)	RH (%)	3440cm^{-1} Free water	3330cm^{-1} Amide A	3210cm^{-1} Bound water	3070cm^{-1} Amide B	3440cm^{-1} Free water	3210cm^{-1} Bound water	1655cm^{-1} Amide I	1530cm^{-1} Amide II	2935cm^{-1} CH_2 asym	2875cm^{-1} CH_3 sym
0	0	4.9	0.1113	0.5913	0.2627	0.0347	0.2976	0.7024	1653	1531	2936	2875
2040	34	19.3	0.3614	0.3728	0.2285	0.0373	0.6126	0.3874	1652	1540	2938	2877
3000	50	42.9	0.4712	0.2800	0.2139	0.0349	0.6877	0.3123	1651	1543	2938	2878
4200	70	61.6	0.5339	0.2326	0.2022	0.0313	0.7253	0.2747	1651	1550	2939	2879
5400	90	80.3	0.6152	0.1747	0.1857	0.0245	0.7682	0.2318	1651	1551	2942	2879
6600	110	60.5	0.5427	0.2302	0.1964	0.0308	0.7342	0.2658	1651	1550	2940	2879
8040	134	40.1	0.4769	0.2778	0.2095	0.0359	0.6948	0.3052	1652	1546	2939	2878
9000	150	19.9	0.3836	0.3514	0.2269	0.0381	0.6283	0.3717	1653	1542	2938	2877
10200	170	5.0	0.1182	0.5714	0.2709	0.0394	0.3038	0.6962	1654	1532	2936	2875

2.4.4. Changes in Weights Using Quartz Crystal Microbalance

Frequency shifts of QCM were converted to weight changes by Sauerbrey's equation (Eq. 2.1) in the water adsorption / desorption on the collagen film. Weights (μg) increased and decreased with RH increase and decrease (Figure 2.3b). Weight changes with RH on the sample-free QCM sensor, possibly due to trace amounts of water adsorbed on the QCM sensor, were less than 9 ng, which was less than 2 % of the weight increase with RH in the presence of the collagen film (Table 2.3). Therefore, the weight changes are considered to be mainly by water adsorption / desorption to the collagen film. These water weights were

divided by the weight of dried collagen film (8.0 μg at RH = 5.1 %) and plotted against RH values (Figure 2.3c). The adsorbed water weights are almost similar for wetting and drying processes, indicating that the collagen film is almost equilibrated between adsorption and desorption of water. Details of water adsorption behavior (adsorption isotherm) with RH (water vapor pressure) need further numerous data points that are not necessarily quasilinear.

2.4.5. Infrared Spectral Changes with Relative Humidity

Infrared spectral changes with RH of the collagen film at 28 ^{o}C are shown for wetting (Figure 2.4a) and drying processes (Figure 2.4b). These are raw transflection spectra of the collagen film in absorbance without any baseline correction or smoothing. Several replicate runs showed similar results but only a representative series of results with absorbance values between 0 and 1 are shown here for quantitative analyses. Twenty spectra (64 scans) were obtained for one RH value maintained for 20 min. A representative spectrum at that RH after its stabilization at about 15 min was selected for further quantitative analyses. Since RH (%) and temperature (T in ^{o}C) were monitored every second, we averaged RH and T for 60 s corresponding to the IR spectrum.

All the IR spectra during the water sorption and desorption processes show a broad band from 3700 to 3000 cm^{-1}. These spectral changes during the wetting and drying processes are mostly similar. This broad band in the 3700 − 3000 cm^{-1} region is due to OH + NH stretching bands (Masuda et al., 2003; Siebert and Hildebrandt, 2008; Kataoka et al., 2011; Fabian and Naumann, 2012) with a strong peak around 3340 cm^{-1} and another small peak at 3080 cm^{-1} due to N−H stretching (often called amide A and B, respectively) (Fabian and Naumann, 2012).

The 2975 and 2875 cm^{-1} bands are due to asymmetric and symmetric CH_3 stretching, respectively (Staroszczyk et al., 2012). The 2935 cm^{-1} band is due to asymmetric stretching of CH_2 (Staroszczyk et al., 2012). The 1445 and 1335 cm^{-1} bands are due to CH_2 bending and CH_2 wagging, respectively (Boryskina et al., 2007; Staroszczyk et al., 2012).

The bending vibration of H_2O molecules is around 1640 cm^{-1} (Masuda et al., 2003; Kataoka et al., 2011), but this band overlaps with adjacent bands resulting in the shoulder around 1655 cm^{-1}.

The 1655 cm^{-1} band is due to C=O stretching of peptides (H−N−C=O) (amide I). The 1530 cm^{-1} band is due to N−H bending and C−N stretching (amide II). The 1230 cm^{-1} band is also due to coupling of N−H bending and C−N stretching of peptides (amide III) (Siebert and Hildebrandt, 2008; Fabian and Naumann, 2012; Staroszczyk et al., 2012).

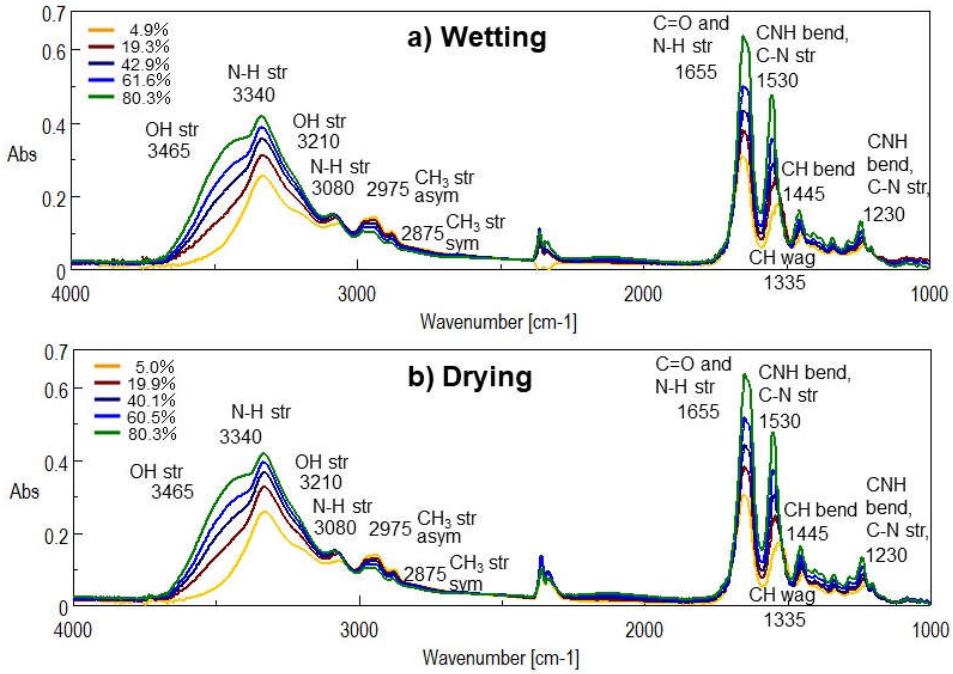

Figure 2.4. Infrared changes with RH of the collagen film. (a) Wetting process (RH = 4.9, 19.3, 42.9, 61.6, and 80.3 %); (b) drying process (RH = 80.3, 60.5, 40.1, 19.9, and 5.0 %).

2.4.6. Changes in the Total OH + NH Band Area with Relative Humidity

The OH + NH stretching band from 3700 to 3000 cm^{-1} for the collagen film increased with increasing humidity and decreased with decreasing humidity (Figure 2.4a, b). The OH + NH stretching band areas were determined with a linear baseline from 3660 to 3010 cm^{-1} for the collagen film during the wetting and drying processes and were plotted against RH in

Figure 2.5a. The increasing and decreasing trends of the OH + NH band area during the wetting and drying process are almost similar (Figure 2.5a) indicating quasi-equilibrium of water adsorption in agreement with the QCM data (Figure 2.3c). As stated above, details of water adsorption behavior (adsorption isotherm) with RH need further numerous data points that are not necessarily quasi-linear.

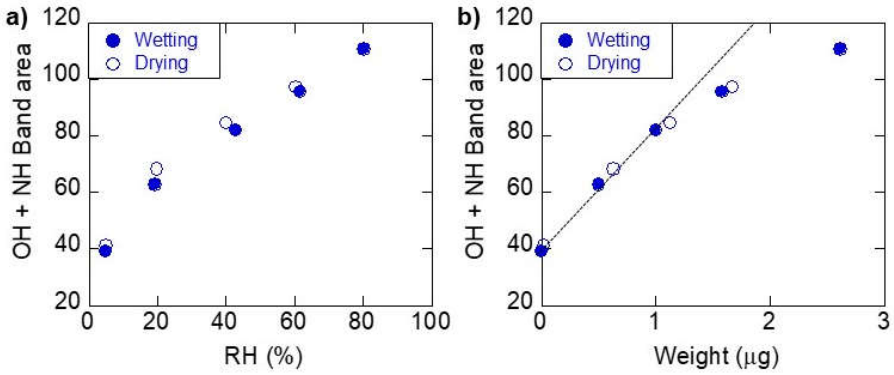

Figure 2.5. Infrared total OH + NH stretching band areas in the 3660 − 3010 cm^{-1} region plotted against (a) RH and (b) weight changes by QCM of the collagen film during the wetting and drying processes.

2.4.7. Total OH + NH Band Area against Adsorbed Weight Using Quartz Crystal Microbalance

The OH + NH band area during the wetting and drying process (Figure 2.5a) were plotted against the weight changes observed by QCM in Figure 2.3b (Figure 2.5b). The OH + NH band area increases linearly with the adsorbed weight until about 1.2 μg (correlation coefficient R = 0.993). However, the OH + NH band areas at higher RH (60 %, 80 %) deviate from the linear trend to the lower side (Figure 2.5b). Origins of this deviation will be discussed later.

2.4.8. Changes in Infrared Peak Positions with Relative Humidity

Peak maximum positions of the amide I and II bands are plotted in Figure 2.6. The peak positions of the amide I band were determined by local maxima in a narrow range from 1657

cm^{-1} to 1647 cm^{-1} for avoiding contribution from H_2O bending band. The shoulder of the amide I band, including the H_2O bending band, are situated around 1637 cm^{-1} and do not influence the peak maxima of the amide I band. Therefore, the peak shift of the amide I band with RH is considered to be independent of the increase of adsorbed water. The peak position of the amide I band decreased slightly from 1653 cm^{-1} to 1651 cm^{-1} for increasing RH and increased up to 1654 cm^{-1} for decreasing RH (Figure 2.6c). On the other hand, the peak position of the amide II band increased significantly from 1531 cm^{-1} to 1551 cm^{-1} for increasing RH and decreased down to 1532 cm^{-1} for decreasing RH (Figure 2.6d).

Peak maximum positions of asymmetric stretching of CH_2 and symmetric stretching of CH_3 are plotted in Figure 2.7. These peak positions were determined by local maxima after the baseline correction with a linear baseline from 3010 to 2850 cm^{-1} in order to remove effects of absorption tails of OH + NH stretching bands. The peak position of the CH_2 band increased from 2936 cm^{-1} to 2942 cm^{-1} for increasing RH and decreased down to 2936 cm^{-1} for decreasing RH (Figure 2.7c). The peak position of the CH_3 band also increased from 2875 cm^{-1} to 2879 cm^{-1} for increasing RH and decreased down to 2875 cm^{-1} for decreasing RH (Figure 2.7d).

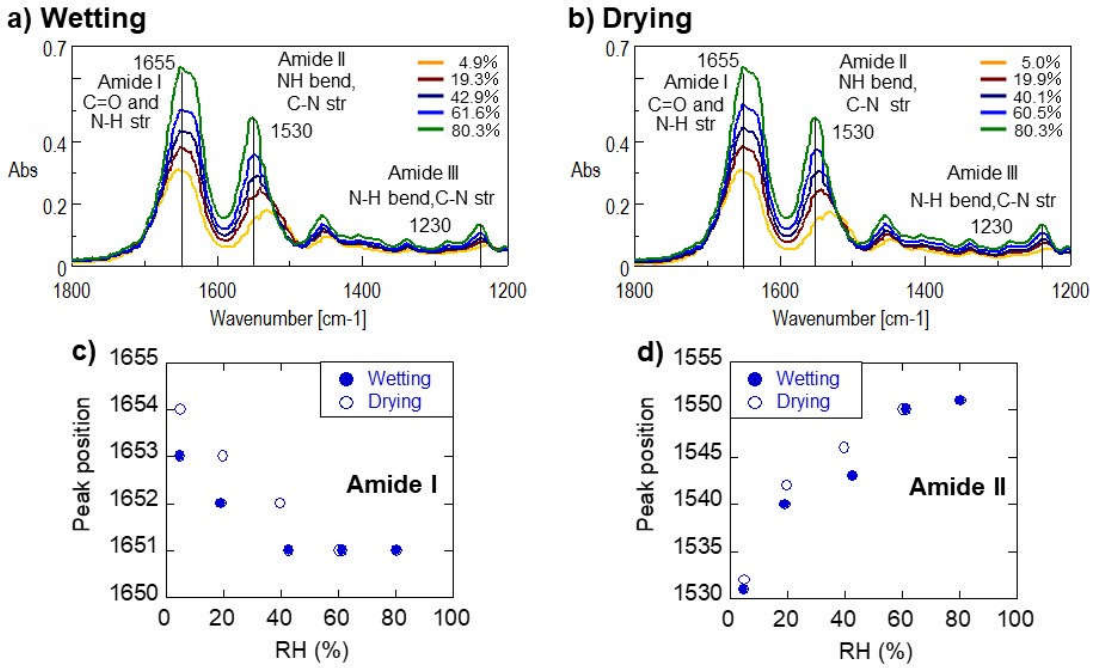

Figure 2.6. Infrared spectral changes of amide region during (a) wetting, (b) drying, and peak positions of (c) Amide I (1655 cm^{-1}) and (d) Amide II (1530 cm^{-1}) of the collagen film.

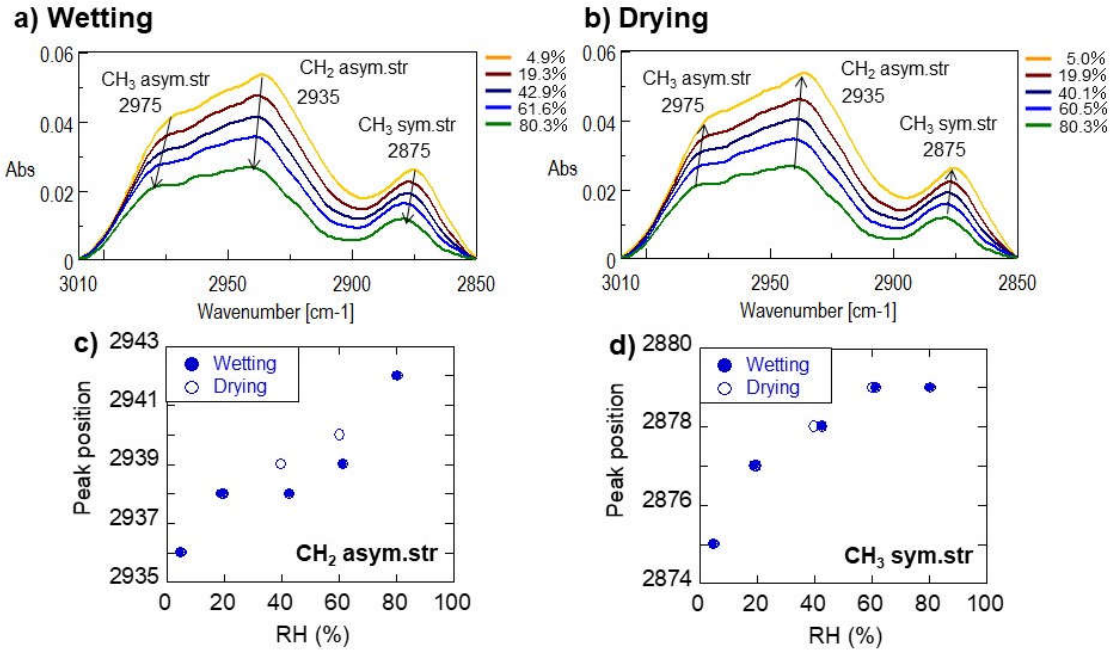

Figure 2.7. Infrared spectral changes of CH stretching region during (a) wetting, (b) drying, and peak positions of (c) asymmetric CH_2 (2935 cm^{-1}) and (d) symmetric CH_3 (2875 cm^{-1}) of the collagen film.

2.4.9. Difference Spectra from the Dry Collagen Film

In order to study detailed changes in IR spectra during the wetting and drying processes, all the spectra were subtracted by the driest collagen film spectrum at RH = 4.9 % (Figure 2.8a, b). The difference spectra during the wetting process show a broad OH + NH stretching band in the 3700 − 3000 cm^{-1} region with four different peaks at 3465, 3340, 3210 and 3080 cm^{-1} (Figure 2.8a). The same bands are also observed for the drying process (Figure 2.8b). These bands increased with increasing RH.

The CH stretching bands in the 3000 − 2800 cm^{-1} region are negative, indicating that their bands decreased for increasing RH. This is in agreement with the band intensity decrease with RH (Figure 2.7). The CH bending band around 1445 cm^{-1} also shows similar behavior.

The amide I, II and III bands are positive, indicating that their bands increased for increasing RH. This is in agreement with the band intensity increase with RH (Figure 2.6).

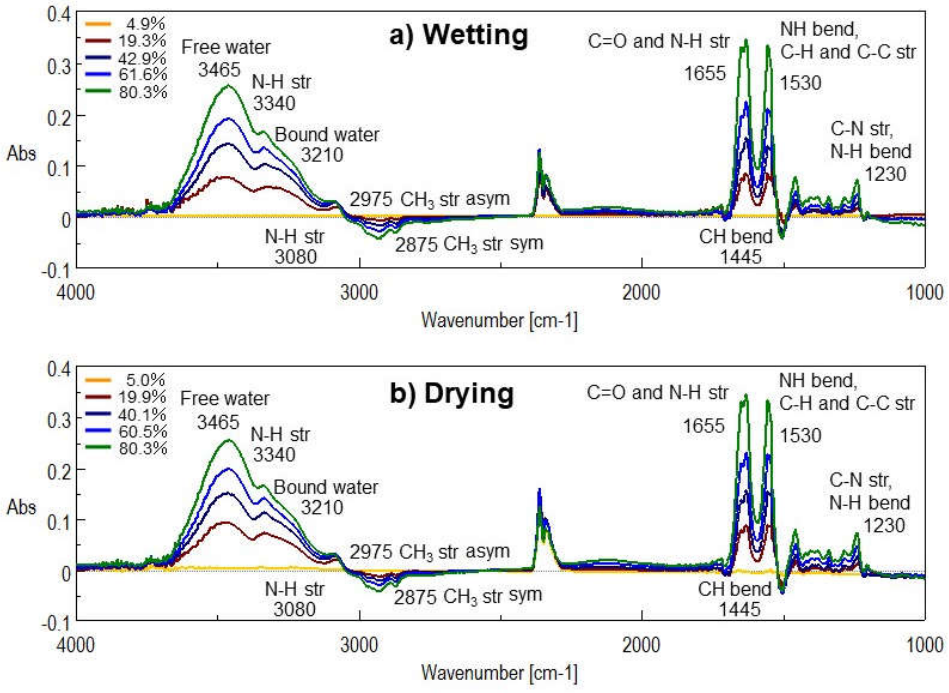

Figure 2.8. Difference spectra from the driest collagen film spectrum (RH = 4.9 %) during (a) wetting and (b) drying processes.

2.5. Discussion

The amide and OH + NH bands show a general increase and decrease with RH. This can be related to complex combined effects of decrease of refractive indices of the collagen film (1.553 at RH = 2.0 % to 1.531 at RH = 83.2 %) (Figure 2.2a), its slight thickening (from 1.97 ± 0.23 μm at RH = 5.7 % to 2.37 ± 0.23 μm at RH = 80.4 %) (Figure 2.2b) and subsequent increase of travel length of IR light through the collagen film by transflection (twice transmission path length). The effects of standing wave in the IR transflection method (Staroszczyk et al., 2012; Bassan et al., 2013) should also be considered. However, CH band intensities behave in an opposite way. Therefore, detailed quantitative treatments of IR band intensities need correction of these combined effects and will be reported in a future report.

2.5.1. OH+NH Band Area versus Weight Changes Using Quartz Crystal Microbalance

Despite the above difficulties of quantitative treatments of IR band intensities, the OH + NH band area during the wetting and drying processes plotted against the weight changes observed using QCM shows a linear relation for RH = 5 % to 40 % (Figure 2.5b). This indicates that weights gained by the collagen film are due to water adsorption.

However, the OH + NH band area deviates to the lower side from the linear trend at higher RH (60 %, 80 %) (Figure 2.5b). This deviation can be due to the difference in the measured areas, OH band saturation, and viscoelasticity of the collagen film. While the IR microspectroscopic measurement on the collagen film were conducted on a 300 x 300 μm^2 area preferentially at low absorbance locations, the frequency shift observed by QCM is for the whole film on the Au electrode. Therefore, OH band areas at a limited area might be underestimated. Moreover, some locations with a thicker film have strong OH + NH absorptions leading to saturation of the bands preventing the quantitative treatments. The Sauerbrey equation of QCM measurement is valid for adsorption of thin rigid materials attaching to the quartz resonator but is no longer valid for viscoelastic ‘‘soft’’ material. The collagen film at high RH (> 40 %) can become soft because of significant water adsorption.

In fact, the thickness of the collagen film increased for higher RH > 40 % possibly due to its swelling by incorporating adsorbed water (Figure 2.2b).

The combined IR and QCM measurements performed here are useful for lower RH conditions but need further quantitative improvements such as correction of QCM data for viscoelastic materials. These will be reported in a future paper.

2.5.2. Origins of Infrared Peak Shifts

The peak position of the amide I band shifts slightly from 1653 cm^{-1} to 1651 cm^{-1} for increasing RH (Figure 2.6c), while the peak position of the amide II band shifts significantly from 1531 cm^{-1} to 1551 cm^{-1} for increasing RH (Figure 2.6d). The lower wavenumber shift (red shift) of C=O stretching (amide I) can be understood by increasing hydrogen bonding of water molecules to peptides at lower RH (Boryskina et al., 2007). The opposite higher wavenumber shift (blue shift) of N−H bending (amide II) can also be understood by this hydrogen bonding (Boryskina et al., 2007).

The asymmetric stretching of CH_2 and symmetric stretching of CH_3, after the baseline correction to remove effects of absorption tails of OH + NH, show peak shifts from 2936 to 2942 cm^{-1} (Figure 2.7c) and from 2875 to 2879 cm^{-1} (Figure 2.7d), respectively, for increasing RH. These higher wavenumber shifts (blue shift) for CH stretching vibrations cannot be explained by normal hydrogen bonding. In fact, these blue shifts of CHs have been reported for various compounds such as acetone-water mixture (Mizuno et al., 1998). Recent molecular simulation studies suggested that these shifts can be due to anomalous hydrogen bonding of water molecules to hydrophobic CH species through complex mixtures of multiple interactions (Scheiner et al., 2001; Joseph and Jemmis, 2007).

These results suggest that adsorption sites of water molecules on the collagen film are not only by hydrogen bonding to the polar peptide bonds but also include interactions with hydrophobic CH portions.

2.5.3. Curve Fitting of OH + NH Bands

Raw OH + NH bands of collagen show peaks of amide A and B (NH). Their positions mostly remain unchanged with RH (Figure 2.4). OH bands appear as shoulders and so the peak positions can not be determined (Figure 2.4). The difference spectra from the driest collagen film (RH = 4.9 %) shows four peaks at 3465, 3340, 3210 and 3080 cm^{-1} for both wetting and drying processes (Figure 2.8a, b). The peak positions of these four bands do not change significantly with RH, although peak positions of the 3210 cm^{-1} component remain unclear.

In order to study detailed changes in the OH + NH band with RH, Gaussian curve fitting was conducted on original absorbance spectra (Figure 2.9a). First, four Gaussian components at 3465, 3340, 3210 and 3080 cm^{-1} were used without fixing positions and widths of these bands. The fitting results were not satisfactory. Next by changing band positions, four Gaussian bands fixed at 3440, 3330, 3210, and 3070 cm^{-1} gave better fits to the original OH + NH bands. Since no significant band shifts of OH + NH bands were observed in original and difference spectra (Figures 2.4 and 2.8), the bands were fixed at these positions. The bandwidths (half width at half maximum [HWHM]) for NH bands (amides A and B) were fixed at 120 and 60 obtained by the average values. Finally, four Gaussian components fixed at 3440, 3330, 3210 and 3070 cm^{-1} and HWHM fixed at 120 and 60 for 3330 and 3070 cm^{-1} bands, respectively, gave the best fits to the original OH + NH bands. HWHM values for the 3440 cm^{-1} band were 128 − 155 and those for the 3210 cm^{-1} band were 143 − 174. The band areas of these four bands were plotted against RH (Figure 2.9b). The 3330 and 3070 cm^{-1} band components due to amide A and B (NH) are relatively constant for increasing and decreasing RH (Figure 2.9b).

The 3440 and 3210 cm^{-1} band components are considered to be due to OH stretching vibrations of water molecules adsorbing to the collagen film. These band components correspond to H_2O molecules with longer and shorter hydrogen bonding, respectively (Nakamoto et al., 1955). In this study, the longer and shorter H bond components around 3440 and 3210 cm^{-1} are called ‘‘free water’’ and ‘‘bound water,’’ respectively. At low RH = 4.9 %, more bound water (band area: 10.2) than free water (4.3) is retained in the collagen

film (Figure 2.9b). With increasing RH, bound water shows a slight increase, approaching a constant band area value around 20 for RH > 40 %. On the other hand, free water increases greatly from 4.3 at RH = 4.9 % to 22.3 at RH = 19.3 % and then continues to increase quasi-linearly over RH > 40 % to 72.9 at RH = 80.3 %. Bound water adsorbs first at low RH and its adsorption can be saturated over RH > 40 %, while free water continues to increase over RH > 40 % (Figure 2.9b). Increase in the collagen film thickness at higher RH (Figure 2.2b) can be originated from the increase of free water fraction at higher RH.

The band areas of free and bound water were divided by the sum of these areas and plotted against RH (Figure 2.9c). The bound water fraction is around 0.70 (70 %) at RH = 4.9 % but decreases greatly from RH = 19.3 % approaching 0.23 (23 %) at RH = 80.3 %. At higher RH, free water fraction becomes dominant over 70 %.

The adsorption behavior of bound water saturating with increasing RH (Figure 2.9b) is similar to the peak shifts of the amide I and II bands (Figure 2.6c, d). This result suggests binding of water molecules to peptide bonds of the collagen film by hydrogen bonding. On the other hand, the adsorption behavior of free water increasing further at higher RH can be correlated to the peak shift of aliphatic CH_2 groups (2935 cm^{-1}) (Figure 2.7c). The peak shift of the CH_3 groups appears to be saturated at higher RH (Figure 2.7d), possibly due to limited interaction sites of end methyl species on the collagen surface. Free water with longer hydrogen bonding might be loosely bound to aliphatic side chains on the collagen surface. Since hydrophobic CH side chains are present on the surface of helical collagen structures by keeping hydrogen bonded peptide bonds inside the helices, the higher wavenumber CH peak shifts observed at higher RH can be understood by loose adsorption of water molecules on aliphatic CHs on the collagen surface. Bound water adsorbs first at low RH and its adsorption can be saturated over RH > 40 %, while free water continues to increase over RH > 40 % (Figure 2.9b). Therefore, free water fraction increases at higher RH resulting in increase in film thickness (Figure 2.2b).

These results suggest that water molecules adsorbing to the collagen film are strongly hydrogen bonded ones bound to polar sites such as peptides at lower RH, while at higher RH,

freer water molecules are loosely bound to aliphatic CH side chains cropping out on the surface of collagen helices.

The present combined QCM-IR method is found to be useful for studying amounts and natures of water adsorbing on biomolecules.

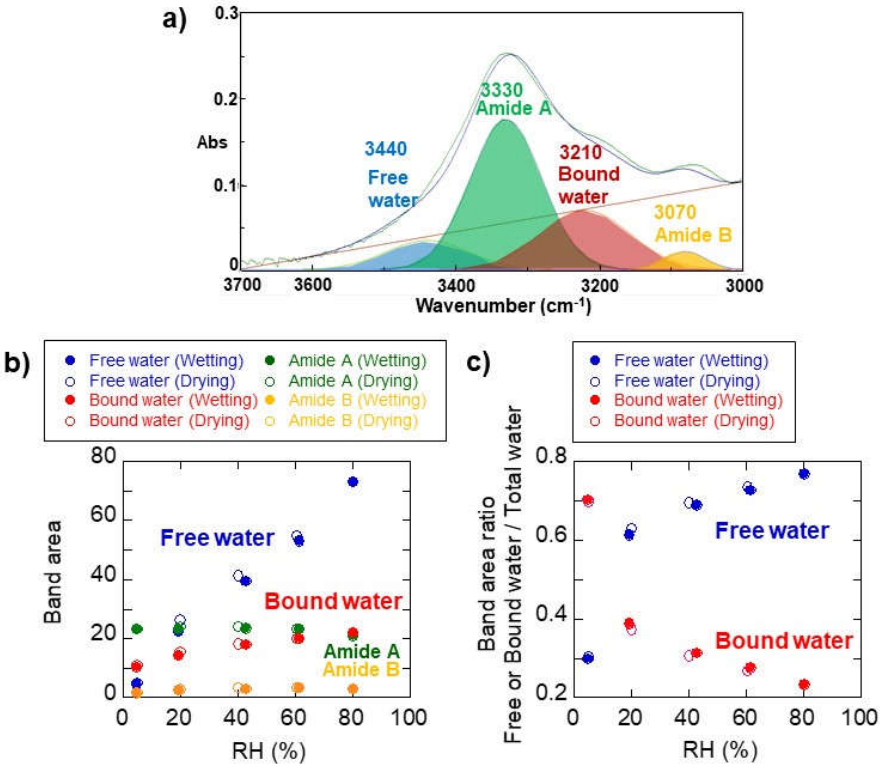

Figure 2.9. (a) Curve fitting of OH + NH stretching bands in the 3700 − 3000 cm^{-1} region by four Gaussian components: free water (3440 cm^{-1}), amide A (3330 cm^{-1}), bound water (3210 cm^{-1}), and amide B (3070 cm^{-1}). (b) Band areas of the four components and (c) factions of free and bound water in the total water (3440 + 3210 cm^{-1} band areas) of the collagen film as a function of RH.

2.6. Conclusion

Water molecules adsorbed on a collagen film were studied by IR microspectroscopy combined with a QCM together with an original RH control system.

1. Weight changes (μg) by QCM increased and decreased with RH corresponding to water adsorption / desorption to the collagen film at 28 °C. The adsorbed water weights were almost

similar for wetting and drying processes, indicating that the collagen film were at close equilibria of water adsorption / desorption.

2. Infrared spectra of the collagen film at 28 ^{o}C during the adsorption / desorption processes show a broad band from 3700 to 3000 cm^{-1} due to OH + NH stretching which increases and decreases during the wetting / drying processes in a similar manner in agreement with the QCM data.

3. The OH + NH band area increases linearly with the adsorbed weight until about 1.2 μg / 8.0 μg dry collagen film at RH = 40 %. However, the OH + NH band areas at higher RH (60 %, 80 %) deviate from the linear trend to the lower side, possibly due to the differences in measured areas, OH band saturation, and viscoelasticity of the collagen film. The combined IR and QCM measurements performed in this study are useful for lower RH conditions but need further quantitative improvements such as correction of QCM data for viscoelastic materials.

4. The lower wavenumber shift (red shift) of C=O stretching (amide I) and the opposite higher wavenumber shift (blue shift) of N−H bending (amide II) can be understood by increasing hydrogen bonding of water molecules to peptides at lower RH.

5. The higher wavenumber shifts (blue shift) of asymmetric stretching of CH_2 and symmetric stretching of CH_3 can be due to anomalous hydrogen bonding of water molecules to hydrophobic CH species through complex mixtures of multiple interactions.

6. The difference spectra from the driest collagen film (RH = 4.9 %) shows four peaks at 3465, 3340, 3210, and 3080 cm^{-1} for both wetting and drying processes. Four Gaussian components at 3440, 3330, 3210 and 3070 cm^{-1} gave the best fits to the original OH + NH bands. The 3330 and 3070 cm^{-1}band components due to amide A and B (NH) are relatively constant for increasing and decreasing RH.

7. The 3440 and 3210cm^{-1} components correspond to H_2O molecules with longer (free water) and shorter (bound water) hydrogen bonding, respectively. At low RH = 4.9 %, more bound water than free water is retained in the collagen film. With increasing RH, bound water shows a slight increase approaching a constant value, while free water increases greatly from RH = 4.9 % to RH = 19.3 % and then continues to increase quasi-linearly to RH = 80.3 %. The

bound water fraction is around 70 % at RH = 4.9 % but decreases greatly from RH = 19.3 % approaching 23 % at RH = 80.3 %. At higher RH, free water fraction becomes dominant over 70 %.

8. The adsorption behavior of bound water saturating with increasing RH is similar to the peak shifts of the amide I and II bands, suggesting the binding of water molecules to peptide bonds of the collagen film by hydrogen bonding at lower RH. On the other hand, the adsorption behavior of free water increasing further at higher RH can be correlated to the peak shift of aliphatic CH_2 groups. Free water with longer hydrogen bonding might be loosely bound to aliphatic side chains on the collagen surface, especially at higher RH.

9. The present combined QCM-IR method is found to be useful for studying amounts and natures of water adsorbing on biomolecules.

Chapter 3. Evaluation of Water Adsorption Capacities of Various Biomaterials: Keratin and Collagen

This chapter has been published as the following paper:
"Water adsorption with relative humidity changes for keratin and collagen as studied by infrared (IR) micro-spectroscopy"
Sachie Kudo and Satoru Nakashima
Skin Research and Technology, Accepted on September 23, 2018 and published online on October, 2018.
John Wiley & Sons Ltd.
(I am now requesting the permission of use from the publisher.)

3.1. Abstract

Background: Natures and amounts of water retained at the surface of stratum corneum (SC) of human skins, affecting skin health and penetration of chemical components, remain unclear.
Methods: A keratin film, a main component of human SC surface, was measured by IR microspectroscopy combined with a quartz crystal microbalance (QCM) and a relative humidity (RH) control system.
Results: Water contents increased with RH up to about 19 wt% and were correlated linearly with the OH + NH band areas in IR spectra of the keratin film. The OH + NH band areas for the triple helix collagen film are about twice as large as those for the keratin film (double helix). The free water component increases with RH by keeping the bound water component minor for the keratin film. About twice of water retention capacity of the collagen film can be due to increasing adsorption of free water, interacting possibly with hydrophobic aliphatic CH surfaces.
Conclusion: The present results suggest relatively low water contents less than about 19 wt% of outermost SC layers of human skin composed mostly of keratin exposed to ambient RH conditions. The triple helix collagen can be used as an effective moisturizing agent.

3.2. Introduction

Water contents at the stratum corneum (SC) of human skins are considered to affect skin health (Tanaka et al., 1998; Edwards and Marks, 2005; Serup, 2005) and penetration of several chemical components (Raut et al., 2014; Li et al, 2016). Water contents of human SC have been evaluated mostly by relative values using electrical methods (Khazaka, 2005; Barel and Clarys, 2014; Tagami, 2014), which correspond to water contents throughout the whole SC layers. On the other hand, confocal Raman microscopy has been employed to determine depth profiles of water contents from about 70 to 20 wt% over the SC with a spatial resolution of about 5 μm (Caspers et al., 2000; Sieg, 2014). Water contents at the SC surface has been reported to increase by keeping the constant deeper water contents (Egawa et al., 2007). An alternative method is required for evaluating water contents at the outermost surface (about 1 μm) of human SC.

Attenuated total reflection infrared (ATR-IR) spectroscopy can be used to examine water contents of the SC surface because of the penetration depth of about 1 μm of evanescent wave (Olsztynska et al., 2018). However, the sample should be placed on an ATR crystal (typically ZnSe) and its weight cannot be determined directly preventing the evaluation of water contents.

Since the outermost SC layers are exposed to ambient human environment with variable relative humidity (RH), their water contents might vary in response to ambient RH (Bouwstra et al., 2008).

α-Keratin is the main constituent of hair, nail, and skin surface (stratum corneum) (Leveque, 2005; Wang et al., 2016). Its structure is mainly in the form of α helix by hydrogen bonding among peptide bonds. Two α helices form double helix chains of about 45 nm long and 2 nm in width. They are assembled into protofilament groups called protofibril with a diameter of about 7 nm (Wang et al., 2016). The double helices form crystalline phases, while others are in amorphous states bound either by strong S−S bonds or by weak H bonds among peptides (Xiao and Hu, 2016). Water sorption properties of α keratin have been studied by

sorption isotherms, thermal analyses, Raman and IR spectroscopy (Leveque, 2005; Barba et al., 2011; Xiao and Hu, 2016). Although different natures of water (bound water and free water) adsorbed to α-keratin have been proposed mainly by thermal analyses (Leveque, 2005), detailed natures of water molecules and their interactions with keratin functional groups still remain unclear.

Although infrared (IR) spectroscopy has been used for studying amide structures of keratins (Xiao and Hu, 2016), it has not been employed extensively to study water bound to keratins except for some limited studies mentioned above. For investigating water molecules bound to biomaterials, infrared (IR) microspectroscopy equipped with a humidity control system has been combined with quartz crystal microbalance (QCM) (Kudo et al., 2017). By this new method, small weight changes in the nano gram range can be determined from a shift of the resonant frequency of the quartz crystal during changes in relative humidity (RH) (Sauerbrey, 1959; Schuttlefield et al., 2007). At the same time, IR spectra can be obtained on the same sample placed on the QCM giving characteristics of water molecules together with those of functional groups of keratins.

The OH stretching frequency in the infrared (IR) spectra was reported to decrease with decreasing hydrogen bond distance among water molecules (Nakamoto et al., 1955). Therefore, higher and lower wavenumber components in the OH band correspond respectively to longer and shorter hydrogen bond components. The longer H bond component is often called as “free water,” while the shorter H bond component as “bound water” (Einhorn-Stoll et al., 2012; Kudo et al., 2017). Water adsorbed on keratins measured by IR microspectroscopy with changing relative humidity is analyzed here based on these different H bond components. Moreover, interactions of water molecules were studied not only for peptide bonds (amide I) but also for aliphatic CH species on external surfaces of keratin double helices.

Moreover, the obtained results for keratins are compared with those for collagens studied by the same method. Collagens are another representative structural proteins present in biological tissues such as animal skins and bones. Natural collagens are considered to be in the triple helix form bound by hydrogen bonding mainly between peptide bonds (Shoulders

and Raines, 2009) with some contribution of water to peptide bonding (Boryskina et al., 2007). Therefore, in this study, natures and amounts of water molecules adsorbed are compared for keratins with double helices and collagens with triple helices both forming fibril structures.

3.3. Material and Methods

3.3.1. Preparation of Keratin Solution

Human hair (of a Japanese woman) was washed with ethanol; external lipids were removed using a mixture of chloroform / methanol (2:1, v / v) for 24 hours. The delipidized hair (20 mg) was mixed with a solution (5 mL) containing 25 mmol L^{-1} Tris-HCl, pH 8.5, 2.6 mol L^{-1} thiourea, 5 mol L^{-1} urea and 5 % 2-mercaptoethanol (2-ME) (Shindai method) or 25 mmol L^{-1} Tris-HCl, pH 9.5, 8 mol L^{-1} urea and 5 % 2-ME (conventional method) at 50 °C for 1 − 3 days. The mixture was filtered and centrifuged at 15 000 g for 20 minutes at room temperature. The obtained supernatant was used as a hair protein fraction (Nakamura et al., 2002). The colloidal suspension solution containing 1 wt% keratin was purchased from Shinshu TLO.

3.3.2. Relative Humidity Control System

In order to study adsorption behavior of water to keratin, a plastic humidity control cell (36 × 36 × 14 mm) with a CaF_2 window (20 mm diameter) was fabricated (Figure 3.1) (Kudo et al., 2017). The relative humidity (RH) of the cell interior was controlled by flowing a mixture of dry air and water-saturated air with varying proportions at a total flow rate of about 1 L min^{-1} (Figure 3.1). The dry air was provided from a dehumidifier (AM-12, JASCO, Tokyo, Japan) through a flow meter (D8500, KOFLOC, Kyoto, Japan). The water-saturated air was made by flowing the dry air from the same dehumidifier via another flow meter through two bottles of pure water (Milli-Q, Electrical resistivity > 18.2 MΩ cm). The humidity and temperature in the cell were monitored every second by a small temperature

and humidity sensor (SHT 35, SENSIRION, Stafa, Switzerland) equipped with a data logger (SCHM-1, SENSIRION) connected to a PC with an USB cable. The humidity was increased from 1.2 % to 85.4 % by changing the flow rates of humid and dry air by two flow meters.

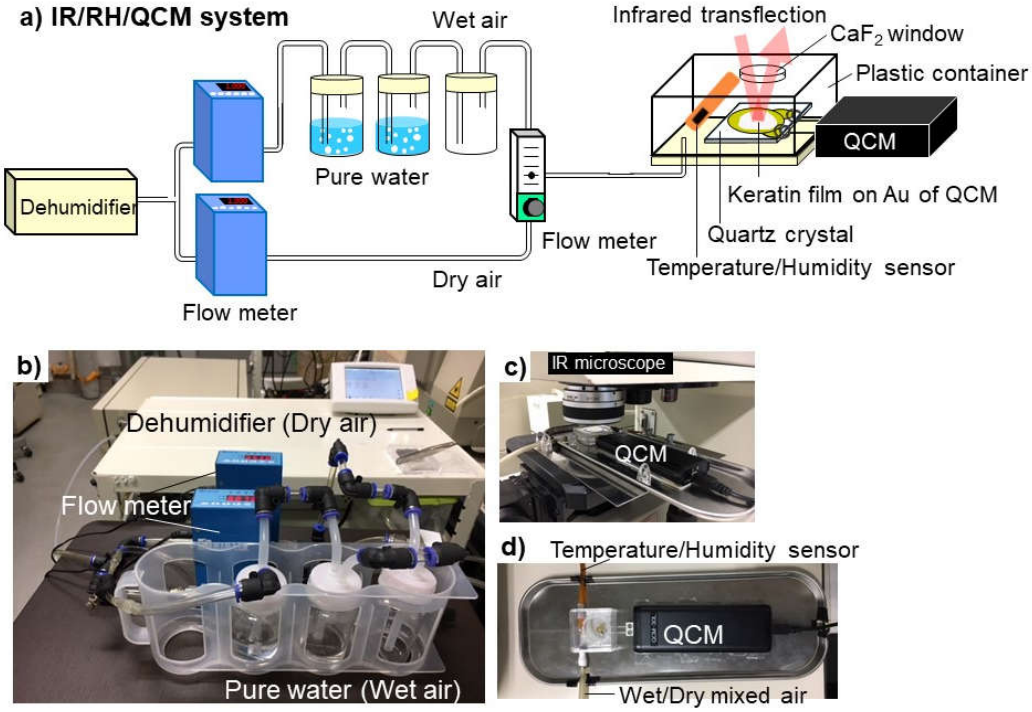

Figure 3.1. Infrared (IR) microspectroscopy combined with relative humidity (RH) control system and quartz crystal microbalance (QCM). (a) A schematic image of the system, (b) A photograph of the RH control system, (c) A photograph of the RH control cell under an IR microscope, (d) A close-up photograph of the RH control cell with QCM.

3.3.3. Quartz Crystal Microbalance (QCM)

A quartz crystal microbalance (QCM) system (QCM-30L, SEIKO EG&G, Tokyo, Japan) was used in this study for measuring weights of adsorbed water on a keratin film placed on a gold (Au) electrode coating on an AT-cut quartz of QCM sensor in a plastic container (Figure 3.1) (Kudo et al., 2017). Changes in resonant frequency of quartz from the initial value (F_0) around 9.0 MHz were monitored at every second when water was adsorbed /

desorbed under various relative humidity. These frequency changes can be converted to mass changes by Sauerbrey's equation (Sauerbrey, 1959):

$$\Delta F = -\frac{2F_0^{\,2}}{\sqrt{\rho_Q \mu_Q}} \frac{\Delta m}{A} \qquad (3.1)$$

where ΔF is the change in resonance frequency (Hz), Δm is the mass change (kg), F_0 is the resonant frequency (Hz) at around 9.0 MHz, ρ_Q is the density of quartz (2.65×10^3 kg m^{-3}), μ_Q is the shear modulus of quartz (2.95×10^{10} kg m^{-1} s^{-2}), and A is the surface area of the electrode (1.96×10^{-5} m^2) (Lucklum et al., 1997).

3.3.4. Preparation of the Keratin Film

One drop of the 1 % keratin suspension was placed by a micropipette on the Au electrode coating on the quartz crystal microbalance (QCM) in a plastic container. Dried air was flowed in the plastic container with a flow rate more than 1 L min^{-1} for about 5 min until the stable weight monitored by QCM. The obtained transparent keratin film had a weight of 7.9 μg (at RH = 3.0 %).

3.3.5. IR Microspectroscopy

In order to evaluate natures of adsorbed water on the keratin film, infrared (IR) transflection (transmission-reflection) spectra of the keratin film on the Au electrode on QCM quartz crystal were measured under different relative humidities (RH = 1.2 to 85.4 %). The keratin film on the QCM in the plastic cell with a CaF_2 window was placed under an FTIR microscope (Jasco IRT30 + FTIR620: a Cassegrainian objective mirror with a magnification of 16, MCT detector, ceramic IR source and KBr beam splitter) (Figure 3.1). The environment outside the RH cell was the ambient experimental room with normal air conditioning with the temperature around 24 °C and RH of about 40 % (Figure 3.1). No evacuation or gas purging had been conducted on the IR microscope.

A background reflection spectrum was measured on the Au coated quartz crystal without any sample using an aperture size of 300 × 300 μm^2 and then a sample transflection spectrum

was measured on the keratin film with the same aperture. All the spectra were obtained by accumulating 64 scans at a wavenumber resolution of 4 cm^{-1}. The transflection method has been reported to be used quantitatively in IR microspectroscopy (Alipour et al., 2016).

3.4. Results

3.4.1. Temperature and Relative Humidity Changes

Temperature in the cell during water adsorption / desorption experiments on the keratin film was mostly kept constant around 25.0 ± 2.5 °C during the increase and decrease in relative humidity (RH) from 1.2 to 85.4 and then to 1.8 % (Table 3.1, Figure 3.2a, b). The RH value became relatively stable within 10 minutes with some small fluctuations at each humidity value with errors of less than 0.2 % (Table 3.1). After keeping the same RH values for 60 − 120 minutes until the stable weight monitored by QCM, the RH values were increased or decreased (Figure 3.2a, b).

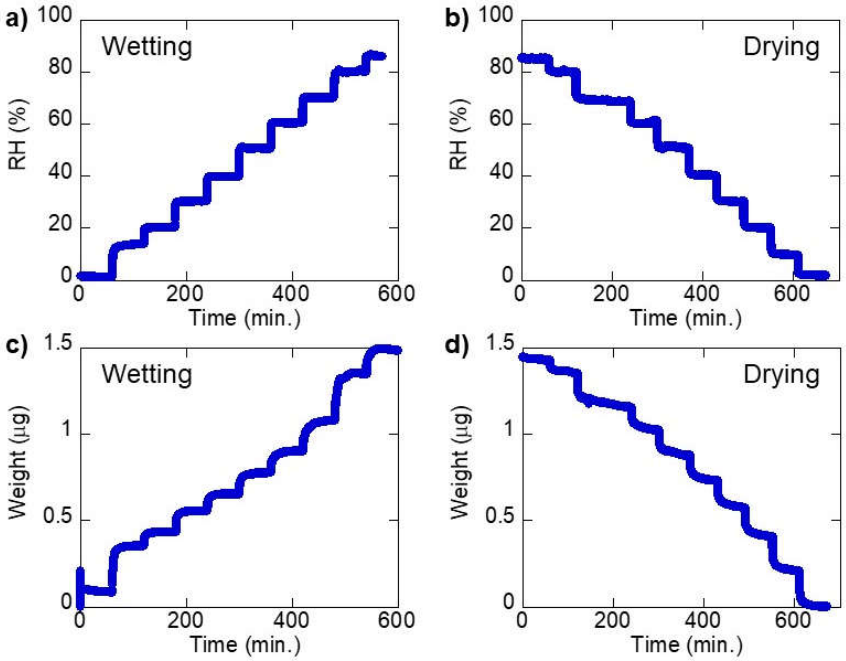

Figure 3.2. Changes in relative humidity (RH: %) during (a) wetting and (b) drying. Changes in weights (µg) of the keratin film during (c) wetting and (d) drying.

Table 3.1. Time (minutes), temperature (°C), relative humidity (RH: %), frequency shifts of QCM (Hz) and mass changes (μg) with errors, weight ratio and total OH + NH band area during wetting and drying processes of the keratin film.

	Time (min)	Temp (°C)	Max error	RH (%)	Max error	ΔF (Hz)	Max error	Δm (μg)	Max error	Weight ratio (μg / μg)	Total OH + NH Band area
Wetting	55	22.6	0.04	1.2	0.09	-80	0.9	0.09	0.0001	0.011	45.00
	115	23.3	0.02	13.8	0.1	-327	1.07	0.35	0.0012	0.045	53.95
	175	23.8	0.05	20.3	0.16	-402	1.22	0.44	0.0013	0.055	57.15
	235	24.1	0.03	30.3	0.09	-513	0.8	0.56	0.0009	0.070	61.30
	295	24.3	0.02	39.7	0.1	-603	0.57	0.65	0.0006	0.083	64.68
	355	24.5	0.03	50.6	0.05	-717	0.6	0.78	0.0006	0.098	68.62
	415	24.5	0.02	60.5	0.12	-834	1.03	0.90	0.0011	0.114	72.80
	475	24.4	0.03	69.9	0.1	-995	0.55	1.08	0.0006	0.136	78.07
	535	24.5	0.03	80.2	0.13	-1243	0.62	1.35	0.0007	0.170	84.61
	595	24.6	0.03	85.4	0.1	-1370	1.3	1.48	0.0014	0.188	87.99
Drying	55	25.0	0.03	85.1	0.1	-1317	1.13	1.43	0.0012	0.181	87.91
	115	25.4	0.02	79.7	0.1	-1247	1.12	1.35	0.0012	0.171	84.53
	235	26.9	0.03	68.8	0.13	-1066	0.87	1.15	0.0009	0.146	76.03
	295	27.0	0.06	60.8	0.16	-945	1.15	1.02	0.0012	0.130	71.33
	365	26.8	0.04	50.7	0.07	-810	0.85	0.88	0.0009	0.111	67.51
	425	26.4	0.03	40.2	0.07	-674	1.07	0.73	0.0012	0.092	63.42
	485	26.1	0.02	30.0	0.05	-531	1.02	0.58	0.0011	0.073	59.43
	545	25.8	0.03	20.0	0.11	-377	0.55	0.41	0.0006	0.052	55.12
	605	25.6	0.0	9.7	0.13	-193	0.58	0.21	0.0006	0.027	47.91
	665	25.1	0.1	1.8	0.08	-1	1.03	0.00	0.0011	0.000	41.21

3.4.2. Changes in Weights by Quartz Crystal Microbalance (QCM)

Frequency shifts of QCM were converted to weight changes by Sauerbrey's equation (3.1) in the water adsorption / desorption on the keratin film (Table 3.1). Weights (μg) increased and decreased with RH increase and decrease (Figure 3.2c, d). Weight changes with RH on the sample-free QCM sensor, due possibly to trace amount of water adsorbed on the QCM sensor, are less than 9 ng, which was less than 10 % of the weight increase with RH in the presence of the keratin film. Therefore, the weight changes are considered to be mainly by water adsorption / desorption to the keratin film. These water weights were divided by the weight of dried keratin film (7.9 μg at RH = 3.0 %) and plotted against RH values (Table 3.1, Figure 3.3). The adsorbed water weights are slightly different for wetting and

drying processes, indicating some hysteresis of water adsorption / desorption to the keratin film.

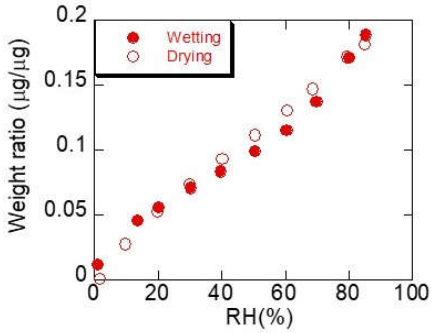

Figure 3.3. Weight ratio of water to dry keratin film (μg / μg) plotted against RH, during wetting (red filled circles) and drying (red open circles) processes of the keratin film.

3.4.3. IR Spectral Changes with RH

IR spectral changes with relative humidity of the keratin film at 25 °C showed similar changes for wetting and drying processes for several replicate runs. Therefore, only a representative series of spectral changes with absorbance values between 0 and 1 for wetting process will be presented here (Figure 3.4). These are raw transflection spectra (64 scans) of the keratin film in absorbance without any baseline correction or smoothing at each RH value after the weight stabilization by QCM. Since RH (%) and temperature (T: °C) were monitored every 1 second, we averaged RH and T for 60 seconds corresponding to the IR spectrum.

All the IR spectra during the water adsorption processes show a broad band from 3700 to 3000 cm^{-1} (Figure 3.4). This broad band in the 3700 − 3000 cm^{-1} region is due to OH + NH stretching bands (Masuda et al., 2003; Kataoka et al., 2011; Siebert and Hildebrandt, 2008; Fabian and Naumann, 2012) with a strong peak around 3300 cm^{-1} and another small peak at 3070 cm^{-1} due to N−H stretching (often called as amide A and B, respectively) (Fabian and Naumann, 2012).

The 2959 and 2874 cm^{-1} bands are due to asymmetric and symmetric CH_3 stretching, respectively (Fabian and Naumann, 2012). The 2934 cm^{-1} band is due to asymmetric

stretching of CH_2 (Staroszczyk et al., 2012). The 1455 and 1340 cm^{-1} bands are due to CH_2 bending and CH_2 wagging, respectively (Boryskina et al., 2007; Staroszczyk et al., 2012).

The bending vibration of H_2O molecules is around 1636 cm^{-1} (Masuda et al., 2003; Kataoka et al., 2011) but this band overlaps with the following adjacent amide I band. The 1645 cm^{-1} band is due to C=O stretching of peptides (H−N−C=O) (amide I). The 1540 cm^{-1} band is due to C−N−H bending and C−N stretching (amide II). The 1240 cm^{-1} band is also due to coupling of C−N−H bending and C−N stretching of peptides (amide III) (Siebert and Hildebrandt, 2008; Fabian and Naumann, 2012; Staroszczyk et al., 2012).

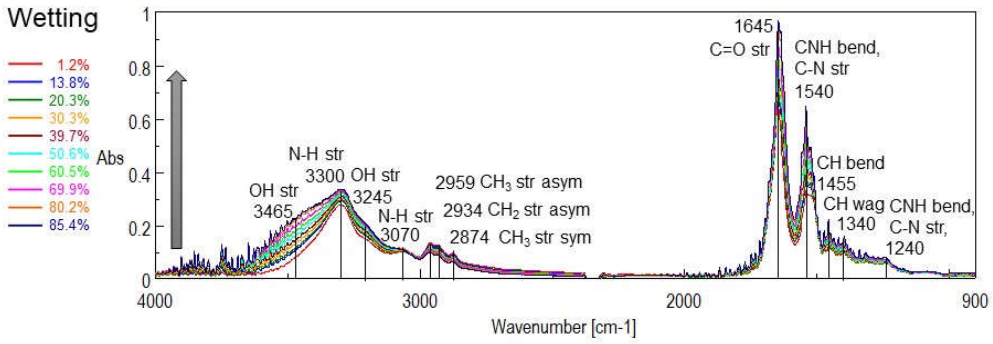

Figure 3.4. IR spectral changes with relative humidity (RH: %) of the keratin film during wetting process (RH = 1.2 % − 85.4 %, about 10 % intervals.). IR peak positions and their assignments are indicated.

3.4.4. Changes in the Total OH + NH Band Area with RH

The OH + NH stretching band from 3660 to 3010 cm^{-1} for the keratin film increases with increasing humidity (Figure 3.4) and decreases with decreasing humidity (figure not shown). The OH + NH stretching band areas were determined with a linear baseline from 3660 to 3010 cm^{-1} for the keratin film during the wetting / drying processes and were plotted against RH in Figure 3.5a. The increasing and decreasing trends of OH + NH band area during the wetting and drying process are mostly similar (Figure 3.5a).

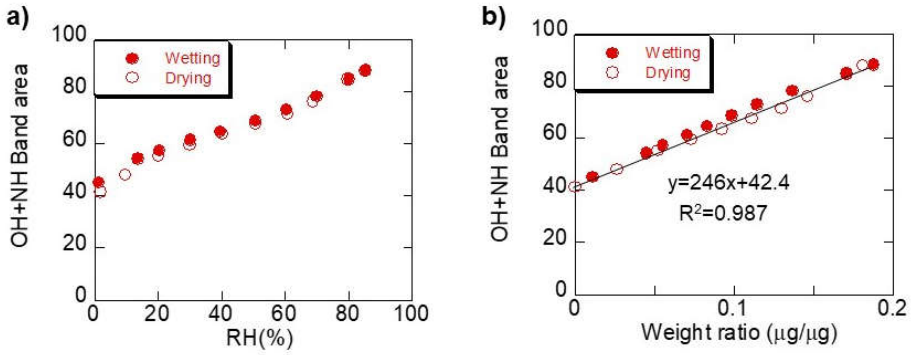

Figure 3.5. IR total OH + NH stretching band areas in the 3660 − 3010 cm^{-1} region plotted against (a) RH, (b) weight ratio (μg / μg) by QCM of the keratin film during the wetting (red filled circles) and drying (red open circles) processes.

3.4.5. Total OH + NH Band Area against Adsorbed Weight by QCM

The OH + NH band areas during the wetting and drying process (Figure 3.5a) were plotted against the weight changes observed by QCM in Figure 3.3 (Figure 3.5b). The OH + NH band area increases linearly with the adsorbed water ratio (correlation coefficient R^2 = 0.987), indicating that the OH + NH band area increase is mainly due to water adsorption.

3.5. Discussion

3.5.1. Water Adsorption to the Keratin Film

As is shown by Figures 3.3 and 3.5a, both weight changes by QCM and OH + NH band areas by IR spectroscopy show increasing trends with RH. These data can be corresponding to adsorption isotherms of water to the keratin film around 25 °C. Since this isotherm shows S type shape, the adsorption process is considered to be multi-layer adsorption (Atkins and de Paula, 2012) of water molecules to the keratin film. A slight difference in the adsorption isotherm between wetting and drying processes (Figure 3.3) might indicate changes in pore structures of the keratin film and associate changes in rate-determining steps such as diffusion.

3.5.2. OH + NH Band Area vs. Weight Changes by QCM

The OH + NH band area during the wetting and drying processes plotted against the weight changes observed by QCM shows a linear relation for RH = 1.2 % − 85.4 % (Figure 3.5b). This indicates that weights gained by the keratin film are due to water adsorption, which can be observed by changes in OH stretching band. The combined IR and QCM measurements performed in this study provide a quantitative calibration for evaluating adsorbed water weight by the IR band area. These points will be reported in a future paper for evaluating adsorbed water to human skins and their model compounds.

3.5.3. Comparison between Keratin and Collagen

In order to discuss adsorption / desorption mechanisms of water for the keratin film, we will compare its adsorption / desorption behavior with the collagen film studied previously (Kudo et al,. 2017), because keratin (α keratin in this study) is reported to be in the form of double helix, while collagen (type I) has a triple helix one, both forming fibril-like structures.

OH + NH Band Area

First, the OH + NH band area during the wetting and drying processes for the keratin film (Figure 3.5a) was compared with that for a triple helix collagen film. The collagen film was newly fabricated by using the same collagen solution extracted from a fish scale (Tilapia) in our previous study (Kudo et al., 2017). The total OH + NH band areas for the collagen film during the wetting / drying processes were plotted against RH in Figure 3.6 together with that for the keratin film. The OH + NH band area for the collagen film is consistently larger by a factor of about 2 than that for the keratin film (Figure 3.6). The water adsorption capacity for the collagen film is about twice as large as that for the keratin film.

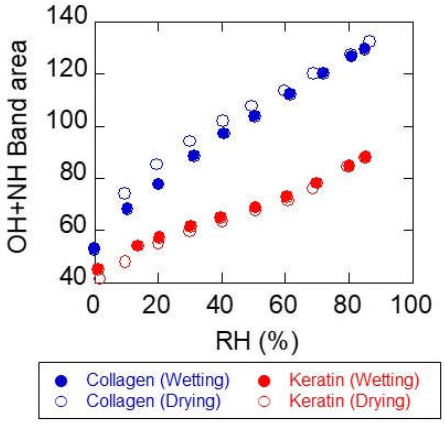

Figure 3.6. IR total OH + NH stretching band areas in the 3660 − 3010 cm^{-1} region plotted against RH of the keratin film (red) and collagen film (blue) during the wetting (filled circles) and drying (open circles) processes.

Aliphatic CH Bands

In order to examine origins of the above difference in the water adsorption capacity between the keratin and collagen, shifts of aliphatic CH bands during wetting process were analyzed. Aliphatic CH bands for the keratin and collagen films after the baseline correction to remove effects of absorption tails of OH + NH are shown in Figure 3.7.

The 2934 cm^{-1} peak due to asymmetric stretching of CH_2 and the 2874 cm^{-1} peak due to symmetric stretching of CH_3 do not show significant shifts for the keratin film (Figure 3.7a). On the other hand, the 2959 cm^{-1} peak due to asymmetric stretching of CH_3 shifts from 2959 to 2963 cm^{-1} for increasing RH for the keratin film (Table 3.2, Figure 3.7a, b).

Concerning aliphatic CH bands for the collagen film, the band shapes are quite different from those for the keratin film. Most of the peaks shift to higher wavenumber region with increasing RH (Figure 3.7c). For instance, the 2973 cm^{-1} peak due to asymmetric stretching of CH_3 shifts from 2973 to 2978 cm^{-1} for increasing RH for the collagen film (Table 3.2, Figure 3.7d). These higher wavenumber shifts of CH bands for collagen are considered to be due to interactions of water molecules on the aliphatic hydrophilic surfaces of the collagen triple helix (Kudo et al., 2017).

The differences in the CH band shape and less changes in its band shifts for the keratin film might indicate less interaction of water molecules on aliphatic side chains cropping out from the double helix of the keratin film, leading to less water retention capability.

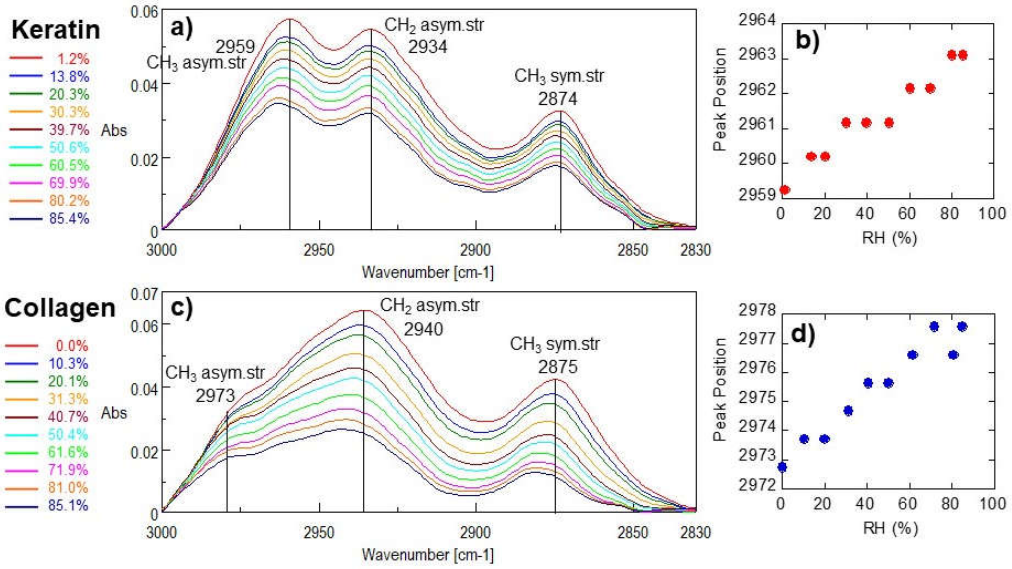

Figure 3.7. IR spectral changes of aliphatic CH region during RH increase (wetting) for the (a) keratin and (b) collagen films. Changes with RH in peak positions of asymmetric stretching of CH_3 for the (c) keratin (2959 cm^{-1}) and (d) collagen (2973 cm^{-1}) films.

Table 3.2. Changes with relative humidity (RH: %) in band areas of Gaussian components of OH + NH (4 components) and amide I (3 components) bands for the keratin and collagen films.

		Band area (OH+NH)				Band area (Amide I)			Peak position
	RH (%)	3405 cm^{-1} Free water	3300 cm^{-1} Amide A	3180 cm^{-1} Bound water	3065 cm^{-1} Amide B	1651 cm^{-1} α helix	1645 cm^{-1} other	1636 cm^{-1} H_2O	2959 cm^{-1} CH_3 asym
Keratin	1.2	28.2	47.3	10.5	3.0	41.9	4.2	5.7	2959
	13.8	40.5	45.4	10.2	3.0	41.0	3.0	11.4	2960
	20.3	43.6	44.8	10.1	3.1	40.7	2.8	11.5	2960
	30.3	48.6	43.6	10.3	3.2	40.0	2.8	13.2	2961
	39.7	50.7	42.6	10.5	3.3	39.4	2.9	14.5	2961
	50.6	56.2	41.2	10.8	3.5	39.0	2.9	16.2	2961
	60.5	62.5	39.8	11.5	3.9	38.9	2.9	18.0	2962
	69.9	70.3	38.3	12.4	4.4	39.4	3.2	20.1	2962
	80.2	80.1	36.4	13.5	4.9	40.7	3.1	23.0	2963
	85.4	85.3	35.6	14.3	5.2	41.4	3.3	24.5	2963
	RH (%)	3440 cm^{-1} Free water	3330 cm^{-1} Amide A	3210 cm^{-1} Bound water	3070 cm^{-1} Amide B	1660 cm^{-1} α helix	1653 cm^{-1} other	1636 cm^{-1} H_2O	2973 cm^{-1} CH_3 asym
Collagen	0	13.7	58.4	27.1	4.1	16.2	0.5	8.4	2973
	10.3	36.4	59.5	30.7	5.6	16.8	0.8	10.6	2974
	20.1	52.8	59.5	32.9	6.0	17.7	0.9	11.9	2974
	31.3	73.7	58.6	35.5	6.5	17.5	1.0	13.5	2975
	40.7	90.6	57.4	37.2	6.9	17.6	1.0	14.2	2976
	50.4	104.6	56.4	38.8	7.2	17.8	1.1	15.5	2976
	61.6	123.0	55.2	40.4	7.1	18.5	1.4	17.1	2977
	71.9	143.4	53.2	42.4	7.1	19.8	1.6	18.9	2978
	81	163.6	49.7	43.6	6.9	21.4	2.0	21.1	2977
	85.1	172.2	47.7	44.4	7.0	22.5	2.3	22.1	2978

Amide I and II Bands

Concerning amide I and II bands for the keratin film, peak positions around 1651, 1645, 1636, 1540 and 1508 cm^{-1} do not change significantly with RH changes (Figure 3.8a). Peaks around 1660, 1653, 1636, 1557 and 1542 cm^{-1} for the collagen film do not change neither during RH changes (Figure 3.8b). However, their band shapes are quite different between keratin and collagen.

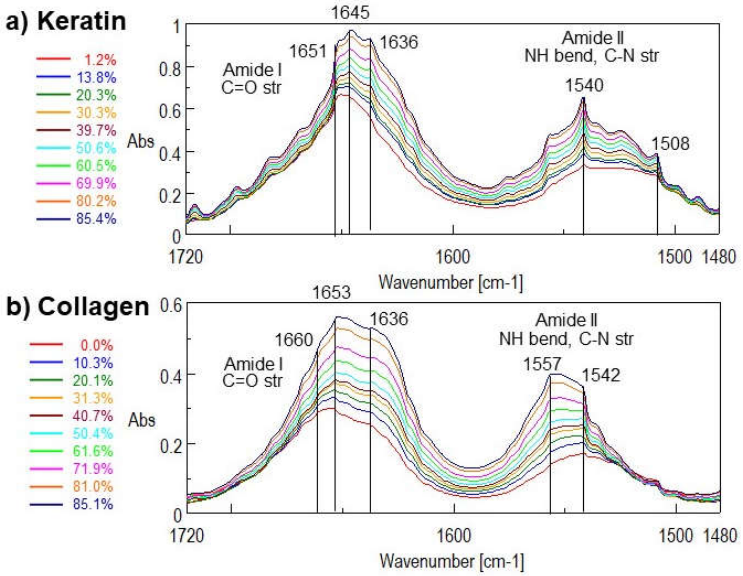

Figure 3.8. IR spectral changes with RH of amide I and II region during RH increase (wetting) of (a) the keratin film and (b) the collagen film.

In order to examine differences in the amide bands between keratin and collagen and with increasing RH, the amide I band has been analyzed by Gaussian curve fitting, since this band includes a component by bending vibration of H_2O molecules. Second derivatives of the amide I bands showed negative peaks at 1651, 1645 and 1636 cm^{-1} for the keratin film and 1660, 1653 and 1636 cm^{-1} for the collagen film. By fixing only the band centers at these positions, the amide I bands were fitted by three Gaussian components (Table 3.2). Representative fitting results at the driest conditions are shown for the keratin film (at RH = 1.2 %) (Figure 3.9a) and the collagen film (at RH = 0.0 %) (Figure 3.9b). The 1636 cm^{-1} components in both of the films are considered to be due to bending band of H_2O molecules.

The larger higher wavenumber components at 1651 and 1660 cm^{-1}, respectively, for the keratin and collagen films might be attributed to α helix components, while the smaller lower wavenumber components at 1645 and 1653 cm^{-1}, respectively, for the keratin and collagen films to other components (Figure 3.9a, b), because α helix forms are the major in these double and triple helix materials.

The band areas of these three Gaussian components of the amide I band were plotted against RH (Figure 3.9c, d). The 1636 cm^{-1} components due to H_2O molecules show S-shape increases with RH in agreement with the OH + NH band increases in Figure 3.6. The lower wavenumber "other" components remain small both for the keratin and collagen films. While the higher wavenumber "α helix" component of the keratin film remain mostly unchanged, that for the collagen film show an S-shape increase with RH in association with an increase in H_2O component (Figure 3.9c, d).

Proportions of the 1636 cm^{-1} components due to H_2O molecules increasing in S-shape with RH are larger for the collagen film than those for the keratin film, in agreement with the larger water retention capacity of the collagen film in Figure 3.6. Increases in the "α helix" component with RH for the collagen film might be due to stabilization of triple helix by water participation in hydrogen bond networks (Boryskina et al., 2007).

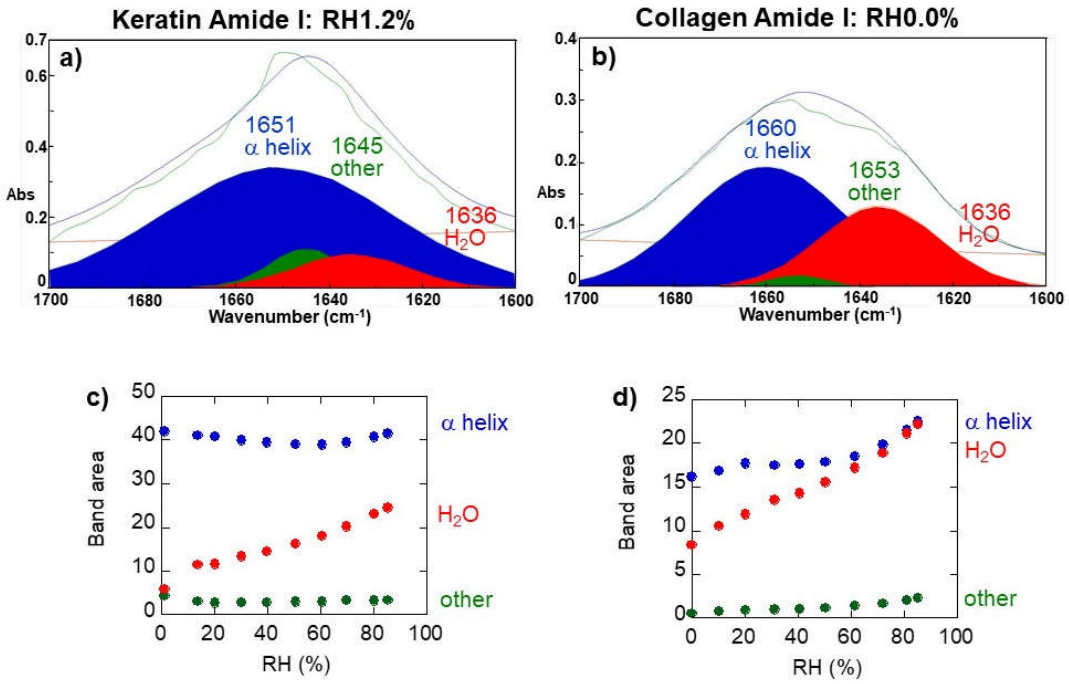

Figure 3.9. Representative fitting results of the amide I band by three Gaussian components for (a) the keratin film (at RH = 1.2 %) and (b) the collagen film (at RH = 0.0 %). Changes with RH of band areas of three Gaussian components during wetting process of (c) the keratin film and (d) the collagen film. 1651 or 1660 cm^{-1} component (α helix: blue), 1645 or 1653 cm^{-1} component (other: green), 1636 cm^{-1} component (H_2O: red).

OH + NH Bands

The OH + NH bands in the 3700 − 3010 cm^{-1} region were also analyzed by Gaussian curve fitting (Table 3.2). The band center positions were determined by trial and error for obtaining better fitting results. Band centers were fixed at 3405, 3300, 3180 and 3065 cm^{-1} for the keratin film and at 3440, 3330, 3210,and 3070 cm^{-1} for the collagen film. Band widths for 3300, 3180 and 3065 cm^{-1} components for the keratin film and those for 3330, 3210 and 3070 cm^{-1} components for the collagen film were also fixed. Representative fitting results for the driest conditions for the keratin film (at RH = 1.2 %) and for the collagen film (at RH = 0.0 %) are shown in Figure 3.10a, b. The 3300 and 3330 cm^{-1} components and the 3065 and 3070 cm^{-1} components are considered to be due to NH stretching vibrations of amide A and

amide B, respectively. While amide B components remain mostly unchanged, amide A components decrease for higher RHs (Figure 3.10c, d). The 3405 and 3440 cm^{-1} components and the 3180 and 3210 cm^{-1} components are considered to be due to OH stretching vibrations of longer and shorter hydrogen bonds, respectively. We will call these as “free water” and “bound water,” respectively. The free water component increases with RH with S-shape by keeping the bound water component minor for the keratin film (Figure 3.10c). On the other hand, for the collagen film, the bound water component is larger than the free water one at the lowest RH. The free water increases greatly with RH at higher RHs for the collagen film. The bound water also shows a slight increase with RH for the collagen film. (Figure 3.10d).

These results suggest that the collagen film has more bound water interacting with possibly polar functional groups than the keratin film. However, about twice of water retention capacity of the collagen film than the keratin film can be due to increasing adsorption of free water with weak hydrogen bonding. At least part of these free water molecules might interact with hydrophobic aliphatic CH surfaces of triple helices of the collagen film.

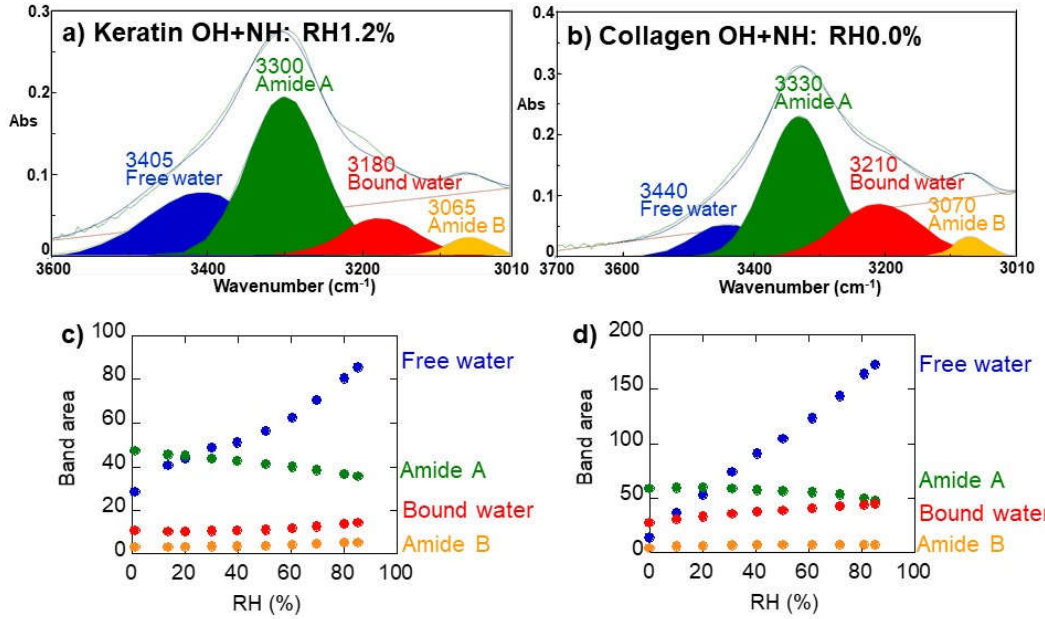

Figure 3.10. Representative fitting results of the OH + NH stretching bands by four Gaussian components for (a) the keratin film (at RH = 1.2 %) and (b) the collagen film (at RH = 0.0 %). Changes with RH of band areas of four Gaussian components during wetting process of (c) the keratin film and (d) the collagen film. 3405 or 3440 cm^{-1} component (free water: blue), 3300 or 3330 cm^{-1} component (amide A: green), 3180 or 3210 cm^{-1} component (bound water: red), and 3065 or 3070 cm^{-1} component (amide B: orange)

3.5.4. Implications

The present results suggest relatively low water contents from 7 to 19 wt% of outermost SC layers of human skin composed mostly of keratin exposed to ambient RH conditions (30 % − 85 %). However, in order to apply these results to real human skins, the following future works are needed.

First, the calibration curve obtained for the keratin film between water contents by QCM and OH + NH band areas by IR spectra can be used to determine water contents of the outermost layers (about 1 μm thick) of stratum corneum (SC) of human skins by using attenuated total reflection infrared (ATR-IR) spectroscopy in our next paper. This is because water contents at the SC surface cannot be determined by other methods.

Secondly, as is indicated by some hydration experiments of human skins measured by confocal Raman microscopy, water contents at the SC surface increase by keeping the constant deeper water contents (Egawa et al., 2007). Moreover, water contents at the SC surface are considered to affect skin health (Tanaka et al., 1998; Edwards and Marks, 2005; Serup, 2005) and diffusion of chemical components including water itself (Li et al., 2016). Therefore, transport properties of SC should be evaluated in relation to the surface water contents.

Thirdly, since the triple helix collagen is found to retain about twice as much water as keratin (double helix), which is the main component of human SC, the triple helix collagen can be used as an effective moisturizing agent. We will report in our future paper effects of adding the triple helix collagen solution to human SC.

3.6. Conclusion

In order to evaluate water contents of human skin surface exposed to ambient RH conditions, water molecules adsorbed on a keratin film were studied by IR microspectroscopy combined with a quartz crystal microbalance (QCM) together with a relative humidity (RH) control system.

1. Increased weights divided by the weight of dried keratin film (7.9 μg at RH = 3.0 %) increased with RH up to about 19 wt% with an S-shape, suggesting multi-layer adsorption.
2. The OH + NH band areas (3660 − 3010 cm^{-1}) in IR spectra of the keratin film correlates linearly with the increased weights, indicating water adsorption.
3. The OH + NH band areas for the collagen film are about twice as large as those for the keratin film, indicating larger water retention capacity of collagen.
4. Aliphatic CH band shapes are quite different for the collagen and keratin films. CH bands for the collagen film show systematic peak shifts, suggesting interaction of water molecules with hydrophobic CH surfaces of collagen triple helices.
5. Gaussian curve fitting of the amide I bands by three components show that the 1636 cm^{-1} components due to H_2O molecules show S-shape increases with RH in agreement with the OH + NH band increases. The lower wavenumber “other” components remain small both for

the keratin and collagen films. While the higher wavenumber "α helix" component of the keratin film remain mostly unchanged, that for the collagen film show an S-shape increase with RH in association with increase of H_2O component.

6. Gaussian curve fitting of the OH + NH bands in the 3700 − 3010 cm^{-1} region show that while amide B components (3065 or 3070 cm^{-1}) remain mostly unchanged, amide A components (3300 or 3330 cm^{-1}) decrease at higher RHs both for the keratin and collagen films.

7. The free water component (3405 cm^{-1}) with longer H bonds increases with RH with S-shape by keeping the bound water component (3180 cm^{-1}) with shorter H bonds minor for the keratin film. On the other hand, for the collagen film, the bound water component (3210 cm^{-1}) is larger than the free water one (3440 cm^{-1}) at the lowest RH and the free water increases greatly with RH at higher RHs.

8. About twice of water retention capacity of the collagen film than the keratin film can be due to increasing adsorption of free water with weak hydrogen bonding. At least part of these free water molecules might interact with hydrophobic aliphatic CH surfaces of triple helices of the collagen film. Therefore, the triple helix collagen can be used as an effective moisturizing agent.

9. The calibration curve obtained for the keratin film between water contents by QCM and OH + NH band areas by IR spectra can be used to determine water contents of the outermost layers (about 1 μm thick) of stratum corneum (SC) of human skins by means of attenuated total reflection infrared (ATR-IR) spectroscopy. Effects of water contents at the human SC surface should be examined in the future in relation to skin health and transport properties.

Chapter 4. Evaluation of Water Adsorption Capacities of Various Biomaterials: Lecithin

4.1. Abstract

Soybean lecithin, one of phospholipids, was selected as a representative cellular membrane, and water molecules bound to lecithin was analyzed by using IR microspectroscopy equipped with a humidity control system. The water weight ratio increases gradually from nearly 0 wt% at RH = 4.3 % to 4.4 wt % at RH = 55.5 % and then greatly until 19.6 wt% at RH = 91.5 %. Infrared OH band area increases linearly with the water weight ratio. The 1230 cm^{-1} band due to PO_2^- and the 1735 cm^{-1} band due to C=O shift to lower wavenumbers (red shift), while the 1060 cm^{-1} band due to PO_2^- and P−O−C shift to higher wavenumber (blue shift) with increasing RH. This can be explained by increasing hydrogen bonding by water molecules to phosphates and carboxylic acids and/or esters. Band areas of 1230 and 1060 cm^{-1} bands of phosphates increase with increasing RH. Band areas of phosphates correlate positively with the band area of bound water. Bound water molecules with shorter H bonds might be bound to these phosphate groups. Band areas of aliphatic CH stretching bands decrease throughout the RH increase and are negatively correlated to the increasing adsorption of free water. Free water molecules with longer H bonds might interact loosely with aliphatic chains of the lecithin film.

4.2. Introduction

In this study, soybean lecithin, one of phospholipids, was selected as a representative cellular membrane, and water molecules bound to lecithin was analyzed by using IR microspectroscopy equipped with a humidity control system.

There are some studies on interactions between water molecules and lecithin. Pohle et al. (1997) compared the behavior of water molecules bound to lecithins and cephalins, and they suggested that lecithins took up more water than cephalins, independently of the nature of their acyl chains. Shchipunov and Shumilina (1995) studied how polar solvents such as water,

glycerol and formamide bound to the lecithin, and they indicated that polar solvents were hydrogen-bonded with the phosphate group. However, quantities of water molecules bound to the phospholipid and their sorption-desorption behaviors are not known.

In this study, adsorption behavior of water molecules on lecithin was investigated by IR microspectroscopy combined with a QCM and a humidity control system for the better understanding of water molecules bound to the phospholipid.

4.3. Materials and Methods

4.3.1. Lecithin Emulsion

Soybean lecithin "DAIGO" (Wako Chemical Industries Co., Japan) is a drug product composed of 95 − 98 % phospholipid. The soybean lecithin used in this study is composed of phosphatidyl choline (PC), phosphatidyl serine (PS) and inositol phospholipid, and also include unsaturated fatty acids (in particular linoleic acid) (Figure. 4.1). Lecithin emulsion (0.29 wt%) was prepared by dissolving 29 mg lecithin in 10 mL of pure water (Milli-Q, Electrical resistivity > 18.2 MΩ cm).

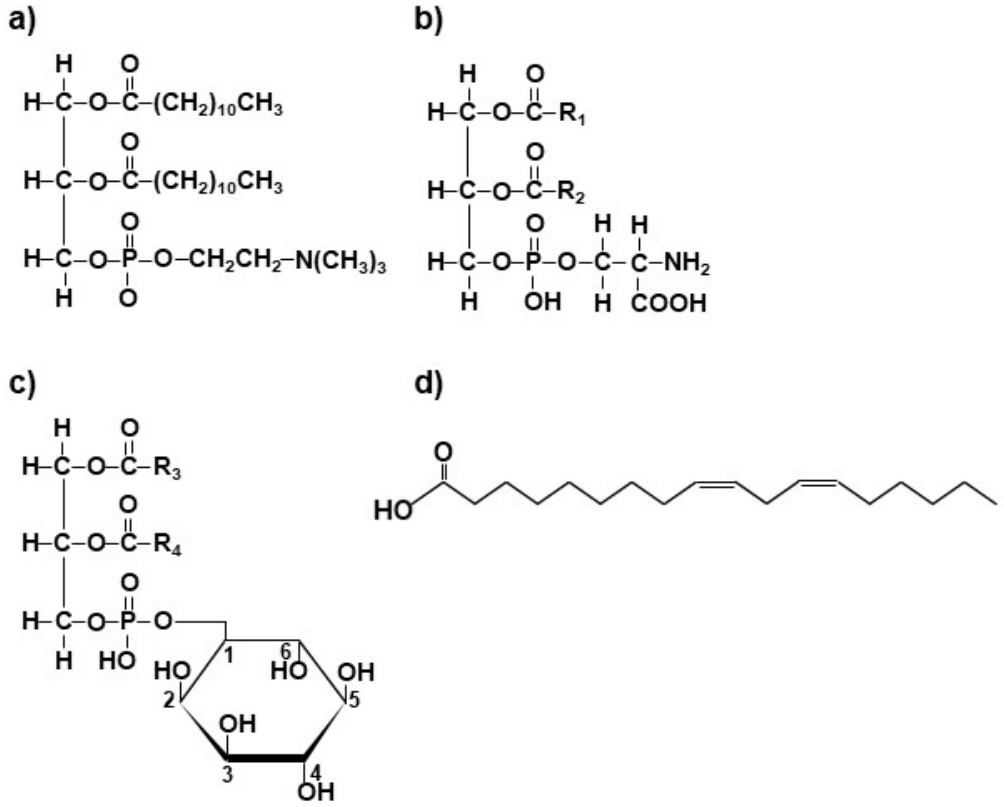

Figure 4.1. The chemical structure of (a) phosphatildyl choline, (b) phosphatidyl serine, (c) inositol phospholipid and (d) linoleic acid.

4.3.2. Relative Humidity Control System

In order to study adsorption behavior of water to lecithin, a plastic humidity control cell (36 × 36 × 14 mm) with a CaF_2 window (10 mm diameter) was fabricated (Figure 4.2). The RH of the cell interior was controlled by flowing a mixture of dry air and water-saturated air with varying proportions at a total flow rate of about 1 L min^{-1} (Figure 4.2). The water-saturated air was made by flowing air through two bottles of pure water (Milli-Q, Electrical resistivity > 18.2MΩ cm) by an air pump. The dry air was provided from a dehumidifier (Jasco, AM-12). The humidity and temperature in the cell were monitored every second by a small temperature and humidity sensor (SHT 75, SENSIRION) equipped with a data logger (SHTDL-2-L, SENSIRION) connected to a PC with a USB cable. The humidity was increased from about 4.3 % to 91.5 % by changing the flow rates of dry and humid air.

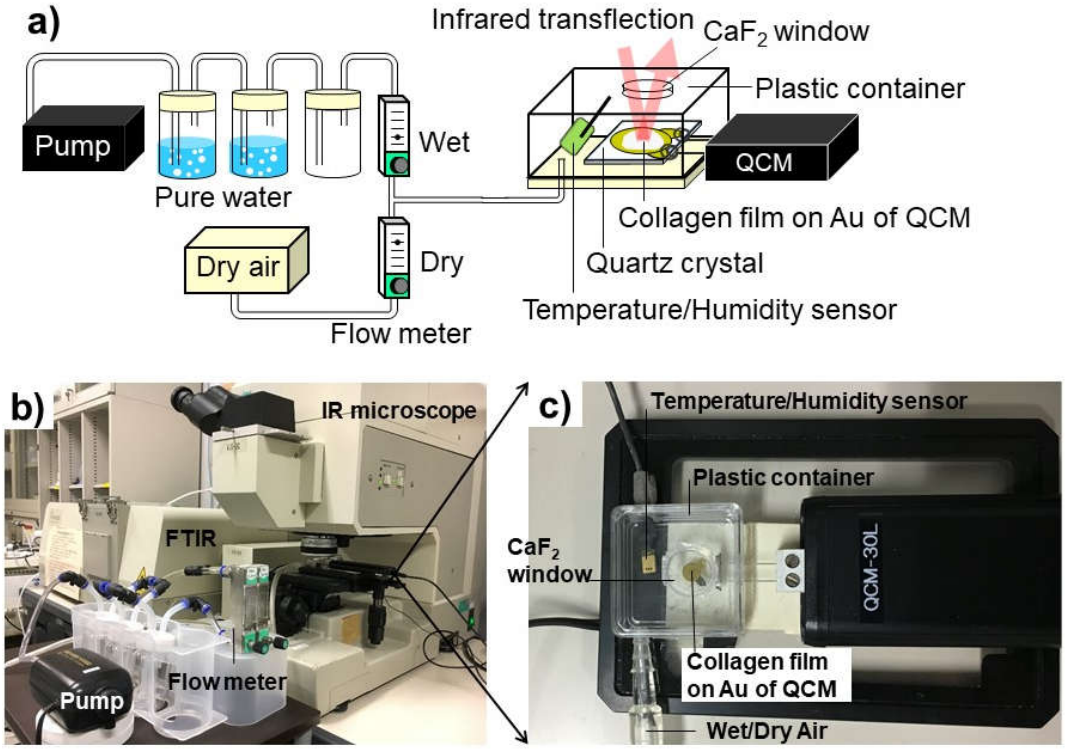

Figure 4.2. Infrared microspectroscopy combined with RH control system and QCM. (a) A schematic image of the system; b) a photograph of the whole system; (c) a close-up photograph of the RH control cell with QCM.

4.3.3. Quartz Crystal Microbalance

A QCM system (SEIKO EG&G, QCM-30L) was used in this study for measuring weights of adsorbed water on a lecithin film placed on a gold (Au) electrode coating on an AT-cut quartz of QCM sensor in a plastic container (Figure 4.2). Changes in resonant frequency of quartz from the initial value (F_0) around 9.0 MHz were monitored at every second when water was adsorbed / desorbed under various relative humidity. These frequency changes can be converted to mass changes by Sauerbrey's equation (Sauerbrey, 1959):

$$\Delta F = -\frac{2F_0^{\,2}}{\sqrt{\rho_Q \mu_Q}} \frac{\Delta m}{A} \qquad (4.1)$$

where ΔF is the change in resonance frequency (Hz), Δm is the mass change (kg), F_0 is the resonant frequency (Hz) at around 9.0MHz, ρ_Q is the density of quartz (2.65×10^3 kg m^{-3}), μ_Q is the shear modulus of quartz (2.95×10^{10} kg m^{-1} s^{-2}) and A is the surface area of the electrode (1.96×10^{-5} m^2) (Lucklum et al., 1997).

4.3.4. Preparation of Lecithin Film

One drop (less than 2 μL) of the 0.29 % lecithin suspension was placed by a micropipette on the Au electrode coating on an AT-cut quartz of the QCM in a plastic container (Figure 4.2). Dried air was flowed in the plastic container with a flow rate of more than 1 L min^{-1} for about 20 min until the stable weight monitored by QCM. The obtained transparent lecithin film had a weight of 12.8 μg (at RH = 4.9 %).

4.3.5. Infrared Microspectroscopy

In order to evaluate nature of adsorbed water on the lecithin film, IR transflection (transmission-reflection) spectra of the lecithin film on the Au electrode on QCM quartz crystal were measured under different RH (4.3 − 91.5 %). The lecithin film on the QCM in the plastic cell with a CaF_2 window was placed under a Fourier transform IR spectroscopy

(FT-IR) microscope (Jasco IRT30+FTIR620: a Cassegrain objective mirror with a magnification of 16, MCT detector, ceramic IR source, and KBr beam splitter) (Figure 4.2). The environment outside the RH cell was the ambient experimental room with normal air conditioning with the temperature around 20 ^{o}C and RH of about 30 % (Figure 4.2). No evacuation or gas purging was conducted on the IR microscope.

A background reflection spectrum was measured on the Au-coated quartz crystal without any sample using an aperture size of 625 × 625 μm^2 and then a sample transflection spectrum was measured on the lecithin film with the same aperture. All the spectra were obtained by accumulating 64 scans at a wavenumber resolution of 4 cm^{-1}. The transflection method has been reported to be used quantitatively in IR microspectroscopy (Alipour et al., 2016).

4.4. Results

4.4.1. Temperature and Relative Humidity Changes

Temperature in the cell during water adsorption experiments on the lecithin film was mostly kept constant at 22.0 ± 2 °C during the increase in relative humidity (RH) from 4.3 to 91.5 % (Table 4.1, Figure 4.3a). The RH value became relatively stable within 5 min with some small fluctuations at each humidity value with errors of less than 0.2 % (Table 4.1). After keeping the same RH values for 20 − 30 min for obtaining stable RH values, the RH values were increased (Figure 4.3a). Concerning RH values around 60 %, the humidity / temperature sensor stopped working. Therefore, the RH and temperature values before and after this interruption were averaged to obtain RH value of 61.4 % and temperature value of 24.0 ^{o}C (Table 4.1).

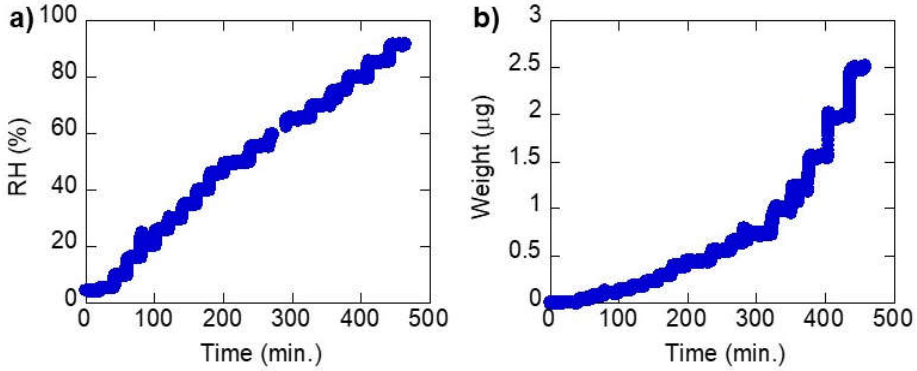

Figure 4.3. Changes in (a) relative humidity (RH: %) and (b) weights (μg) of the lecithin film during wetting.

Table 4.1 Time, temperature, relative humidity (RH), frequency shift (ΔF), mass changes (Δm), water contents (μg / μg) and total OH band area during wetting process of a lecithin film.

Time (min)	Temp (°C)	Max error	RH (%)	Max error	ΔF (Hz)	Max error	Δm (mg)	Max error	Weight ratio (H_2O) (μg / μg)	Total OH Band area
18	20.4	0.02	4.3	0.04	-1	0.53	0.00	0.0006	0.000	13.94
38	21.1	0.02	5.3	0.04	-7	0.68	0.01	0.0007	0.001	13.71
58	21.6	0.02	9.6	0.04	-34	0.67	0.04	0.0007	0.003	14.43
78	21.8	0.04	16.0	0.10	-73	0.65	0.08	0.0007	0.006	14.91
98	22.3	0.03	20.6	0.08	-101	1.05	0.11	0.0011	0.009	15.04
118	22.6	0.01	25.9	0.14	-136	1.92	0.15	0.0021	0.012	15.13
138	23.0	0.03	30.0	0.15	-167	1.90	0.18	0.0021	0.014	15.37
158	23.4	0.02	34.9	0.16	-214	2.88	0.23	0.0031	0.018	16.04
178	23.6	0.02	40.2	0.21	-360	5.57	0.39	0.0061	0.031	17.48
198	23.7	0.02	45.9	0.19	-358	5.27	0.39	0.0057	0.031	18.81
235	23.9	0.03	49.9	0.20	-413	6.58	0.45	0.0072	0.035	20.03
263	24.1	0.03	55.5	0.16	-516	8.08	0.56	0.0088	0.044	21.96
288	24.0	0.05	61.4	1.60	-692	10.00	0.75	0.0109	0.059	25.44
323	24.0	0.04	65.4	0.19	-678	9.58	0.74	0.0104	0.058	25.84
353	23.8	0.02	70.0	0.12	-918	11.15	1.00	0.0121	0.078	28.06
378	23.8	0.02	75.2	0.12	-1111	14.62	1.21	0.0159	0.095	30.61
408	23.8	0.03	79.5	0.09	-1431	8.15	1.56	0.0089	0.122	34.89
438	23.7	0.04	85.4	0.09	-1826	2.85	1.98	0.0031	0.156	41.77
463	23.5	0.03	91.5	0.09	-2293	8.65	2.49	0.0094	0.196	52.16

4.4.2. Changes in Weights by Quartz Crystal Microbalance (QCM)

Frequency shifts of QCM were converted to weight changes by Sauerbrey's equation (4.1) in the water adsorption on the lecithin film (Table 4.1). Weight changes with RH on the sample-free QCM sensor, due possibly to trace amount of water adsorbed on the QCM sensor, were less than 9 ng. The maximum weight increase of the lecithin film was 2493 ng and the error can be less than 0.4 %. However, for the minimum weight increase at RH = 9.6 % of 37.3 ng, the error can be as large as 24 %. Although QCM measurements have small errors due to their frequency changes at the same RH values (Table 4.1), water adsorption to QCM sensor might contribute to larger errors of water adsorption to the lecithin film.

Weights (μg) of the lecithin film increased with RH increase (Figure 4.3b). However, weights once decreased slightly when RH was increased. The origin of these slight weight decreases is unknown. Despite these errors, the weight changes are considered to be mainly by water adsorption to the lecithin film. These water weights were divided by the weight of dried lecithin film (12.8 μg at RH = 4.9 %) and plotted against RH values (Table 4.1, Figure 4.4). The water weight ratio increases gradually from nearly 0 wt% at RH = 4.3 % to 4.4 wt% at RH = 55.5 % and then greatly until 19.6 wt% at RH = 91.5 %.

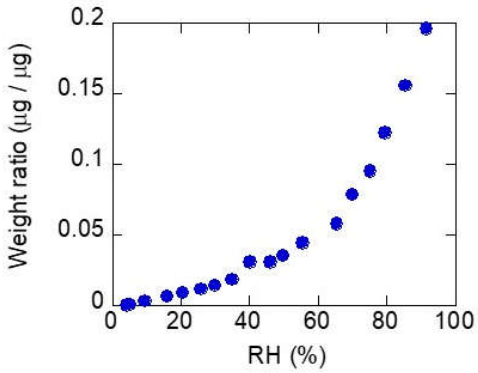

Figure 4.4. Weight ratio of water to dry lecithin film (μg / μg) plotted against RH, during wetting.

4.4.3. IR Spectral Changes with RH

IR spectral changes with RH of the lecithin film at 22 °C showed similar changes for wetting processes for duplicate runs. Therefore, only a representative series of spectral changes with absorbance values between 0 and 1 for wetting process will be presented here (Figure 4.5). These are raw transflection spectra (64 scans) of the lecithin film in absorbance without any baseline correction or smoothing at each RH value after the weight stabilization by QCM. Since RH (%) and temperature (T in °C) were monitored every 1 second, we averaged RH and T for 60 seconds corresponding to the IR spectrum.

All the IR spectra during the water adsorption processes show a broad band from 3600 to 3000 cm^{-1} (Figure 4.5). This broad band in the 3600 − 3000 cm^{-1} region is due to OH stretching bands (Masuda et al., 2003; Siebert and Hildebrandt, 2008; Kataoka et al., 2011; Fabian and Naumann, 2012) with a peak around 3410 cm^{-1} and a shoulder at 3240 cm^{-1}.

The 2925 and 2850 cm^{-1} bands are due to asymmetric and symmetric CH_2 stretching, respectively (Tantipolphan et al., 2007; Kuligowski et al., 2008; Staroszczyk et al., 2012). The 1465 and 1380 cm^{-1} bands are due to CH_2 scissoring and CH_3 symmetric bending, respectively (Garidel et al., 2010).

The 1735 cm^{-1} band is due to C=O stretching of fatty acids and esters. The 1650 cm^{-1} band is assigned to the bending vibration of H_2O molecules (Masuda et al., 2003; Kataoka et al., 2011).

The peak at 1230 cm^{-1} is assigned to asymmetric PO_2^- stretching (Tantipolphan et al., 2007). The peak at 1060 cm^{-1} can be due to overlapping PO_2^- and P−O−C bands (Kuligowski et al., 2008).

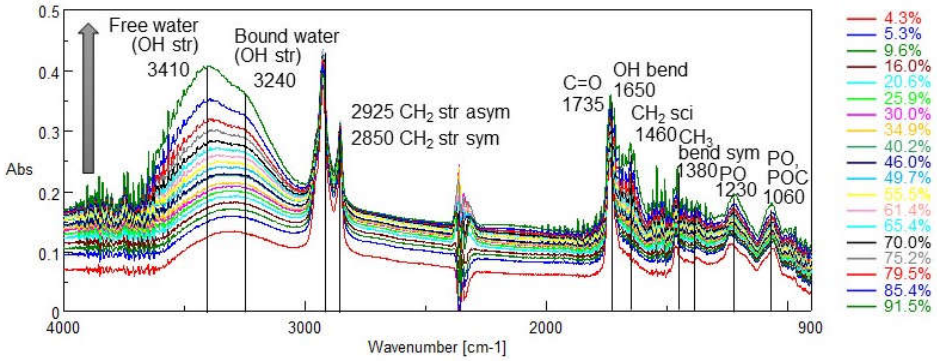

Figure 4.5. IR spectral changes with relative humidity (RH: %) of the lecithin film during wetting process (RH = 4.3 % − 91.5 %, about 5 % intervals.). IR peak positions and their assignments are indicated.

4.4.4. Changes in the Total OH Band Area with RH

The OH stretching band areas were determined with a linear baseline from 3600 to 3040 cm^{-1} for the lecithin film during the wetting processes and were plotted against RH in Figure 4.6a (Table 4.2). The OH stretching band of the lecithin film increased with increasing humidity.

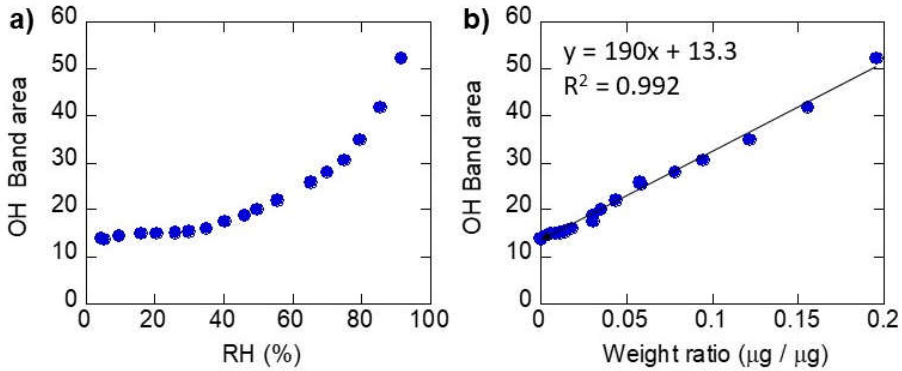

Figure 4.6. IR total OH stretching band area in the 3600 − 3040 cm^{-1} region plotted against (a) RH, (b) weight ratio (μg / μg) by QCM of the lecithin film during the wetting process.

Table 4.2 Band areas of free water, bound water, CH, PO_2^-, P−O−C and peak positions of C=O, PO_2^- and P−O−C bands during wetting process of a lecithin film.

	Band area					Peak position		
RH (%)	3410 cm^{-1} Free water	3240 cm^{-1} Bound water	3000-2830 cm^{-1} CH	1255-1160 cm^{-1} PO	1125-1045 cm^{-1} P-O-C	1735 cm^{-1} C=O	1230 cm^{-1} P-O	1060 cm^{-1} P-O-C
4.3	11.22	21.38	16.0307	0.9300	0.6921	1737	1232	1058
5.3	11.76	20.81	16.0287	0.9182	0.6809	1736	1231	1058
9.6	13.16	21.00	16.0034	0.9392	0.6879	1736	1232	1058
16.0	14.53	21.37	15.9297	0.9633	0.7203	1736	1231	1057
20.6	15.95	20.22	15.8544	0.9829	0.6762	1736	1232	1058
25.9	17.25	20.02	15.7961	1.0166	0.6936	1736	1232	1057
30.0	18.81	19.33	15.7085	1.0106	0.7212	1735	1232	1058
34.9	20.72	20.21	15.6535	1.0264	0.7580	1735	1232	1058
40.2	25.71	22.54	15.5031	1.0806	0.7469	1735	1224	1058
45.9	26.58	22.12	15.3782	1.1105	0.7955	1735	1224	1057
49.9	28.93	23.12	15.2538	1.1190	0.7798	1735	1224	1058
55.5	33.27	24.43	15.0023	1.1651	0.8173	1735	1224	1058
61.4	35.54	24.80	14.8518	1.2186	0.8155	1735	1224	1058
65.4	40.87	27.23	14.5522	1.2813	0.9069	1735	1223	1065
70.0	45.29	29.05	14.2685	1.3409	0.9692	1735	1223	1066
75.2	51.18	31.04	13.8664	1.4143	0.9989	1734	1223	1066
79.5	58.03	36.49	13.5428	1.4919	1.0972	1734	1223	1066
85.4	70.17	43.71	12.8949	1.6414	1.1639	1734	1223	1066
91.5	89.22	56.47	11.7155	1.9244	1.3259	1734	1222	1066

4.4.5. Total OH Band Area against Adsorbed Weight by QCM

The OH band areas during the wetting process (Figure 4.6a) were plotted against the weight changes observed by QCM in Figure 4.4 (Figure 4.6b). The OH band area increases linearly with the adsorbed water ratio (correlation coefficient $R^2 = 0.992$), indicating that the OH band area increase is mainly due to water adsorption.

4.5. Discussion

4.5.1. Difference IR Spectra during the Wetting Process of Lecithin Film

In order to examine IR spectral changes during wetting processes of the lecithin film, the IR spectrum at the driest RH condition (RH = 4.3 %) was subtracted from all the spectra at larger RHs. The obtained difference spectra are shown Figure 4.7.

In the OH stretching region two bands around 3410 and 3240 cm^{-1} increase with RH. These results can be understood by increasing adsorption of water molecules with longer and shorter hydrogen bonds, respectively. The 1650 cm^{-1} band due to bending vibration of H_2O molecules increase also with RH. More detailed analyses will be discussed later.

The bands around 1230 cm^{-1} due to asymmetric PO_2^- stretching and 1060 cm^{-1} due to overlapping PO_2^- and P−O−C increase at higher RHs.

On the other hand, the 2925 and 2850 cm^{-1} bands due to asymmetric and symmetric CH_2 stretching, respectively, decreased with RH.

These results can be originated from band shifts and/or band area changes.

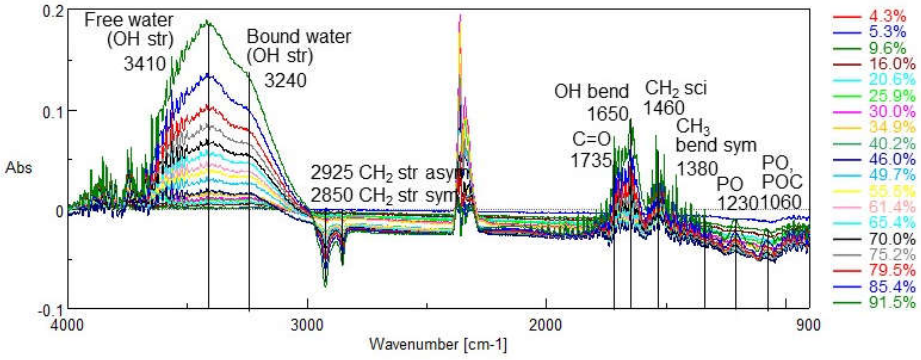

Figure 4.7. Difference spectra from the driest lecithin film spectrum (RH = 4.3 %) during wetting processes.

4.5.2. Peak Shifts of the Lecithin Film

In order to examine shifts of aliphatic CH stretching bands in the 3000 − 2830 cm^{-1} region, band changes with the baseline correction in the same region of the original IR spectra are

shown in Figure 4.8a. The second derivative spectra show 5 negative peaks at 2995, 2955, 2925, 2870 and 2850 cm^{-1} (Figure 4.8b). These are corresponding to stretching of unsaturated CH, asymmetric CH_3, asymmetric CH_2, symmetric CH_3 and symmetric CH_2, respectively. These peaks do not shift significantly with RH.

The peak positions of the 1230 cm^{-1} band due to asymmetric PO_2^- stretching and the 1060 cm^{-1} band due to PO_2^- and P−O−C were determined in the original IR spectra and plotted against RH (Figure 4.9a, b). The 1230 cm^{-1} band shifts from about 1232 to 1222 cm^{-1} with increasing RH (Figure 4.9a). On the other hand, 1060 cm^{-1} band shifts from about 1058 to 1066 cm^{-1} with increasing RH (Figure 4.9b). The lower wavenumber shift (red shift) of the 1230 cm^{-1} band and the higher wavenumber shift (blue shift) of the 1060 cm^{-1} band can be explained by increasing hydrogen bonding by water molecules to phosphates. The hydrogen bonding to P−O stretching vibration lowers the frequency, while H bonds to P−O−C bending raise the frequency (Kudo et al., 2017; Kuligowski et al., 2008).

Among analyses of peak shifts examined in this study, the peak shifts of the 1735 cm^{-1} band due to C=O stretching have been recognized (Figure 4.9c). The 1735 cm^{-1} band shifts slightly from 1736 to 1734 cm^{-1}. This slight lower wavenumber shift of C=O stretching can be explained by hydrogen bonding of water molecules to carboxylic acids and/or esters.

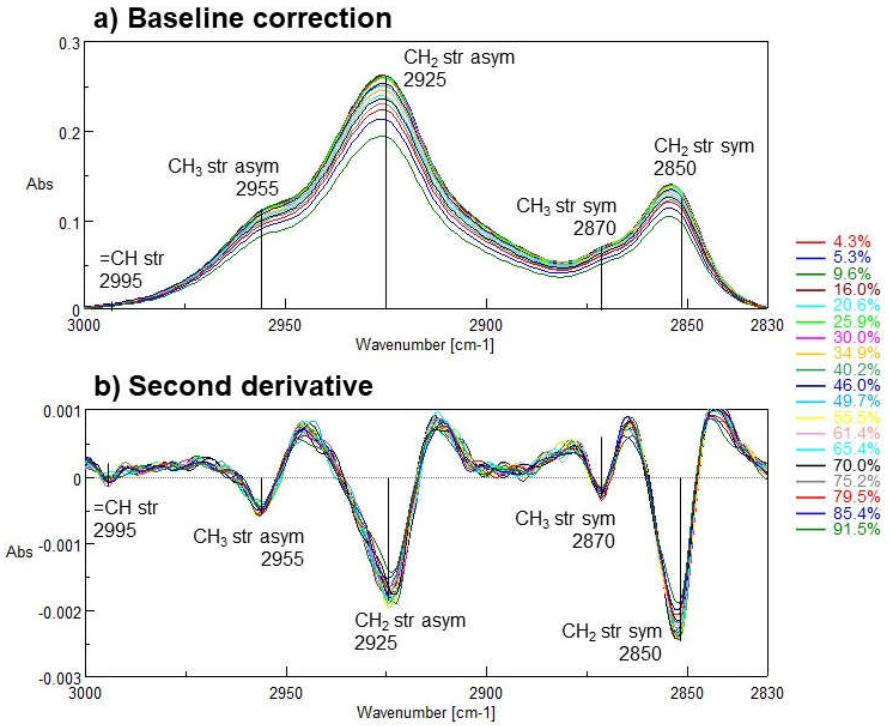

Figure 4.8. Infrared spectral changes of CH stretching region during wetting. (a) Original CH bands after baseline correction and (b) Second derivatives of the original CH bands.

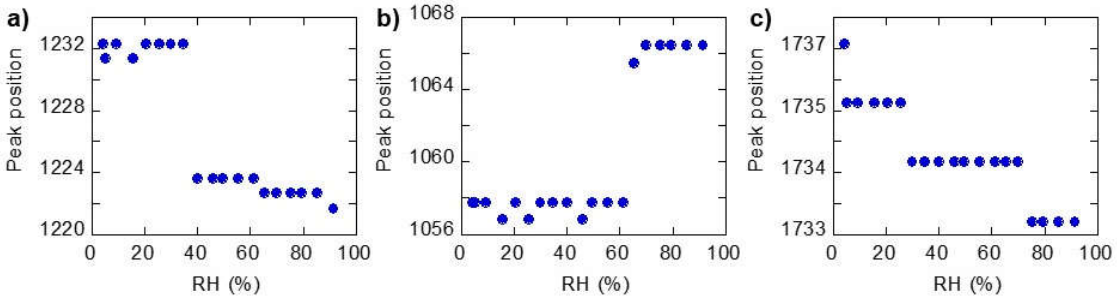

Figure 4.9. Peak positions of (a) asymmetric PO_2^- stretching (1230 cm^{-1}), (b) PO_2^- and P−O−C (1060 cm^{-1}) and (c) C=O stretching (1735 cm^{-1}) of the lecithin film.

4.5.3. Analyses of the OH Stretching Band

In the OH stretching band, two peaks around 3410 and 3240 cm^{-1} increased with RH (Figure 4.5, 4.7a). Therefore, the OH band was fitted by two Gaussian components. First, the experimental OH bands were fitted by two Gaussian components without fixing peak

positions and full width at half maximum (FWHM). Since the FWHM values were around 220 and 260 for higher and lower wavenumber components, these FWHM values were fixed. Peak positions of two components were not fixed, because hydrogen bonding to water molecules might change with increasing RH. Under these conditions with fixed FWHM, the OH bands were fitted by two Gaussian components. A representative fitting result is shown Figure 4.10a. We call the bands around 3410 and 3240 cm^{-1} as free water and bound water, respectively.

The band positions of free and bound water were plotted in Figure 4.10b. Both of them shift to lower frequency sides with increasing RH. These results can be understood by increasing hydrogen bonding among water molecules adsorbed to the lecithin film.

The band areas of free and bound water were plotted in Figure 4.10c. The band area of bound water is larger than that of free water at low RHs and remains relatively stable until RH = 60 %. The band area of bound water then increases at higher RHs. The band area of free water is small at lower RHs, but increases at medium RHs and increases greatly at high RHs.

The band area fraction of bound water decreases from about 0.66 to about 0.38, while that of free water increases from about 0.34 to about 0.62 with increasing RH (Figure 4.10d).

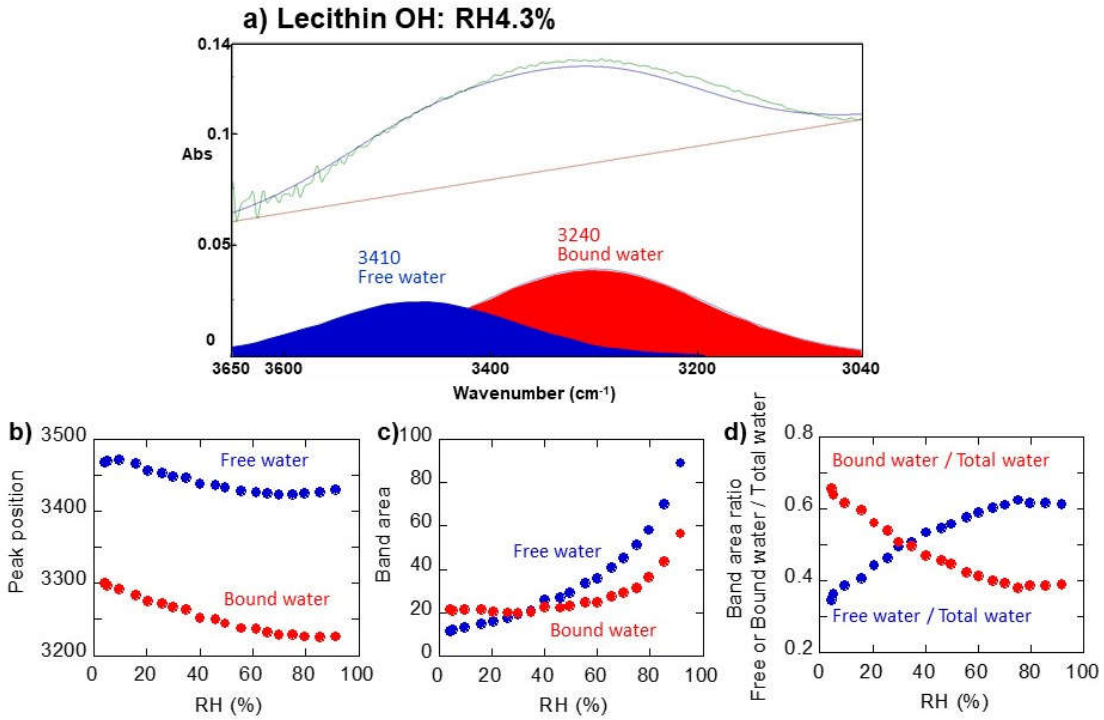

Figure 4.10. (a) Curve fitting of OH stretching band in the 3650 − 3040 cm^{-1} region by two Gaussian components: free water (3410 cm^{-1}) and bound water (3240 cm^{-1}). (b) Peak positions of free and bound water against RH. (c) Band areas of free and bound water, and (d) factions of free and bound water in the total water (3410 + 3240 cm^{-1} band areas) of the lecithin film as a function of RH.

4.5.4. Analyses of Band Areas

Band areas of 1230 cm^{-1} band due to asymmetric PO_2^- stretching (1255 − 1160 cm^{-1}) and the 1060 cm^{-1} band due to PO_2^- and P−O−C (1125 − 1045 cm^{-1}) were determined in the original IR spectra and plotted against RH (Figure 4.11a, b). They increase greatly at higher RHs. This increase appears to be similar to that of bound water (Figure 4.10c).

Band areas of aliphatic CH stretching bands (3000 − 2830 cm^{-1}) were determined in the original IR spectra and plotted against RH (Figure 4.11c). They decrease throughout the RH increase. This decrease is similar to that of free water (Figure 4.10c).

In order to examine the above correlations with bound and free water, their band areas were plotted against those of bound and free water (Figure 4.12). Band areas of 1230 and

1060 cm^{-1} bands of phosphates correlate positively with that of bound water with two different quasi-linear trends (Figure 4.12a, b). The later trends correspond to significant increases of bound water at very high RHs. Bound water molecules with shorter H bonds might be bound to these phosphate groups.

In contrast, band areas of aliphatic CHs show an excellent negative linear trend with that of free water (Figure 4.12c). Since these band area decreases have been observed for triple helix collagen in our previous study (Kudo et al., 2017), free water molecules with longer H bonds might interact loosely with aliphatic chains of the lecithin film.

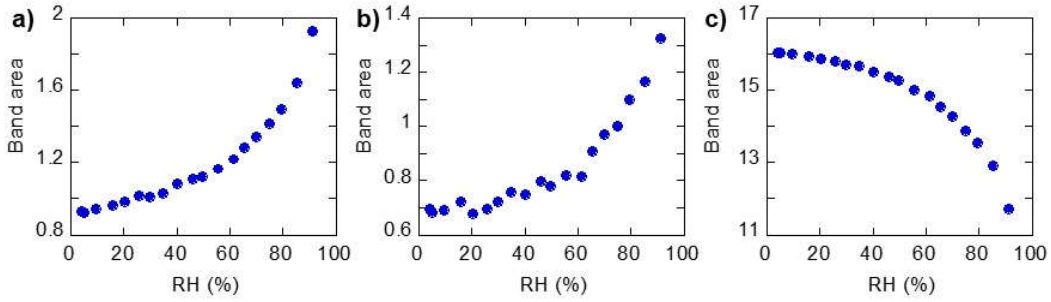

Figure 4.11. Band areas of (a) asymmetric PO_2^- stretching band (1255 − 1160 cm^{-1}), (b) PO_2^- and P−O−C band (1125 − 1045 cm^{-1}) and (c) aliphatic CH stretching bands (3000 − 2830 cm^{-1}) of the lecithin film as a function of RH.

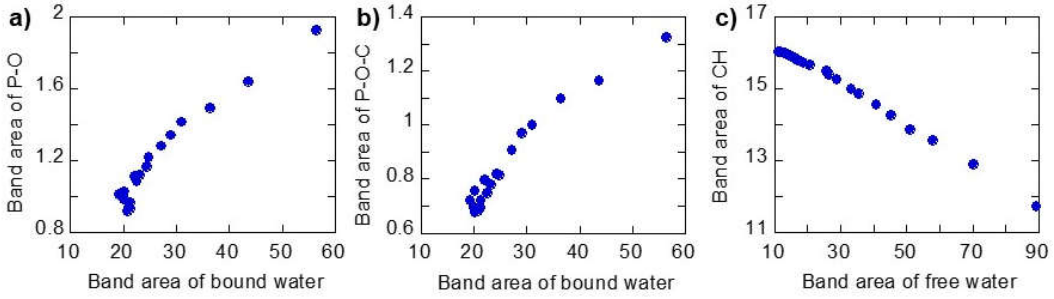

Figure 4.12. Band areas of (a) asymmetric PO_2^- stretching band (1255 − 1160 cm^{-1}) and (b) PO_2^- and P−O−C band (1125 − 1045 cm^{-1}) against band area of bound water and (c) aliphatic CH stretching bands (3000 − 2830 cm^{-1}) against band area of free water of the lecithin film.

4.5.5. Hydration Model of the Lecithin Film

Based on the above results, the following hydration model of the lecithin film can be proposed. At low RHs, bound water molecules with shorter H bonds are already bound to

polar phosphate group of lecithin. At high RHs, further bound water molecules can be adsorbed near these phosphate groups (Figure 4.10, 4.11, 4.12).

Free water molecules with longer H bonds are not abundant at low RHs (Figure 4.10c). With increasing RH, free water molecules might be bound loosely to aliphatic chains of the lecithin film. Since further free water molecular layers can be added on to the lecithin film, increasing water adsorption at high RHs is observed (Figure 4.10c).

4.6. Conclusion

In this study, soybean lecithin, one of phospholipids, was selected as a representative cellular membrane, and water molecules bound to lecithin was analyzed by using IR micro-spectroscopy equipped with a humidity control system.

1. The water weight ratio increases gradually from nearly 0 wt% at RH = 4.3 % to 4.4 wt% at RH = 55.5 % and then greatly until 19.6 wt% at RH = 91.5 %.
2. Infrared OH band area increases linearly with the water weight ratio, indicating that the OH band area increase is mainly due to water adsorption.
3. The 1230 cm^{-1} band due to asymmetric PO_2^- stretching shifts from about 1232 to 1222 cm^{-1} (red shift) with increasing RH, possibly due to water adsorption.
4. The 1060 cm^{-1} band due to PO_2^- and P−O−C shifts from about 1058 to 1066 cm^{-1} (blue shift) with increasing RH. This can be explained by increasing hydrogen bonding by water molecules to phosphates.
5. The 1735 cm^{-1} band due to C=O stretching shifts slightly from 1736 to 1734 cm^{-1} (red shift), indicating hydrogen bonding of water molecules to carboxylic acids and/or esters.
6. The band positions of free and bound water shift to lower frequency sides with increasing RH. These results can be understood by increasing hydrogen bonding among water molecules adsorbed to the lecithin film.
7. The band area of bound water is larger than that of free water at low RHs and remains relatively stable until RH = 60 %. The band area of bound water then increases at higher RHs.
8. The band area of free water is small at lower RHs, but increase at medium RHs and increase greatly at high RHs.

9. Band areas of 1230 and 1060 cm^{-1} bands of phosphates increase with increasing RH. They correlate positively with the band area of bound water. Bound water molecules with shorter H bonds might be bound to these phosphate groups.

10. Band areas of aliphatic CH stretching bands in the 3000 − 2830 cm^{-1} region decrease throughout the RH increase. This decrease is negatively correlated to the increasing adsorption of free water. Since these band area decreases have been observed for triple helix collagen in our previous study, free water molecules with longer H bonds might interact loosely with aliphatic chains of the lecithin film.

11. At low RHs, bound water molecules with shorter H bonds are already bound by polar phosphate group of lecithin. At high RHs, further bound water molecules can be adsorbed near these phosphate groups.

12. Free water molecules with longer H bonds are not abundant at low RHs. With increasing RH, free water molecules might be bound loosely to aliphatic chains of the lecithin film. Since further free water molecular layers can be added on the lecithin film, increasing water adsorption at high RHs is observed.

Chapter 5. Evaluation of Water Adsorption Capacities of Various Biomaterials: Ceramide

5.1. Abstract

Water adsorption to a representative inter−cellular lipid, ceramide, was studied by using IR micro-spectroscopy equipped with a humidity control system. The water weight ratio increases quasi−linearly from nearly 0 wt% at RH = 2.0 % to 1.2 wt% at RH = 84.8 %. The OH + NH band area increases linearly with the water weight ratio, indicating that the OH band area increase is mainly due to water adsorption. No significant peak shifts were observed for aliphatic CHs and amides. The 1045 cm^{-1} band due to C−O stretching shift from 1046 to 1042 cm^{-1} with increasing RH. The free water component increases only slightly with RH, while the bound water component increases slightly at low RHs and more from about RH = 60 %. Since the peak shift of C−O was observed at higher RHs than 60 %, bound water with shorter H bonds is considered to be adsorbed to C−O bonds. These are significantly different from lecithin with phosphate groups adsorbing bound water and aliphatic chains interacting with free water molecules.

5.2. Introduction

In Chapter 4, soybean lecithin, one of phospholipids, was selected as a representative cellular membrane, and water molecules bound to lecithin was analyzed by using IR microspectroscopy equipped with a humidity control system. Other types of lipids are present in biological systems such as inter-cellular lipids (Jung et al., 2015). For example, different types of ceramides are present in inter-cellular spaces in animal skins (Jung et al., 2015; Masukawa et al., 2008). Among them, ceramide 3 has been selected in this study. It is composed of phytosphingosine [P] unit and non-hydroxyl fatty acid [N] unit, which are bound to an amide bond (Masukawa et al., 2008). The non-hydroxyl fatty acid is generally stearic acid ($CH_3(CH_2)_{16}COOH$) which can contain a few double bonds (unsaturated parts).

The phytosphingosine unit is originally a long aliphatic chain (around C_{18}) amino alcohol having three hydroxyls (OH).

There are some studies on interactions between water molecules and ceramide (Adhikari et al., 2016). They used vibrational sum frequency generation spectroscopy and molecular dynamic simulation for studying orientation of water molecules on ceramide. Based on these, they proposed both H up and H down orientation of water molecules facing to polar C−OH head groups of ceramide. However, quantities of water molecules bound to ceramide and their sorption-desorption behaviors are not known.

In this study, adsorption behaviors of water molecules on ceramide were investigated by IR microspectroscopy combined with a QCM and a humidity control system for the better understanding of water molecules bound to ceramide.

5.3. Material and Methods

5.3.1. Ceramide

It is composed of phytosphingosine [P] unit and non-hydroxyl fatty acid [N] unit, which are bound by an amide bond, as shown in Figure 5.1 (Masukawa et al., 2008). The non-hydroxyl fatty acid is generally stearic acid ($CH_3(CH_2)_{16}COOH$) which can contain a few double bonds (unsaturated parts). The phytosphingosine unit is originally a long aliphatic chain (around C_{18}) amino alcohol having three hydroxyls (OH). Ceramide 3 powder (DS-CERAMIDE Y30) was purchased from Doosan Co. Ltd. (Korea).

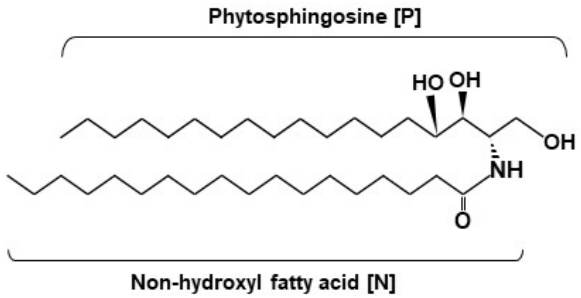

Fig. 5.1. A representative chemical structure of ceramide 3 composed of phytosphingosine [P] unit and non-hydroxyl fatty acid [N] unit bound by an amide bond.

5.3.2. Relative Humidity Control System

In order to study adsorption behavior of water to ceramide, a plastic humidity control cell (36 × 36 × 14 mm) with a CaF_2 window (20 mm diameter) was fabricated (Figure 5.2) (Kudo et al., 2017). The relative humidity (RH) of the cell interior was controlled by flowing a mixture of dry air and water-saturated air with varying proportions at a total flow rate of about 1 L min^{-1} (Figure 5.2). The dry air was provided from a dehumidifier (AM-12, JASCO, Tokyo, Japan) through a flow meter (D8500, KOFLOC, Kyoto, Japan). The water-saturated air was made by flowing the dry air from the same dehumidifier via another flow meter through two bottles of pure water (Milli-Q, Electrical resistivity > 18.2 MΩ cm). The humidity and temperature in the cell were monitored every second by a small temperature and humidity sensor (SHT 35, SENSIRION, Stafa, Switzerland) equipped with a data logger (SCHM-1, SENSIRION) connected to a PC with an USB cable. The humidity was increased from 2.0 % to 84.8 % by changing the flow rates of humid and dry air by two flow meters.

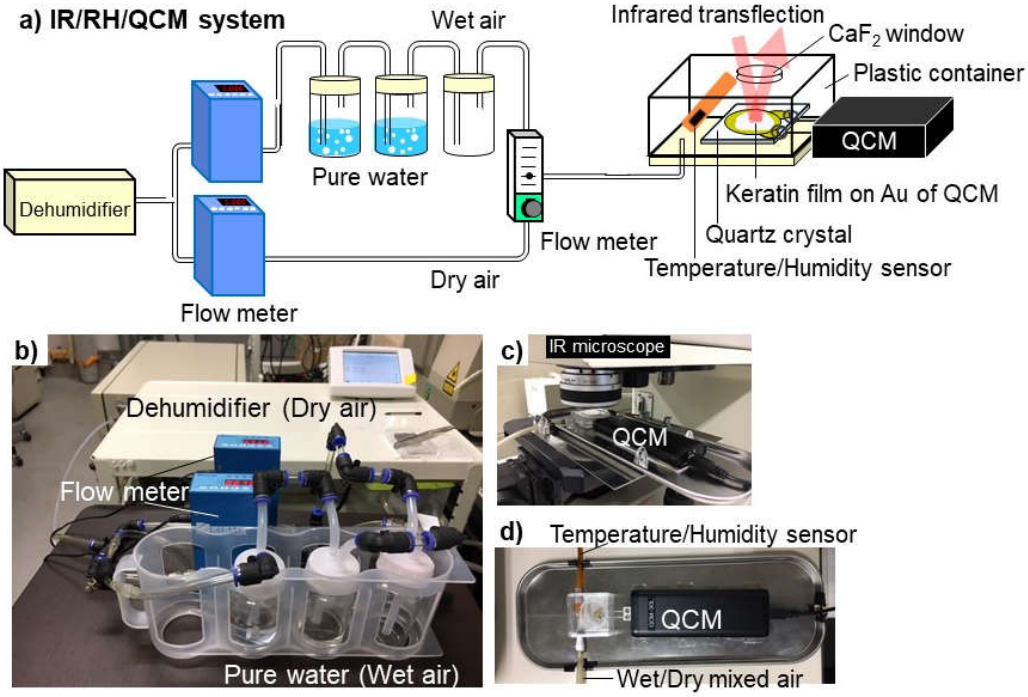

Figure 5.2. Infrared (IR) microspectroscopy combined with relative humidity (RH) control system and quartz crystal microbalance (QCM). (a) A schematic image of the system, (b) A photograph of the RH control system, (c) A photograph of the RH control cell under an IR microscope, (d) A close-up photograph of the RH control cell with QCM.

5.3.3. Quartz Crystal Microbalance (QCM)

A quartz crystal microbalance (QCM) system (QCM-30L, SEIKO EG&G, Tokyo, Japan) was used in this study for measuring weights of adsorbed water on a ceramide film placed on a gold (Au) electrode coating on an AT-cut quartz of QCM sensor in a plastic container (Figure 5.2) (Kudo et al., 2017). Changes in resonant frequency of quartz from the initial value (F_0) around 9.0 MHz were monitored at every second when water was adsorbed / desorbed under various relative humidity. These frequency changes can be converted to mass changes by Sauerbrey's equation (Sauerbrey, 1959):

$$\Delta F = -\frac{2F_0^{\,2}}{\sqrt{\rho_Q \mu_Q}} \frac{\Delta m}{A} \qquad (5.1)$$

where ΔF is the change in resonance frequency (Hz), Δm is the mass change (kg), F_0 is the resonant frequency (Hz) at around 9.0 MHz, ρ_Q is the density of quartz (2.65×10^3 kg m^{-3}), μ_Q is the shear modulus of quartz (2.95×10^{10} kg m^{-1} s^{-2}), and A is the surface area of the electrode (1.96×10^{-5} m^2) (Lucklum et al., 1997).

5.3.4. Preparation of a Ceramide Film

Ceramide 3 powder (DS-CERAMIDE Y30) was dissolved in ethanol to obtain 1 wt% ceramide solution. One drop of the 1 wt% ceramide solution in ethanol was placed by a micropipette on the Au electrode coating on the quartz crystal microbalance (QCM) in a plastic container. Dried air was flowed in the plastic container with a flow rate more than 1 L min^{-1} for about 1 minutes until the stable weight monitored by QCM. The obtained ceramide film had a weight of 10.7 μg (at RH = 2.0 %).

5.3.5. IR Microspectroscopy

In order to evaluate natures of adsorbed water on the ceramide film, infrared (IR) transflection (transmission-reflection) spectra of the ceramide film on the Au electrode on QCM quartz crystal were measured under different relative humidities (RH = 2.0 to 84.8 %).

The ceramide film on the QCM in the plastic cell with a CaF_2 window was placed under an FTIR microscope (Jasco IRT30 + FTIR620: a Cassegrainian objective mirror with a magnification of 16, MCT detector, ceramic IR source and KBr beam splitter) (Figure 5.2). The environment outside the RH cell was the ambient experimental room with normal air conditioning with the temperature around 24°C and RH of about 30 % (Figure 5.2). No evacuation or gas purging was conducted on the IR microscope.

A background reflection spectrum was measured on the Au coated quartz crystal without any sample using an aperture size of 300 × 300 μm^2 and then a sample transflection spectrum was measured on the ceramide film with the same aperture. All the spectra were obtained by accumulating 64 scans at a wavenumber resolution of 4 cm^{-1}. The transflection method was reported to be used quantitatively in IR microspectroscopy (Alipour et al., 2016).

5.4. Results

5.4.1. Temperature and Relative Humidity Changes

Temperature in the cell during water adsorption experiments on the ceramide film was mostly kept constant at 25.0 ± 0.5 °C during the increase in relative humidity (RH) from 2.0 to 84.8 (Table 5.1, Figure 5.3). The RH value became relatively stable within 10 min with some small fluctuations at each humidity value with errors of less than 0.2 % (Table 5.1). After keeping the same RH values for 20 − 90 min to obtain stable RH values, the RH values were increased (Figure 5.3a, c). Representative relative humidity (RH: %) and weights (μg) values of the ceramide film with relatively stable RH and QCM frequency were extracted from these data (Figure 5.3b, d).

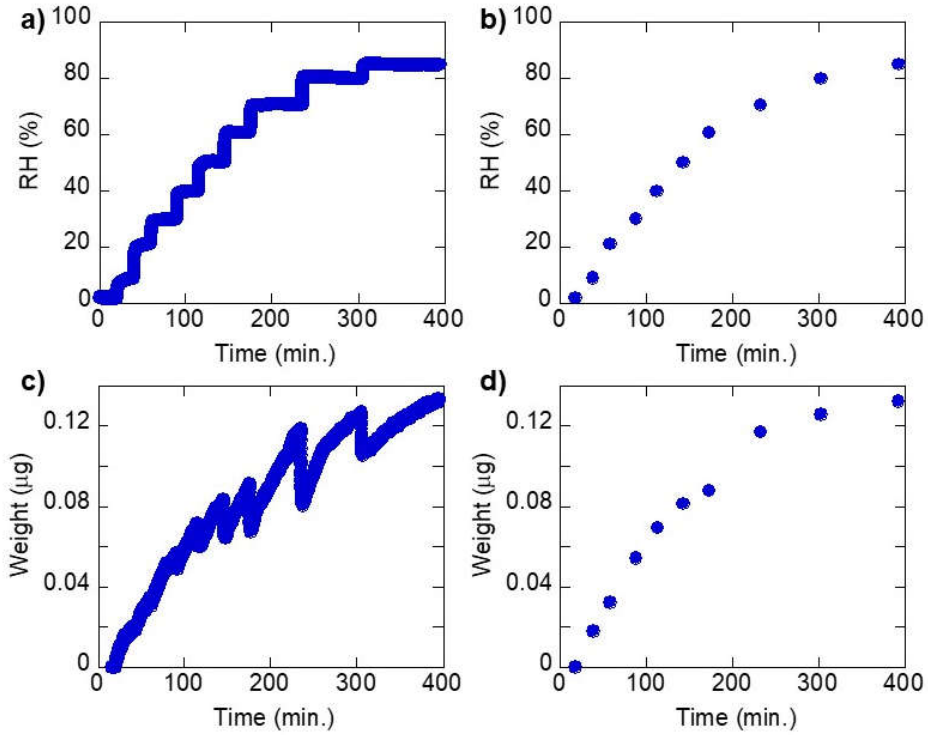

Figure 5.3. Changes with time in (a) relative humidity (RH: %) and (c) weights (μg) of the ceramide film during wetting. Representative (b) relative humidity (RH: %) and (d) weights (μg) of the ceramide film with relatively stable RH and QCM frequency.

Table 5.1. Time, temperature, relative humidity (RH), frequency shift (ΔF), mass changes (Δm), water contents (μg / μg) and total OH + NH band area during wetting process of a ceramide film.

Time (min)	Temp (°C)	Max error	RH (%)	Max error	ΔF (Hz)	Max error	Δm (μg)	Max error	Weight ratio (μg / μg)	Total OH + NH Band area
18	24.6	0.03	2.0	0.06	0	0.62	0.00	0.0000	0.000	20.17
38	24.7	0.04	9.0	0.11	-17	0.57	0.02	0.0006	0.002	20.55
58	24.8	0.02	21.1	0.1	-30	0.77	0.03	0.0008	0.003	20.73
88	24.9	0.03	30.0	0.09	-50	1.03	0.05	0.0011	0.005	21.07
113	24.9	0.03	39.9	0.07	-64	1.1	0.07	0.0012	0.007	21.33
143	24.9	0.03	50.1	0.07	-75	1.02	0.08	0.0011	0.008	21.52
173	25.0	0.03	60.5	0.07	-81	1.23	0.09	0.0013	0.008	21.64
233	24.9	0.02	70.5	0.08	-108	0.63	0.12	0.0007	0.011	22.08
303	24.9	0.03	79.8	0.07	-116	0.55	0.13	0.0006	0.012	22.44
393	25.0	0.04	84.8	0.12	-122	0.65	0.13	0.0007	0.012	22.74

5.4.2. Changes in Weights by Quartz Crystal Microbalance (QCM)

Frequency shifts of QCM were converted to weight changes by Sauerbrey's equation (5.1) in the water adsorption on the ceramide film (Table 5.1). Weight changes with RH on the sample-free QCM sensor, due possibly to trace amount of water adsorbed on the QCM sensor, are less than 9 ng. The maximum weight increase of the ceramide film was 130 ng and the error can be less than 7 %. However, for the minimum weight increase at RH = 9.0 % of 20 ng, the error can be as large as 45 %. Although QCM measurements have small errors due to their frequency changes at the same RH values (Table 5.1), water adsorption to QCM sensor might contribute to larger errors of water adsorption to the ceramide film.

Weights (μg) of the ceramide film increased with RH increase (Figure 5.3). However, weights decreased once when RH was increased. The origin of this sudden weight decreases is unknown. It should be noted that these weight changes might include relatively large errors due to background water adsorption to the QCM sensor. Despite these errors, the weight changes are considered to be mainly by water adsorption to the ceramide film. These water weights were divided by the weight of dried ceramide film (10.7 μg at RH = 2.0 %) and plotted against RH values (Table 5.1, Figure 5.4). The water weight ratio increases quasi-linearly from nearly 0 wt% at RH = 2.0 % to 1.2 wt% at RH = 84.8 %.

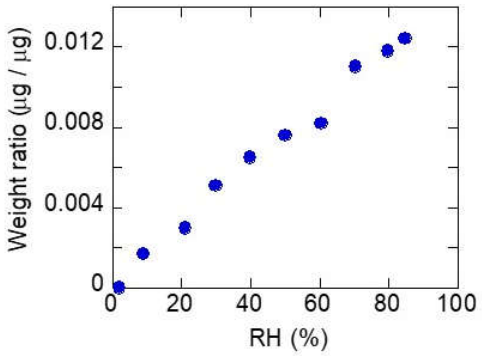

Figure 5.4. Weight ratio of water to dry ceramide film (μg / μg) plotted against RH during wetting.

5.4.3. IR Spectral Changes with RH

IR spectral changes with RH of the ceramide film at 25 °C showed similar changes for wetting processes for duplicate runs. Therefore, only a representative series of spectral changes with absorbance values between 0 and 1 for wetting process will be presented in this chapter (Figure 5.5). These are raw transflection spectra (64 scans) of the ceramide film in absorbance without any baseline correction or smoothing at each RH value after the weight stabilization by QCM. Since RH (%) and temperature (T im °C) were monitored every 1 second, we averaged RH and T for 60 seconds corresponding to the IR spectrum.

All the IR spectra during the water adsorption processes show a broad band from 3500 to 3040 cm^{-1} (Figure 5.5). This broad band in the 3500 − 3040 cm^{-1} region is due to OH + NH stretching bands (Masuda et al., 2003; Kataoka et al., 2011; Siebert and Hildebrandt, 2008; Fabian and Naumann, 2012) with a strong peak around 3300 cm^{-1} and another small peak at 3080 cm^{-1} due to N−H stretching (often called as amide A and B, respectively) (Fabian and Naumann, 2012).

The 2955 and 2872 cm^{-1} bands are due to asymmetric and symmetric CH_3 stretching, respectively (Fabian and Naumann, 2012). The 2925 and 2850 cm^{-1} band is due to asymmetric and symmetric CH_2 stretching, respectively (Staroszczyk et al., 2012). The 1465 cm^{-1} bands are due to CH_2 scissoring (Garidel et al., 2010). A small band at 3005 cm^{-1} can be attributed to CH species bound to unsaturated C=C bonds (Garidel et al., 2010).

The 1635 cm^{-1} band is due to C=O stretching of amides (H−N−C=O) (amide I). However, the bending vibration of H_2O molecules at 1635 cm^{-1} can also contribute to this band (Masuda et al., 2003; Kataoka et al., 2011). The 1540 cm^{-1} band is due to C−N−H bending and C−N stretching (amide II).

A small band around 1045 cm^{-1} is due to C−O stretching (Yoshida and Koike, 2011).

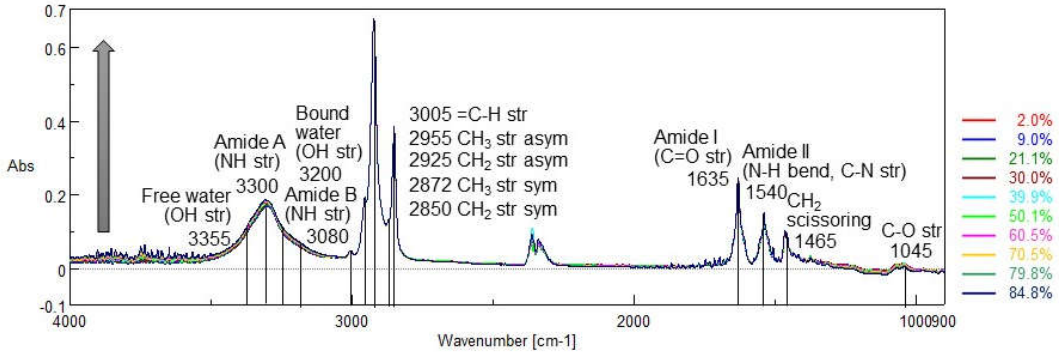

Figure 5.5. IR spectral changes with relative humidity (RH: %) of the ceramide film during wetting process (RH = 2.0 % − 84.8 %, about 10 % intervals.). IR peak positions and their assignments are indicated.

5.4.4. Changes in the Total OH + NH Band Area with RH

The OH + NH stretching band areas were determined with a linear baseline from 3470 to 3040 cm^{-1} for the ceramide film during the wetting processes and were plotted against RH in Figure 5.6a. The OH + NH stretching band areas of the ceramide film increase with increasing humidity.

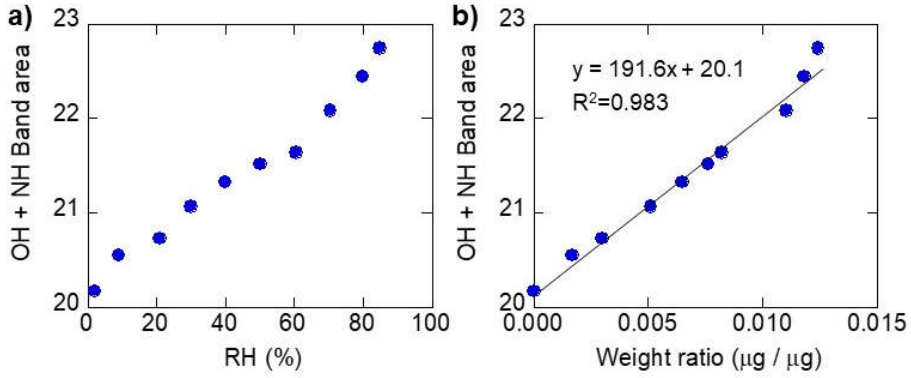

Figure 5.6. IR total OH + NH stretching band area in the 3470 − 3040 cm^{-1} region plotted against (a) RH, (b) Weight ratio (μg / μg) by QCM of the ceramide film during the wetting process.

5.4.5. Total OH + NH Band Brea against Adsorbed Weight by QCM

The OH + NH band areas during the wetting and drying process (Figure 5.6a) were plotted against the weight changes observed by QCM in Figure 5.4 (Figure 5.6b). The OH + NH band area increases linearly with the adsorbed water ratio (correlation coefficient R = 0.983), indicating that the OH + NH band area increase is mainly due to water adsorption.

5.5. Discussion

5.5.1. Water Adsorption to the Ceramide Film

As is shown by Figures 5.4 and 5.6a, both weight changes by QCM and OH + NH band areas by IR spectroscopy showed increasing trends with RH. These data corresponds to adsorption isotherms of water to the ceramide film around 25 °C. This isotherm has a steeper slope at low RH with a small S shape around RH = 50 % and do not show saturation at high RH. Since adsorption processes with S-shape isotherm are considered to be multi-layer adsorption (Atkins and Paula, 2012), multiple layers of water molecules might adsorb to the ceramide film.

5.5.2. OH + NH Band Area vs. Weight Changes by QCM

The OH + NH band area during the wetting processes plotted against the weight changes observed by QCM shows a quasi-linear relation for RH = 2.0 % − 84.8 % (Figure 5.6b). This indicates that weights gained by the ceramide film are due to water adsorption, which can be observed by changes in OH stretching band. The combined IR and QCM measurements performed here provide a quantitative calibration for evaluating adsorbed water weight by the IR band area.

5.5.3. Peak Shifts

In order to examine changes in IR bands with increasing humidity, peak shifts were first investigated. First, CH stretching bands were examined (Figure 5.7a). No significant peak shifts were observed for 2955 and 2872 cm^{-1} bands due to asymmetric and symmetric CH_3 stretching, respectively, 2925 and 2850 cm^{-1} band due to asymmetric and symmetric CH_2 stretching, respectively and the 3005 cm^{-1} band due to C=C−H. The 1465 cm^{-1} band due to CH_2 scissoring did not show recognizable shifts neither (Figure 5.7b).

Concerning amide bands, the amide I and II bands do not change significantly (Figure 5.7b). Water molecules might not be adsorbed to amides.

On the other hand, the band around 1045 cm^{-1} due to C−O stretching shifts from 1046 to 1042 cm^{-1} with increasing RH (Table 5.2, Figure 5.8). Since this lower wavenumber shift (red shift) can be explained by increasing hydrogen bonding, water molecules are supposed to adsorb to C−O bonds.

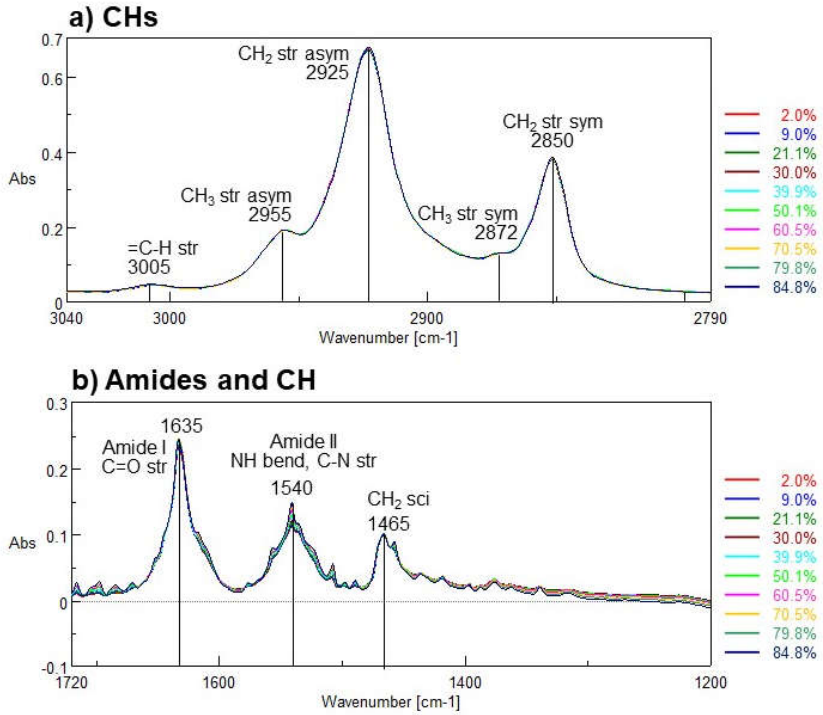

Figure 5.7. IR spectral changes of (a) aliphatic CHs and (b) amides and CH region during wetting of the ceramide.

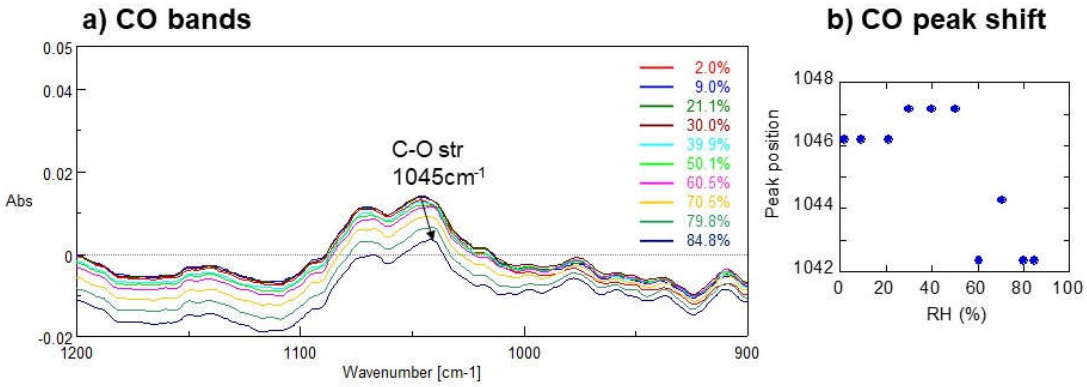

Figure 5.8. Changes in (a) IR spectra and (b) peak position of the band around 1045 cm^{-1} due to C−O stretching during wetting of the ceramide.

Table 5.2. Band areas of free water, amide A, bound water, Amide B and peak position of C−O during wetting process of a ceramide film.

	Band area				Peak position
RH (%)	3355 cm^{-1} Free water	3296 cm^{-1} Amide A	3200 cm^{-1} Bound water	3075 cm^{-1} Amide B	1045 cm^{-1} C-O
2.0	13.81	24.04	5.18	0.13	1046
9.0	14.15	24.25	5.27	0.11	1046
21.1	14.22	24.53	5.42	0.11	1046
30.0	14.46	24.63	5.62	0.07	1047
39.9	14.47	24.78	5.74	0.05	1047
50.1	14.61	24.87	5.84	0.04	1047
60.5	14.62	24.73	6.16	0.01	1042
70.5	14.62	24.70	6.54	0.00	1044
79.8	14.77	24.47	7.37	0.02	1042
84.8	14.88	24.37	7.88	0.00	1042

5.5.4. OH + NH Bands

The OH + NH bands in the 3470 − 3040 cm^{-1} region were analyzed by Gaussian curve fitting (Table 5.2). The band center positions were determined by trial and error for obtaining better fitting results. Band centers were fixed at 3355, 3296, 3200 and 3075 cm^{-1}. Their band correspond to free water, amide A, bound water and amide B, respectively. Band widths for 3296 and 3075 cm^{-1} components were also fixed. A representative fitting result for the driest conditions (at RH = 2.0 %) is shown in Figure 5.9a.

The band areas of amides A and B remain almost constant (Figure 5.9b). The free water component increases only slightly with RH. On the other hand, the bound water component increases slightly at low RHs and more from about RH = 60 % (Figure 5.9b). Since the peak shift of C−O was observed at higher RHs than 60 % (Figure 5.8b), bound water with shorter H bonds is considered to be adsorbed to C−O bonds.

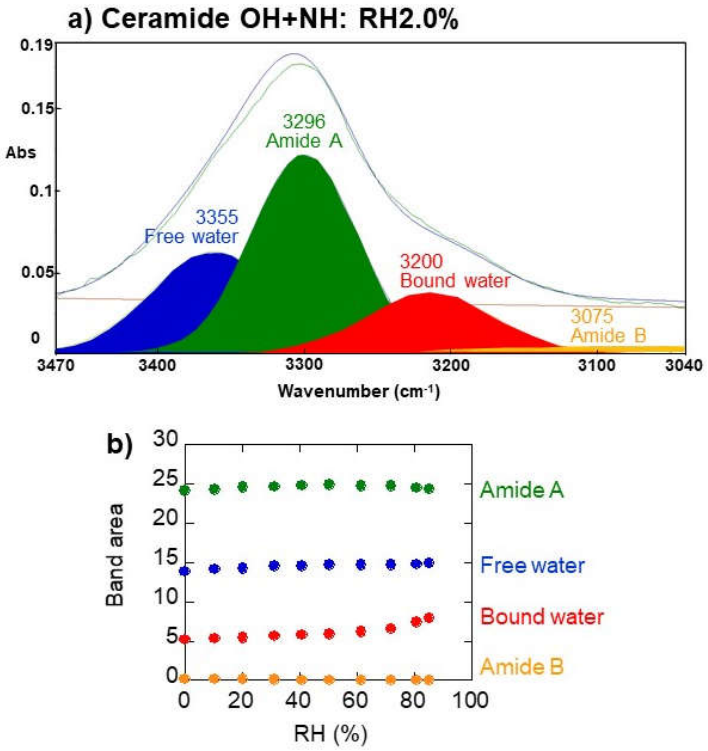

Figure 5.9. (a) Representative fitting results of the OH + NH stretching bands by four Gaussian components for ceramide (at RH = 2.0 %). (b) Changes with RH of band areas of four Gaussian components during wetting process of ceramide. 3355 cm^{-1} component (free water: blue), 3296 cm^{-1} component (amide A: green), 3200 cm^{-1} component (bound water: red), and 3075 cm^{-1} component (amide B: orange).

5.5.5. Comparison between Ceramide and Lecithin

In order to discuss adsorption mechanisms of water for ceramide, we will compare its adsorption behavior with lecithin studied previously (chapter 4).

First, water weight ratios of ceramide and lecithin were plotted against RH (Figure 5.10a). The water weight ratio increases only slightly for ceramide from nearly 0 wt% at RH = 2.0 % to 1.2 wt% at RH = 84.8 %, while it increases greatly for lecithin up to 19.6 wt% at RH = 91.5 %.

Secondly, the OH + NH band area during the wetting process for ceramide is compared with that for lecithin (Figure 5.10b). Although the OH + NH band area for ceramide is larger

than that for lecithin at low RHs, it increases only slightly with RH. This can be due to the presence of amides A and B bands in this region for ceramide.

Thirdly, the OH (+ NH) band areas were plotted against weight ratios for ceramide and lecithin (Figure 5.10c). The linear relation for ceramide is restricted to a small region, while that for lecithin extends to a wide range.

Among water molecular species, the band area of free water is always larger than that of bound water for ceramide (Figure 5.11a). While free water increases only slightly with RH, bound water increases at high RHs. On the other hand, the band area of free water is smaller than that of bound water at low RHs for lecithin (Figure 5.11b). However, free water increases greatly at high RHs.

These significant differences in water adsorption capacities between ceramide and lecithin can be related to their differences in chemical structures. Lecithin is a phospholipid having polar molecules such as phosphates (PO_2^-) and carboxylic acids and/or esters (C=O). Numerous water molecules can be adsorbed to these polar functional groups. In particular, bound water molecules with shorter H bonds might be bound to phosphate groups. Moreover, free water molecules with longer H bonds might interact loosely with aliphatic chains of the lecithin film.

Although amide bonds are present in ceramide, they do not appear to adsorb water. Only C−O bonds is considered to adsorb bound water with shorter H bonds. No interaction of water molecules with aliphatic CH chains of ceramide is noticed.

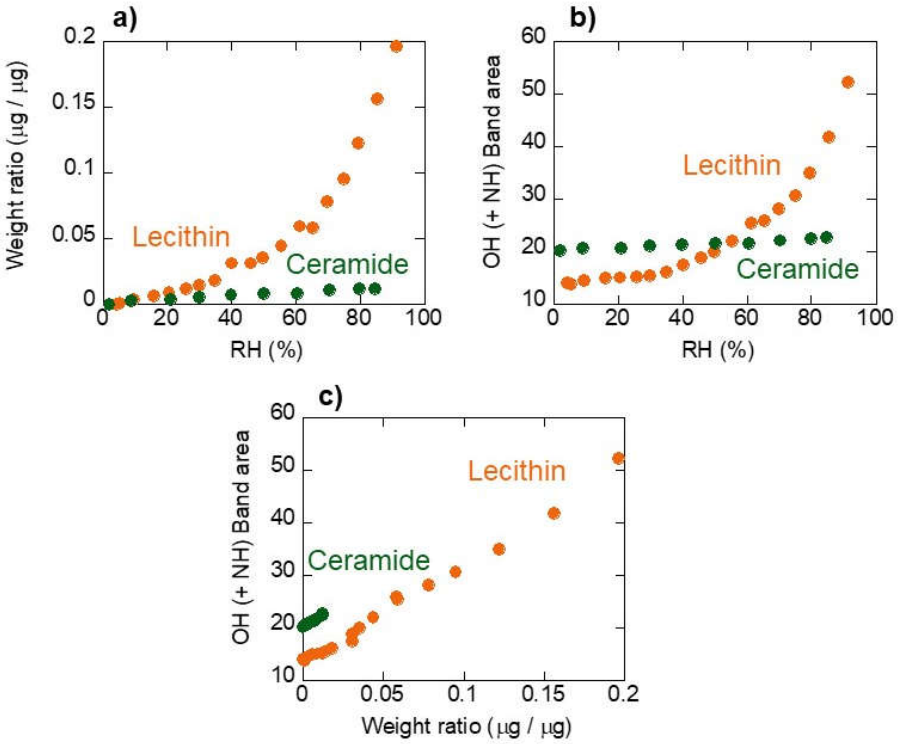

Figure 5.10. (a) Weight ratios and (b) IR OH (+ NH) band areas against RH and (c) OH (+ NH) band areas against weight ratios of ceramide (green) and lecithin (orange) during the wetting process.

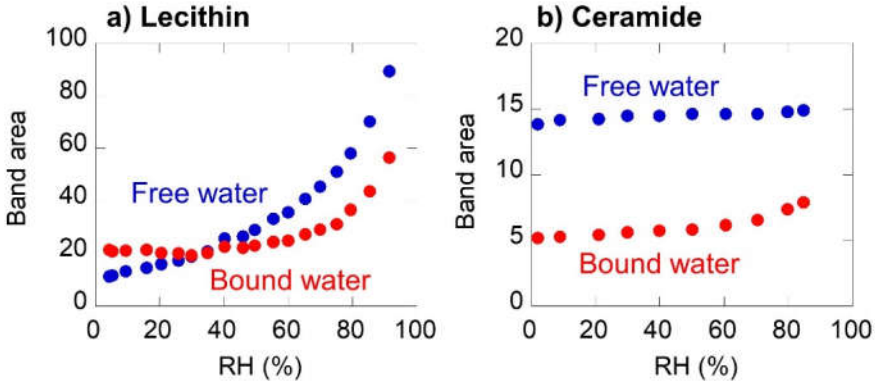

Figure 5.11. Band areas of free (blue) and bound (red) water of (a) ceramide and (b) lecithin against RH during wetting.

5.6. Conclusion

As a representative inter-cellular lipid, ceramide 3 has been selected in this study. It is composed of phytosphingosine [P] unit and non-hydroxyl fatty acid [N] unit, which are bound through an amide bond. Water adsorption to ceramide was studied by using IR microspectroscopy equipped with a humidity control system.

1. The water weight ratio increases quasi-linearly from nearly 0 wt% at RH = 2.0 % to 1.2 wt% at RH = 84.8 %.
2. The OH + NH band area increases linearly with the water weight ratio, indicating that the OH band area increase is mainly due to water adsorption.
3. No significant peak shifts were observed for 2955 (asymmetric CH_3), 2872 (symmetric CH_3), 2925 (asymmetric CH_2), 2850 (symmetric CH_2), 3005 (C=C−H) and 1465 (CH_2 scissoring) cm^{-1} bands.
4. The amide I and II bands do not change significantly. Water molecules might not be adsorbed to amides.
5. The band around 1045 cm^{-1} due to C−O stretching shifts from 1046 to 1042 cm^{-1} (red shift) with increasing RH. This can be explained by increasing hydrogen bonding by water molecules to C−O bonds.
6. The band areas of amides A and B remain almost constant. Although the free water component increases only slightly with RH, the bound water component increases slightly at low RHs and more from about RH = 60 %. Since the peak shift of C−O was observed at higher RHs than 60 %, bound water with shorter H bonds is considered to be adsorbed to C−O bonds.
7. Water weight ratio increases only slightly for ceramide to 1.2 wt% at RH = 84.8 %, while it increases greatly for lecithin up to 19.6 wt% at RH = 91.5 %.
8. While the band area of free water is always larger than that of bound water for ceramide, that of free water is smaller than that of bound water at low RHs, but becomes larger at high RHs for lecithin.
9. These significant differences in water adsorption capacities between ceramide and lecithin can be related to their differences in chemical structures.

10. Bound water molecules with shorter H bonds might be bound to phosphate groups for lecithin. Free water molecules with longer H bonds might interact loosely with aliphatic chains of the lecithin.

11. Only C−O bonds of the ceramide is considered to adsorb bound water with shorter H bonds. No interaction of water molecules with aliphatic CH chains of ceramide is noticed.

Chapter 6. Summary and General Discussion

6.1. Introduction

In this study, we have developed a new measurement system where IR microspectroscopy and QCM measurement can be conducted at the same time on the same sample for studying water adsorption / desorption with a humidity control system. The amount of water adsorbed was quantified by QCM and infrared band shifts and band area changes was analyzed for four biomaterials. The summaries of each chapter will be first given below and the overall discussion will be presented later.

6.2. Development of Evaluation Methods for Water Adsorption to Biomaterials

In this study, we have developed a new measurement system where IR microspectroscopy and quartz crystal microbalance (QCM) measurement can be conducted at the same time on the same sample for studying water adsorption / desorption. We made also an original relative humidity (RH) control system (Figure 6.2.1). The RH of a plastic humidity control cell (36 × 36 × 14 mm) with a CaF_2 window (10 mm diameter) was controlled by flowing a mixture of dry air and water-saturated air with varying proportions at a total flow rate of about 1 L min^{-1}. The humidity and temperature in the cell was monitored every second by a small temperature and humidity sensor equipped with a data logger connected to a PC with a USB cable.

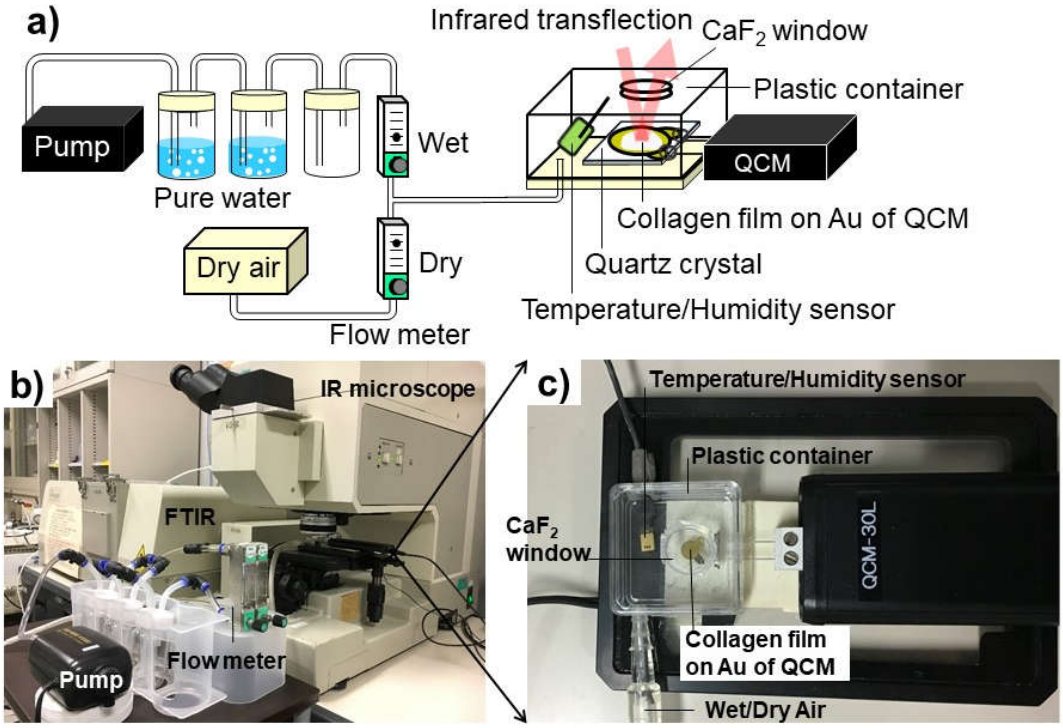

Figure 6.2.1. Infrared microspectroscopy combined with RH control system and QCM. (a) A schematic image of the system; b) a photograph of the whole system; (c) a close-up photograph of the RH control cell with QCM.

Water molecules adsorbed on a collagen film were studied by IR microspectroscopy combined with the QCM together with the original RH control system.

1. Weight changes (μg) by QCM increased and decreased with RH corresponding to water adsorption / desorption to the collagen film at 28 °C. The adsorbed water weights are almost similar for wetting and drying processes, indicating that the collagen film is almost equilibrated between adsorption and desorption of water (Figure 6.2.2).

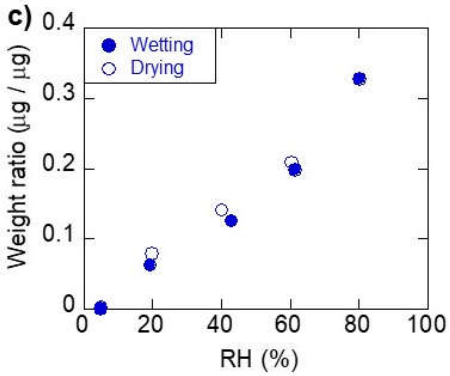

Figure 6.2.2. Weight ratio of water to dry collagen film (µg / µg) plotted against RH, during wetting and drying processes.

2. Infrared spectra of the collagen film at 28 °C during the adsorption / desorption processes show a broad band from 3660 to 3010 cm^{-1} due to OH + NH stretching which increases and decreases during the wetting / drying processes in a similar manner in agreement with the QCM data.

3. The lower wavenumber shift (red shift) of C=O stretching (amide I) and the opposite higher wavenumber shift (blue shift) of N−H bending (amide II) (Figure 6.2.3) can be understood by increasing hydrogen bonding of water molecules to peptides at lower RH.

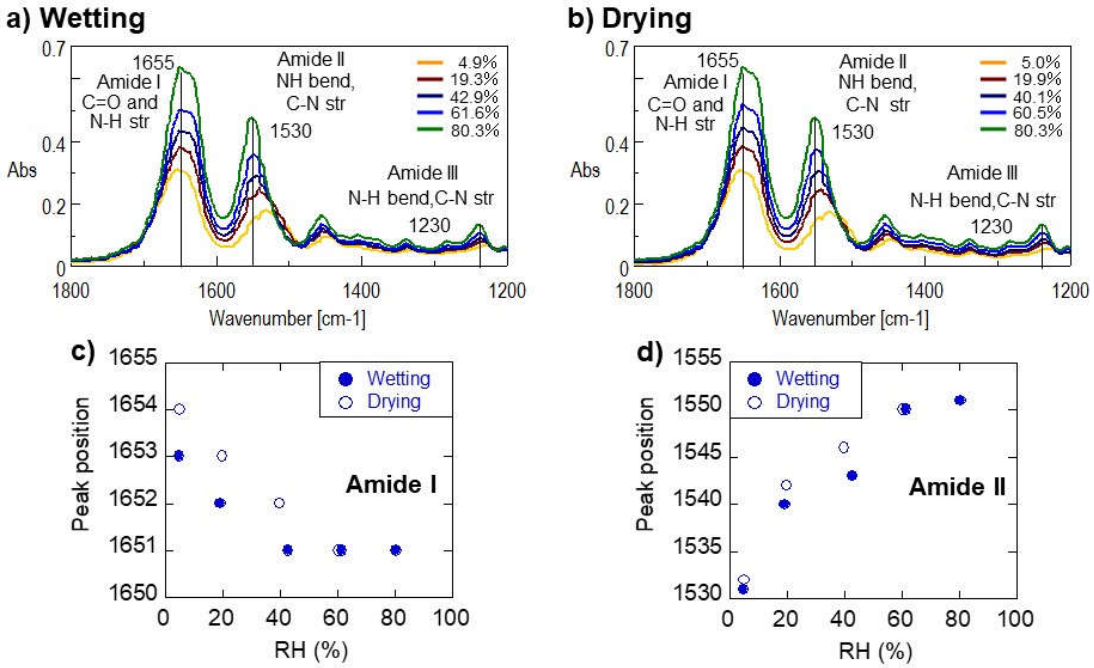

Figure 6.2.3. Infrared spectral changes of amide region during (a) wetting, (b) drying, and peak positions of (c) amide I (1655 cm^{-1}) and (d) amide II (1530 cm^{-1}) of the collagen film.

4. The higher wavenumber shifts (blue shift) of asymmetric stretching of CH_2 and symmetric stretching of CH_3 (Figure 6.2.4) can be due to anomalous hydrogen bonding of water molecules to hydrophobic CH species through complex mixtures of multiple interactions.

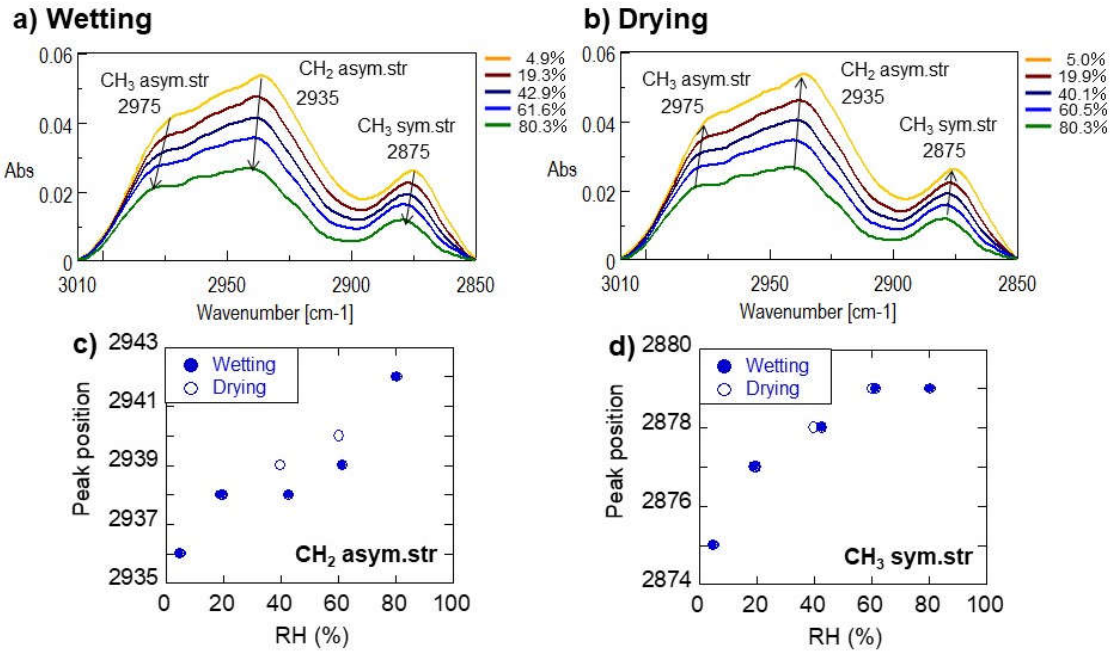

Figure 6.2.4. Infrared spectral changes of CH stretching region during (a) wetting, (b) drying, and peak positions of (c) asymmetric CH_2 (2935 cm^{-1}) and (d) symmetric CH_3 (2875 cm^{-1}) of the collagen film.

5. The difference spectra from the driest collagen film (RH = 4.9 %) showed four peaks at 3465, 3340, 3210 and 3080 cm^{-1} for both wetting and drying processes. Four Gaussian components at 3440, 3330, 3210 and 3070 cm^{-1} gave the best fits to the original OH + NH bands (Figure 6.2.5a). The 3330 and 3070 cm^{-1}band components due to amide A and B (NH) are relatively constant for increasing and decreasing RH.

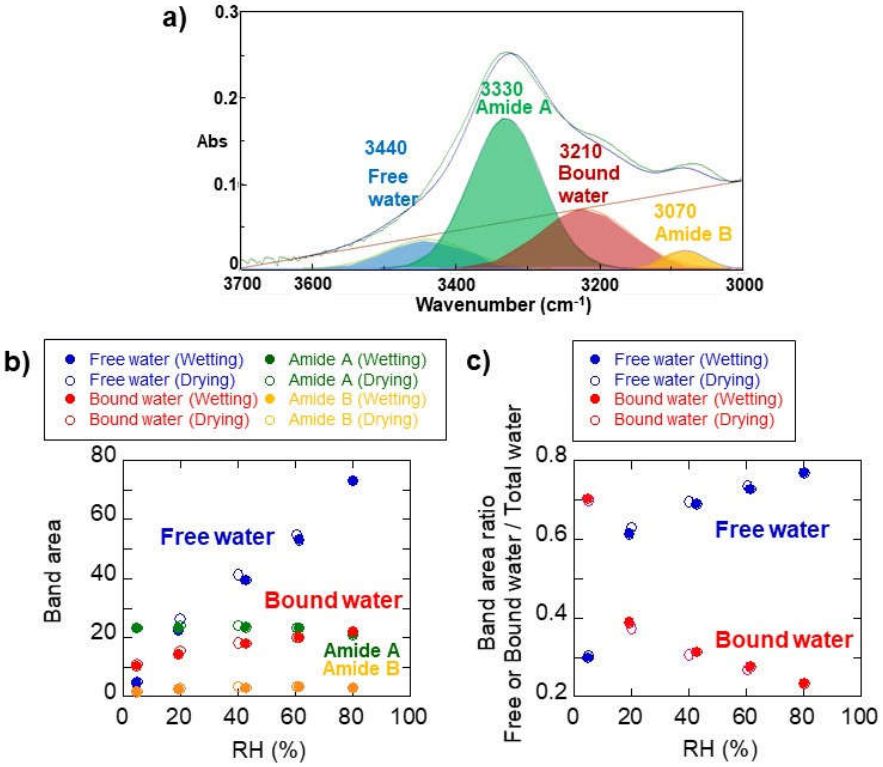

Figure 6.2.5. (a) Curve fitting of OH + NH stretching bands in the 3700 − 3000 cm^{-1} region by four Gaussian components: free water (3440 cm^{-1}), amide A (3330 cm^{-1}), bound water (3210 cm^{-1}) and amide B (3070 cm^{-1}). (b) Band areas of the four components and (c) factions of free and bound water in the total water (3440 + 3210 cm^{-1} band areas) of the collagen film as a function of RH.

6. The 3440 and 3210 cm^{-1} components correspond to H_2O molecules with longer (free water) and shorter (bound water) hydrogen bonding, respectively. At low RH = 4.9 %, more bound water than free water is retained in the collagen film (Figure 6.2.5b). With increasing RH, bound water shows a slight increase approaching a constant value, while free water increases greatly from RH = 4.9 % to RH = 19.3 % and then continues to increase quasi-linearly to RH = 80.3 %. The bound water fraction is around 70 % at RH = 4.9 % but decreases greatly from RH = 19.3 % approaching 23 % at RH = 80.3 %. At higher RH, free water fraction becomes dominant over 70 % (Figure 6.2.5c).

7. The adsorption behavior of bound water saturating with increasing RH (Figure 6.2.5b) is similar to the peak shifts of the amide I and II bands (Figure 6.2.3), suggesting the binding of water molecules to peptide bonds of the collagen film by hydrogen bonding at lower RH. On the other hand, the adsorption behavior of free water increasing further at higher RH (Figure 6.2.5b) can be correlated to the peak shift of aliphatic CH_2 groups (Figure 6.2.4). Free water with longer hydrogen bonding might be loosely bound to aliphatic side chains on the collagen surface, especially at higher RH.

8. The present combined QCM-IR method is found to be useful for studying amounts and natures of water adsorbing on biomolecules.

6.3. Evaluation of Water Adsorption Capacities of Various Biomaterials: Keratin and Collagen

In this study, water adsorbed on keratins measured by IR microspectroscopy combined with QCM and relative humidity control system was analyzed here based on different H bond components. Moreover, interactions of water molecules were studied not only for peptide bonds (amide I) but also for aliphatic CH species on external surfaces of keratin double helices. Natures and amounts of water molecules adsorbed are compared for keratins with double helices and collagens with triple helices both forming fibril structures.

1. Increased weights divided by the weight of dried keratin film (7.9 μg at RH = 3.0 %) increases with RH up to about 19 wt% with S-shape (Figure 6.3.1), suggesting multi-layer adsorption.

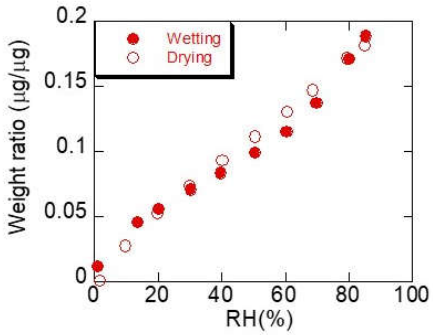

Figure 6.3.1. Weight ratio of water to dry keratin film (µg / µg) plotted against RH, during wetting (red filled circles) and drying (red open circles) processes of the keratin film.

2. The OH + NH band areas (3660 − 3010 cm^{-1}) in IR spectra of the keratin film correlates linearly with the increased weights, indicating water adsorption.

3. The OH + NH band areas for the collagen film are about twice as large as those for the keratin film (Figure 6.3.2), indicating larger water retention capacity of collagen.

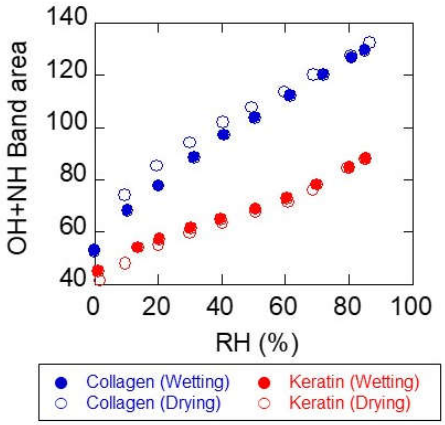

Figure 6.3.2. IR total OH + NH stretching band areas in the 3660 − 3010 cm^{-1} region plotted against RH of the keratin film (red) and collagen film (blue) during the wetting (filled circles) and drying (open circles) processes.

4. Aliphatic CH band shapes are quite different for the collagen and keratin films. While the 2934 cm^{-1} (asymmetric CH_2) and 2874 cm^{-1} (symmetric CH_3) bands do not show significant shifts, the 2959 cm^{-1} (asymmetric CH_3) band shifts from 2959 to 2963 cm^{-1} for increasing

RH for the keratin film (Figure 6.3.3a, b). On the other hand, these CH bands for the collagen film show systematic peak shifts (Figure 6.3.3c, d), suggesting interaction of water molecules with hydrophobic CH surfaces of collagen triple helices.

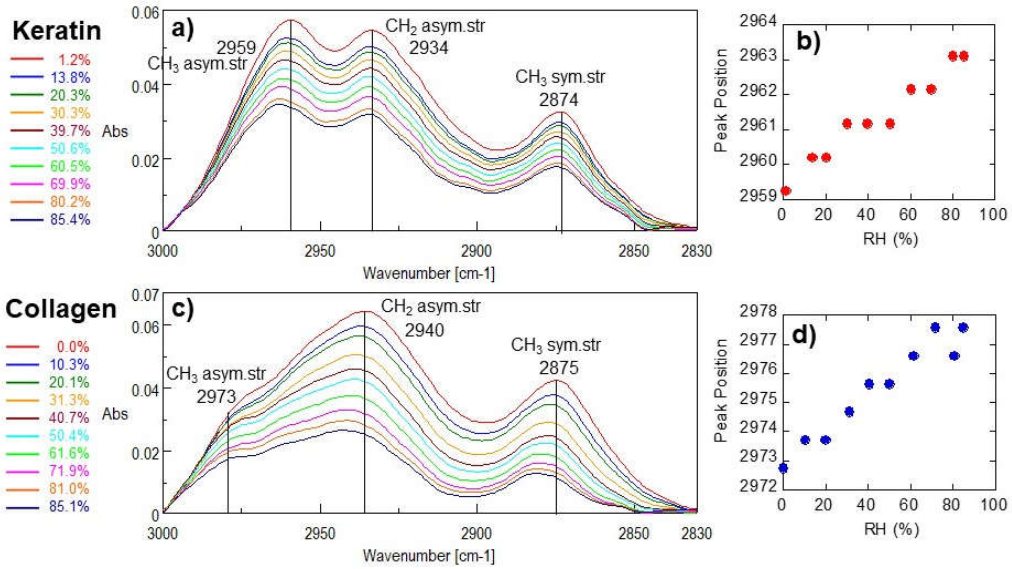

Figure 6.3.3. IR spectral changes of aliphatic CH region during RH increase (wetting) for the (a) keratin and (b) collagen films. Changes with RH in peak positions of asymmetric stretching of CH_3 for the (c) keratin (2959 cm^{-1}) and (D) collagen (2973 cm^{-1}) films.

5. Gaussian curve fitting of the amide I bands by three components (Figure 6.3.4a, b) show that the 1636 cm^{-1} components due to H_2O molecules show an S-shape increases with RH in agreement with the OH + NH band increases. The lower wavenumber "other" components remain small both for the keratin and collagen films. While the higher wavenumber "α helix" components of the keratin film remain mostly unchanged, that for the collagen film show an S-shape increase with RH in association with an increase in H_2O component (Figure 6.3.4c, d).

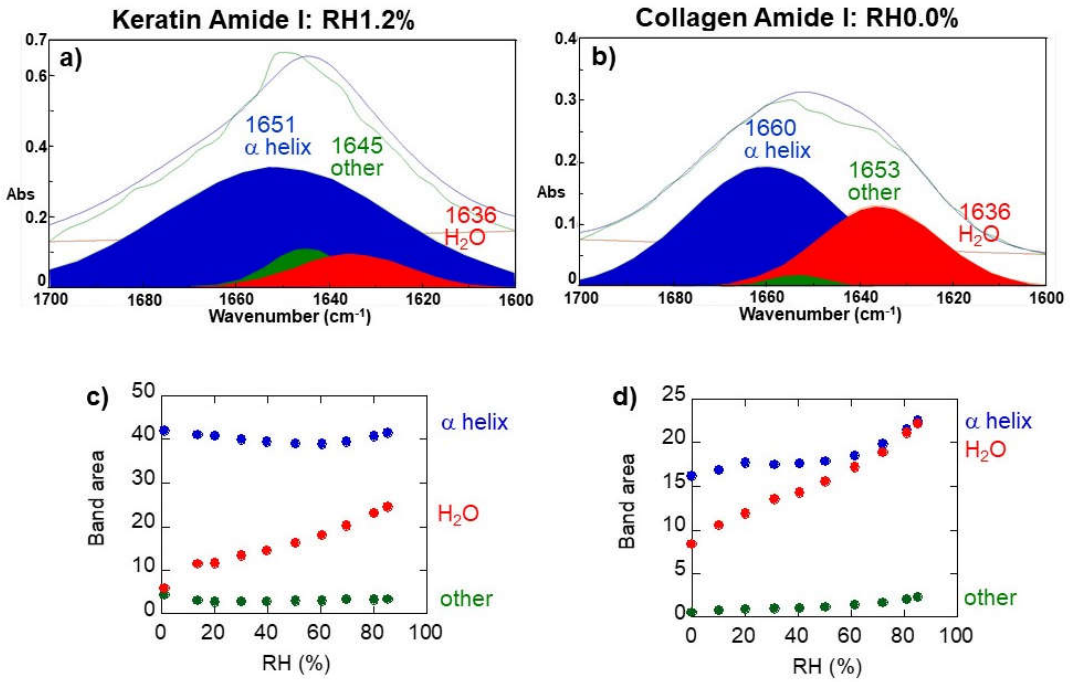

Figure 6.3.4. Representative fitting results of the amide I band by three Gaussian components for (a) the keratin film (at RH = 1.2 %) and (b) the collagen film (at RH = 0.0 %). Changes with RH of band areas of three Gaussian components during wetting process of (c) the keratin film and (d) the collagen film. 1651 or 1660 cm^{-1} component (α helix: blue), 1645 or 1653 cm^{-1} component (other: green), 1636 cm^{-1} component (H_2O: red).

6. Gaussian curve fitting of the OH + NH bands in the 3700 − 3010 cm^{-1} region (Figure 6.3.5a, b) show that while amide B components (3065 or 3070 cm^{-1}) remain mostly unchanged, amide A components (3300 or 3330 cm^{-1}) decreases for higher RHs both for the keratin and collagen films (Figure 6.3.5c, d).

7. The free water component (3405 cm^{-1}) with longer H bonds increases with RH with S-shape by keeping the bound water component (3180 cm^{-1}) with shorter H bonds minor for the keratin film. On the other hand, for the collagen film, the bound water component (3210 cm^{-1}) is larger than the free water one (3440 cm^{-1}) at the lowest RH and the free water increases greatly with RH at higher RHs (Figure 6.3.5c, d).

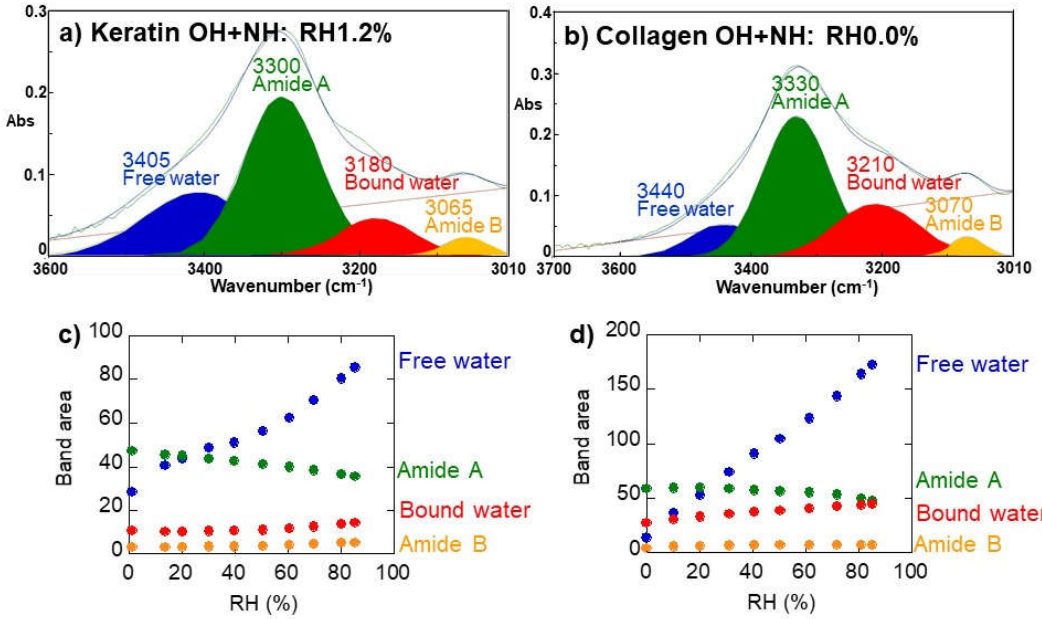

Figure 6.3.5. Representative fitting results of the OH + NH stretching bands by four Gaussian components for (a) the keratin film (at RH = 1.2 %) and (b) the collagen film (at RH = 0.0 %). Changes with RH of band areas of four Gaussian components during wetting process of (c) the keratin film and (d) the collagen film. 3405 or 3440 cm^{-1} component (free water: blue), 3300 or 3330 cm^{-1} component (amide A: green), 3180 or 3210 cm^{-1} component (bound water: red), and 3065 or 3070 cm^{-1} component (amide B: orange)

8. About twice of water retention capacity of the collagen film than the keratin film can be due to increasing adsorption of free water with weak hydrogen bonding. At least part of these free water molecules might interact with hydrophobic aliphatic CH surfaces of triple helices of the collagen film.

6.4. Evaluation of Water Adsorption Capacities of Various Biomaterials: Lecithin

In this study, soybean lecithin, one of phospholipids, was selected as a representative cellular membrane, and water molecules bound to lecithin was analyzed by using IR microspectroscopy equipped with a humidity control system.

1. The water weight ratio increases gradually from nearly 0 wt% at RH = 4.3 % to 4.4 wt% at RH = 55.5 % and then greatly until 19.6 wt% at RH = 91.5 % (Figure 6.4.1).

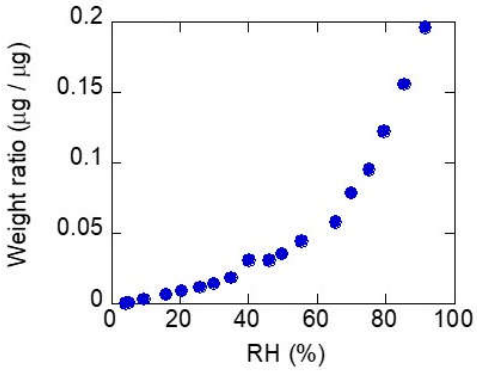

Figure 6.4.1. Weight ratio of water to dry lecithin film (µg / µg) plotted against RH, during wetting.

2. Infrared OH band area increases linearly with the water weight ratio (Figure 6.4.2), indicating that the OH band area increase is mainly due to water adsorption.

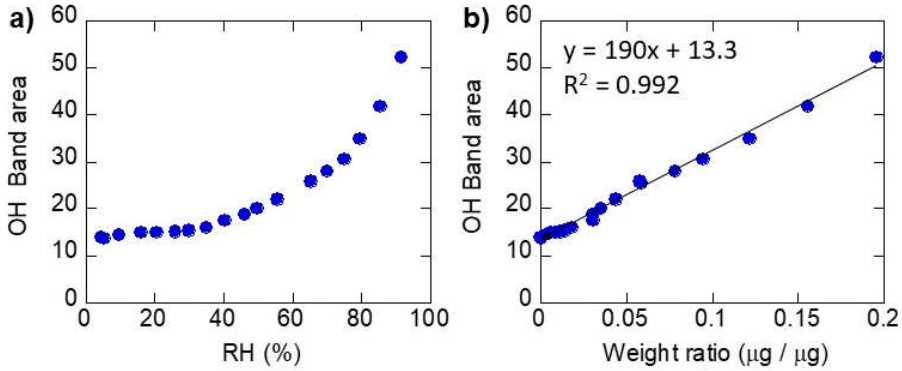

Figure 6.4.2. IR total OH stretching band area in the 3600 − 3040 cm^{-1} region plotted against (a) RH, (b) Weight ratio (µg / µg) by QCM of the lecithin film during the wetting process.

3. The 1230 cm^{-1} band due to asymmetric PO_2^- stretching shifts from about 1232 to 1222 cm^{-1} (red shift) with increasing RH (Figure 6.4.3a), possibly due to water adsorption.

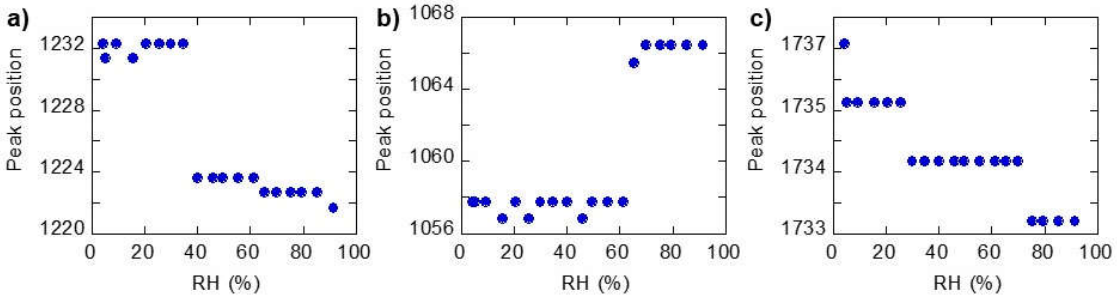

Figure 6.4.3. Peak positions of (a) asymmetric PO_2^- stretching (1230 cm^{-1}), (b) PO_2^- and P−O−C (1060 cm^{-1}) and (c) C=O stretching (1735 cm^{-1}) of the lecithin film.

4. The 1060 cm^{-1} band due to PO_2^- and P−O−C shifts from about 1058 to 1066 cm^{-1} (blue shift) with increasing RH (Figure 6.4.3b). This can be explained by increasing hydrogen bonding by water molecules to phosphates.

5. The 1735 cm^{-1} band due to C=O stretching shifts slightly from 1736 to 1734 cm^{-1} (red shift) (Figure 6.4.3c), indicating hydrogen bonding of water molecules to carboxylic acids and/or esters.

6. The band positions of free and bound water shift to lower frequency sides with increasing RH (Figure 6.4.4b). These results can be understood by increasing hydrogen bonding among water molecules adsorbed to the lecithin film.

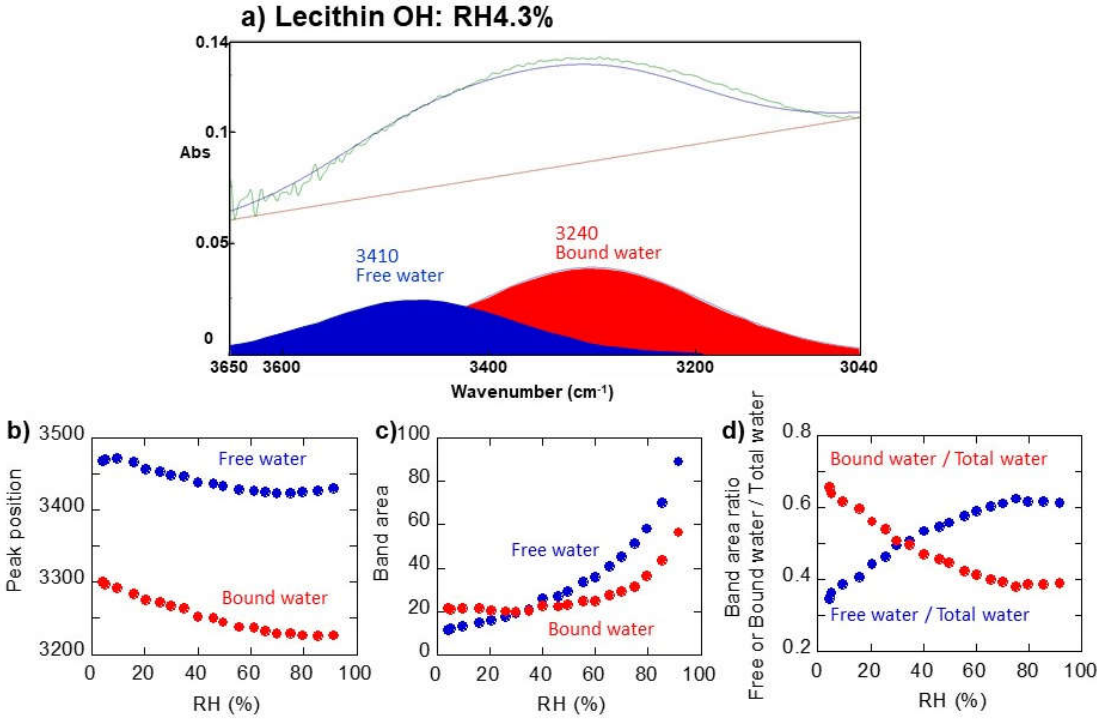

Figure 6.4.4. (a) Curve fitting of OH stretching band in the 3650 − 3040 cm^{-1} region by two Gaussian components: free water (3410 cm^{-1}) and bound water (3240 cm^{-1}). (b) Peak positions of free and bound water against RH. (c) Band areas of free and bound water, and (d) factions of free and bound water in the total water (3410 + 3240 cm^{-1} band areas) of the lecithin film as a function of RH.

7. The band area of bound water is larger than that of free water at low RHs and remains relatively stable until RH = 60 %. The band area of bound water then increases at higher RHs. The band area of free water is small at lower RHs, but increases at medium RHs and increase greatly at high RHs (Figure 6.4.4c).

8. Band areas of 1230 and 1060 cm^{-1} bands of phosphates increase with increasing RH (Figure 6.4.5a, b). The band areas of phosphates correlate positively with the band area of bound water (Figure 6.4.6a, b). Bound water molecules with shorter H bonds might be bound to these phosphate groups.

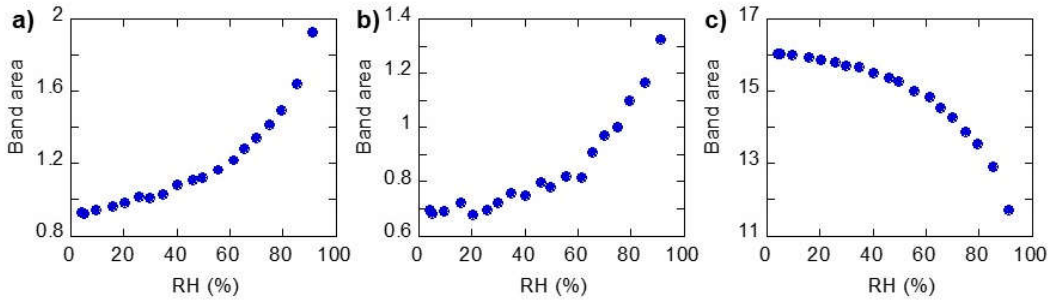

Figure 6.4.5. Band areas of (a) asymmetric PO_2^- stretching band (1255 − 1160 cm^{-1}), (b) PO_2^- and P−O−C band (1125 − 1045 cm^{-1}) and (c) aliphatic CH stretching bands (3000 − 2830 cm^{-1}) of the lecithin film as a function of RH.

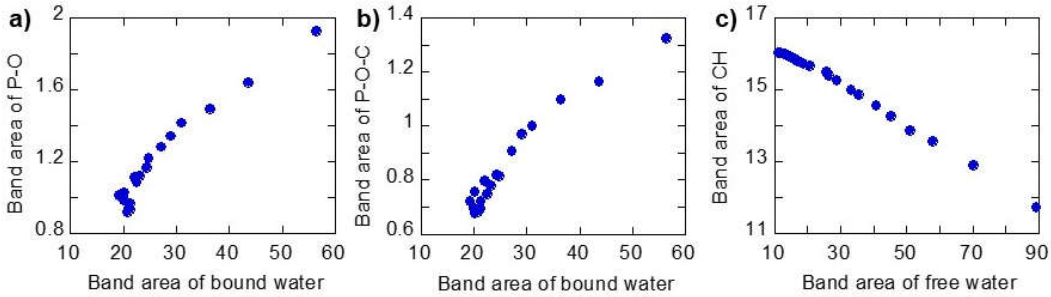

Figure 6.4.6. Band areas of (a) asymmetric PO_2^- stretching band (1255 − 1160 cm^{-1}) and (b) PO_2^- and P−O−C band (1125 − 1045 cm^{-1}) against band area of bound water and (c) aliphatic CH stretching bands (3000 − 2830 cm^{-1}) against band area of free water of the lecithin film.

9. Band areas of aliphatic CH stretching bands in the 3000 − 2830 cm^{-1} region decrease throughout the RH increase (Figure 6.4.5c). This decrease is negatively correlated to the increasing adsorption of free water (Figure 6.4.6c). Since these band area decreases have been observed for triple helix collagen in our previous study, free water molecules with longer H bonds might interact loosely with aliphatic chains of the lecithin film.

10. At low RHs, bound water molecules with shorter H bonds are already bound by polar phosphate group of lecithin. At high RHs, further bound water molecules can be adsorbed near these phosphate groups.

11. Free water molecules with longer H bonds are not abundant at low RHs. With increasing RH, free water molecules might be bound loosely to aliphatic chains of the lecithin film. Since further free water molecular layers can be added to the lecithin film, increasing water adsorption at high RHs was observed.

6.5. Evaluation of Water Adsorption Capacities of Various Biomaterials: Ceramide

As a representative inter-cellular lipid, ceramide 3 has been selected in this study. It is composed of phytosphingosine [P] unit and non-hydroxyl fatty acid [N] unit, which are bound by an amide bond. Water adsorption to ceramide was studied by using IR microspectroscopy equipped with a humidity control system.

1. The water weight ratio increases quasi-linearly from nearly 0 wt% at RH = 2.0 % to 1.2 wt% at RH = 84.8 % (Figure 6.5.1).

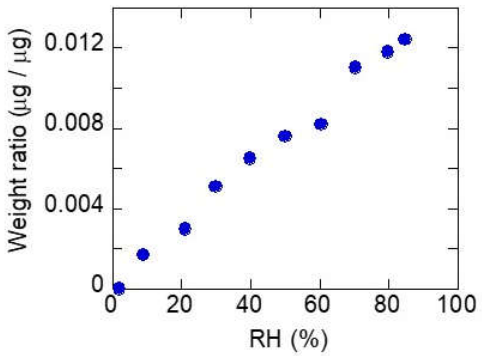

Figure 6.5.1. Weight ratio of water to dry ceramide film (μg / μg) plotted against RH during wetting.

2. The OH + NH band area increases linearly with the water weight ratio (Figure 6.5.2), indicating that the OH band area increase is mainly due to water adsorption.

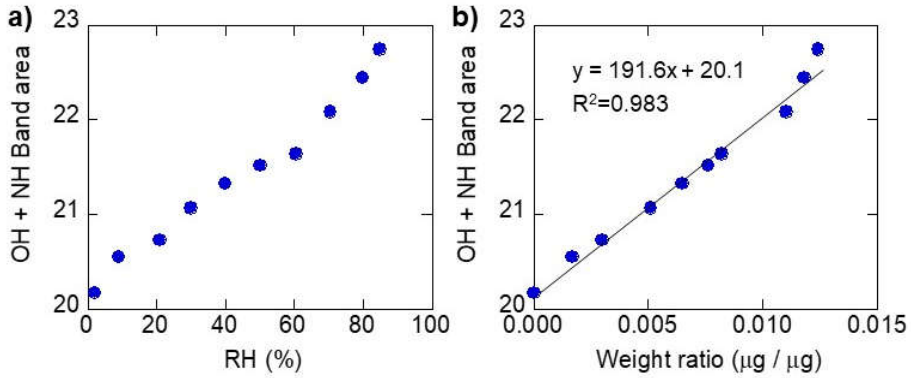

Figure 6.5.2. IR total OH + NH stretching band area in the 3470 − 3040 cm^{-1} region plotted against (a) RH, (b) Weight ratio (μg / μg) by QCM of the ceramide film during the wetting process.

3. No significant peak shifts were observed for 2955 (asymmetric CH_3), 2872 (symmetric CH_3), 2925 (asymmetric CH_2), 2850 (symmetric CH_2), 3005 (C=C−H) and 1465 (CH_2 scissoring) cm^{-1} bands. The amide I and II bands also did not change significantly. Water molecules might not be adsorbed to aliphatic CHs and amides.

4. The band around 1045 cm^{-1} due to C−O stretching shifts from 1046 to 1042 cm^{-1} (red shift) with increasing RH (Figure 6.5.3). This can be explained by increasing hydrogen bonding by water molecules to C−O bonds.

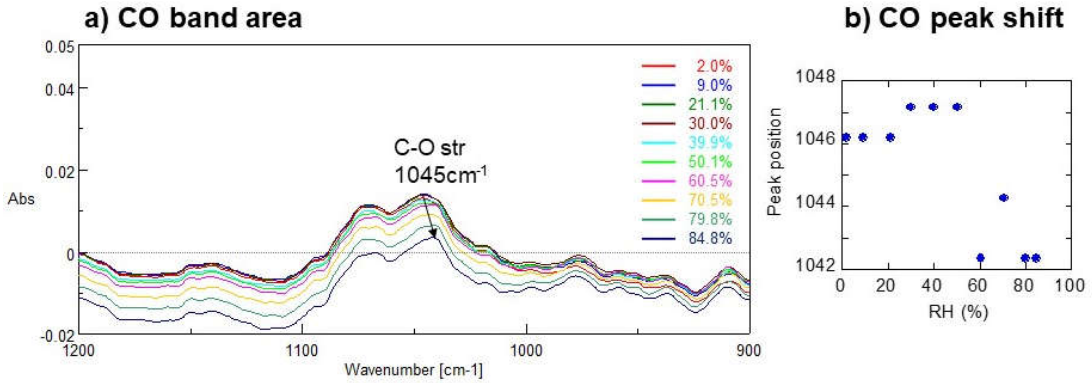

Figure 6.5.3. Changes in (a) IR spectra and (b) peak position of the band around 1045 cm^{-1} due to C−O stretching during wetting of the ceramide.

5. The band areas of amides A and B remain almost constant. Although the free water component increases only slightly with RH, the bound water component increases slightly at low RHs and more from about RH = 60 % (Figure 6.5.4). Since the peak shift of C−O was observed at higher RHs than 60 % (Figure 6.5.3b), bound water with shorter H bonds is considered to be adsorbed to C−O bonds.

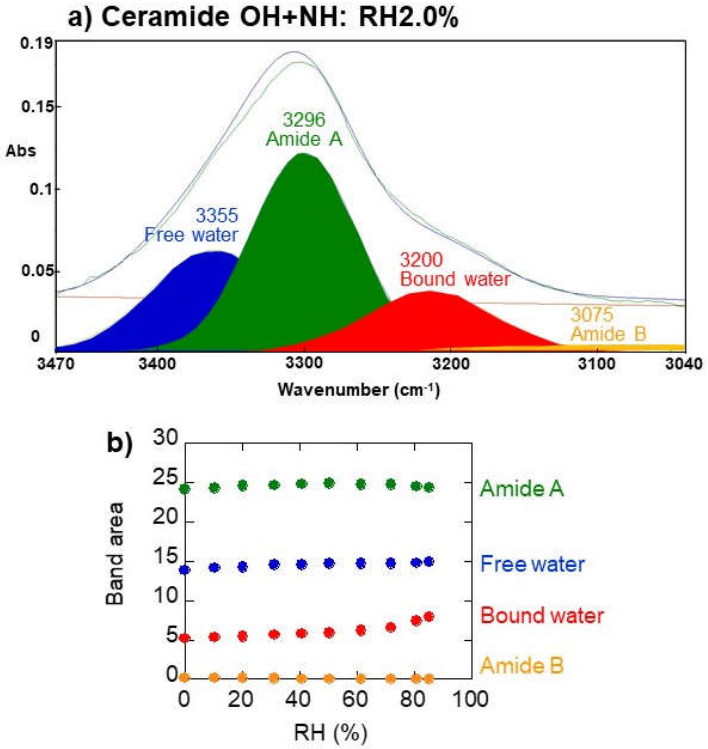

Figure 6.5.4. (a) Representative fitting results of the OH + NH stretching bands by four Gaussian components for ceramide (at RH = 2.0 %). (b) Changes with RH of band areas of four Gaussian components during wetting process of ceramide. 3355 cm^{-1} component (free water: blue), 3296 cm^{-1} component (amide A: green), 3200 cm^{-1} component (bound water: red), and 3075 cm^{-1} component (amide B: orange).

6. Water weight ratio increases only slightly for ceramide to 1.2 wt% at RH = 84.8 %, while it increases greatly for lecithin up to 19.6 wt% at RH = 91.5 % (Figure 6.5.5).

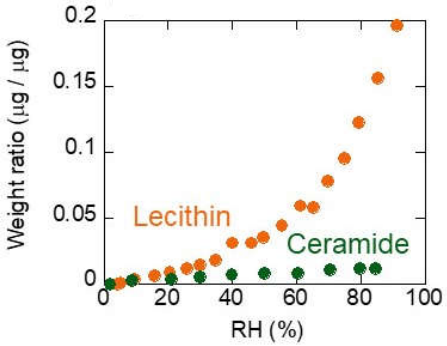

Figure 6.5.5. Weight ratios against RH of ceramide (green) and lecithin (blue) during the wetting process.

7. While the band area of free water is always larger than that of bound water for ceramide, that of free water is smaller than that of bound water at low RHs, but becomes larger at high RHs for lecithin (Figure 6.5.6).

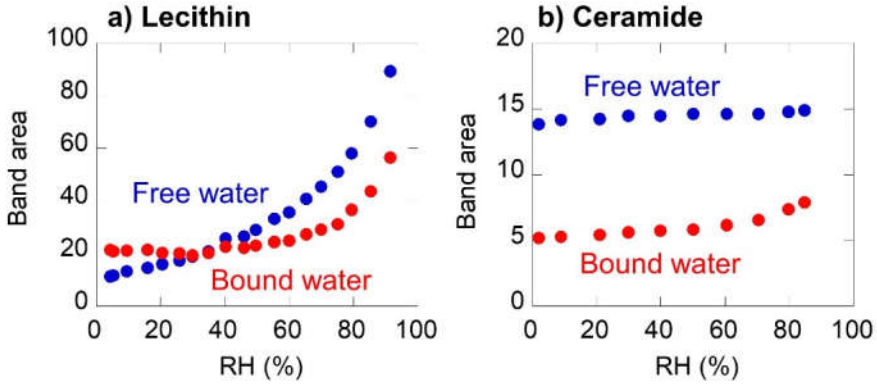

Figure 6.5.6. Band areas of free (blue) and bound (red) water of (a) ceramide and (b) lecithin against RH during wetting.

8. These significant differences in water adsorption capacities between ceramide and lecithin can be related to their differences in chemical structures.

9. Bound water molecules with shorter H bonds might be bound to phosphate groups for lecithin. Free water molecules with longer H bonds might interact loosely with aliphatic chains of the lecithin.

10. Only C−O bonds of the ceramide is considered to adsorb bound water with shorter H bonds. No interaction of water molecules with aliphatic CH chains of ceramide is noticed.

6.6. Overall Discussion

Based on the above results, adsorption behavior of water to various biomaterials will be discussed below.

6.6.1. Water Weight Ratio

Water weight ratios (μg / μg) adsorbed on collagen, keratin, lecithin and ceramide determined by QCM were plotted against RH in Figure 6.6.1. At RH values of about 80 %, water weight ratios are 24.6 wt% (RH = 81.0 %) for collagen, 17.0 wt% (RH = 80.2 %) for keratin, 12.2 wt% (RH = 79.5 %) for lecithin and 1.2 wt% (RH = 79.8 %) for ceramide. Water retention capacity is the largest for collagen and the smallest for ceramide among four biomaterials studied.

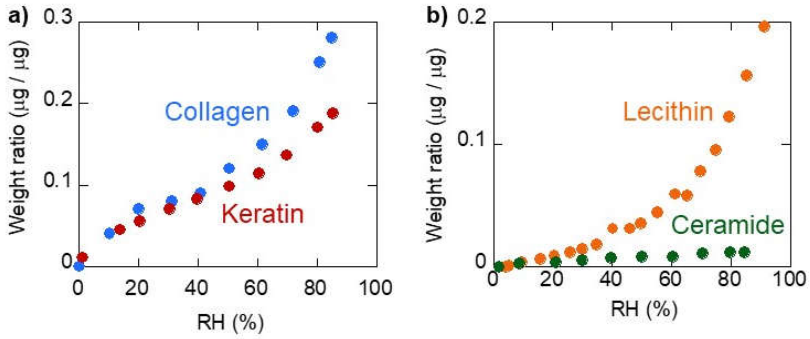

Figure 6.6.1. Water weight ratios (μg / μg) to dry films plotted against RH for (a) collagen and keratin and (b) lecithin and ceramide, during wetting.

6.6.2. OH (+NH) Bands

Changes with RH in infrared OH (+NH) bands measured by IR microspectroscopy are shown in Figure 6.6.2. Besides amide bands (NH stretching) around 3340 − 3300 and 3080 − 3070 cm^{-1}, free water with longer H bonds around 3465 − 3355 cm^{-1} and bound water with

shorter H bonds around 3245 − 3200 cm^{-1} can be recognized. Free water components increase greatly for keratin, collagen and lecithin.

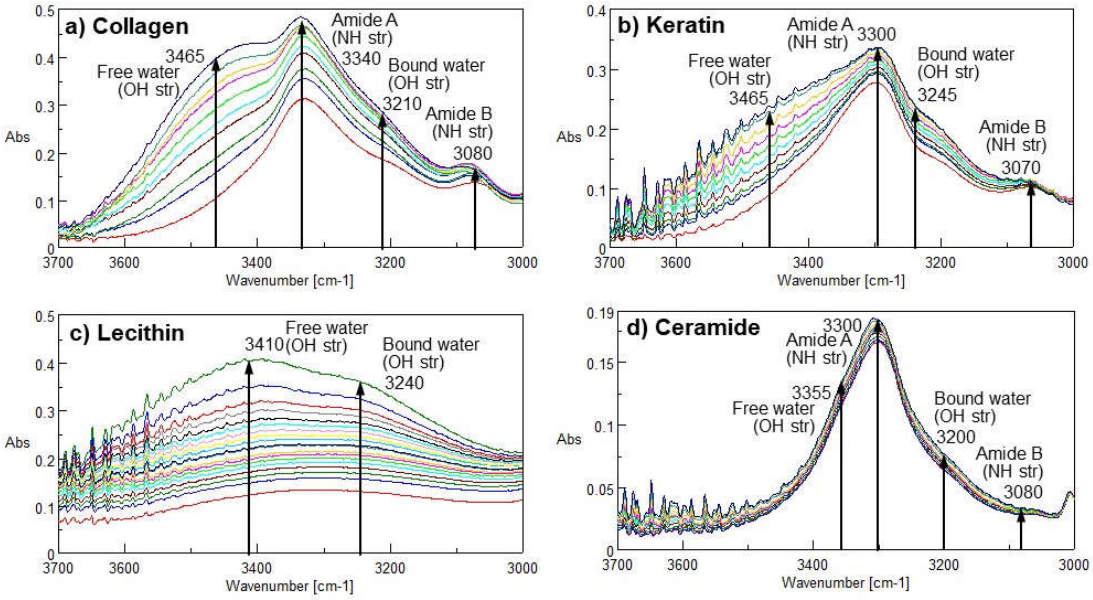

Figure 6.6.2. IR spectral changes of OH (+NH) bands for (a) collagen, (b) keratin, (c) lecithin and (d) ceramide, during wetting. Arrows indicate increasing RH.

6.6.3. OH (+NH) Band Areas

Changes with RH in OH (+NH) band areas are shown in Figure 6.6.3a, b. The band areas increase greatly with increasing RH for collagen, keratin and lecithin, but show only a slight increase for ceramide.

The OH (+NH) band areas can be quasi-linearly correlated with the water weight ratios measured by QCM for keratin, lecithin and ceramide (Figure 6.6.3c, d). However, the OH (+NH) band areas for collagen show attenuation for large water weight ratios (Figure 6.6.3c). This can be due to saturation of the OH (+NH) bands at higher RHs.

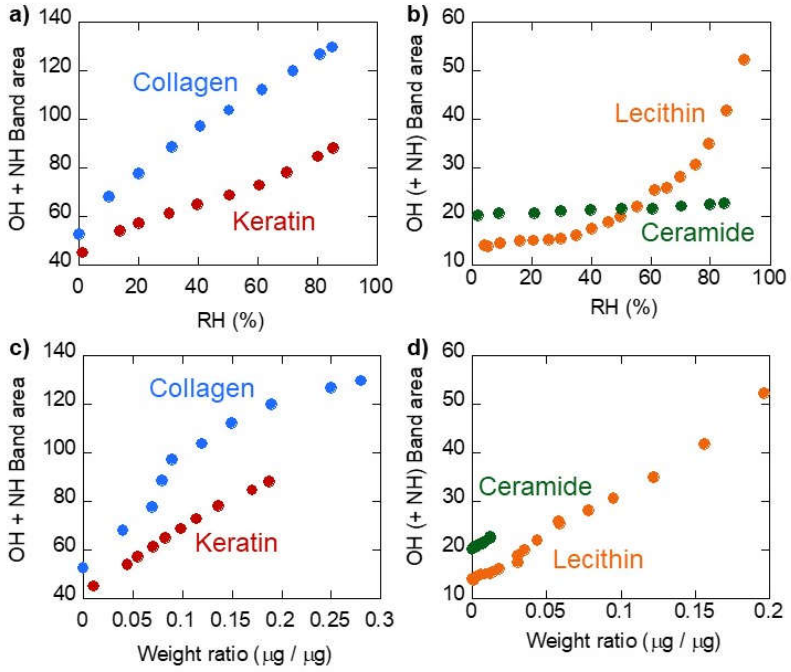

Figure 6.6.3. IR total OH (+NH) stretching band areas plotted against RH for (a) collagen and keratin and (b) lecithin and ceramide, and against water weight ratio (μg / μg) by QCM for (c) collagen and keratin and (d) lecithin and ceramide.

6.6.4. CH Bands

Changes with RH in infrared aliphatic CH stretching bands measured by IR microspectroscopy are shown in Figure 6.6.4. These band shapes are quite different for different biomaterials. Some band shifts can be recognized for collagen and keratin, while no significant band shifts can be noticed for ceramide and lecithin.

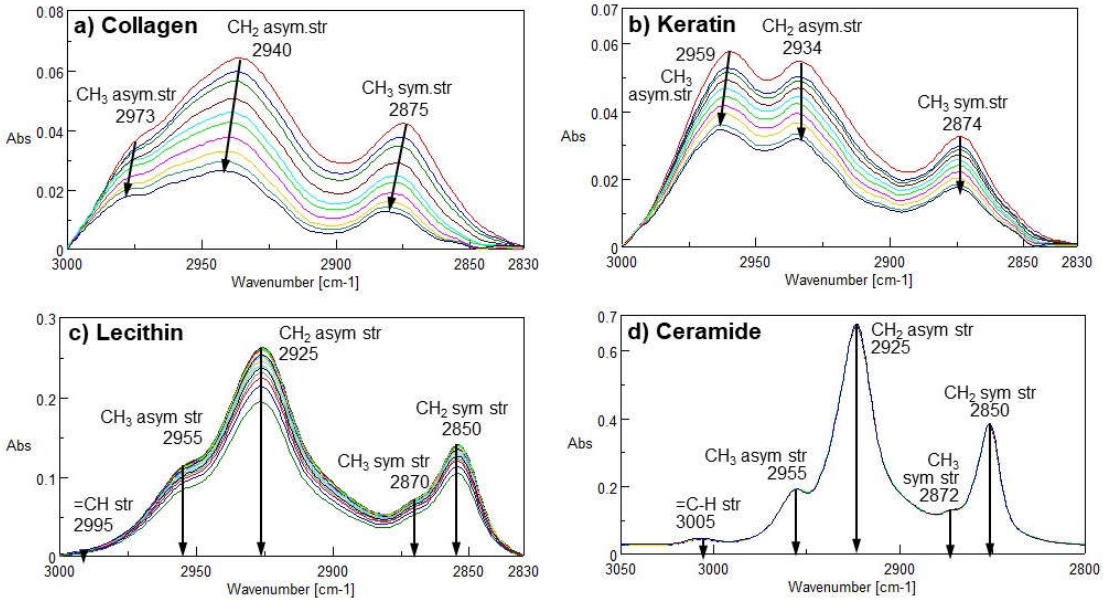

Figure 6.6.4. Infrared spectral changes of CH stretching region of (a) collagen, (b) keratin, (c) lecithin and (d) ceramide. Arrows indicate increasing RH.

6.6.5. CH Peak Positions

Changes with RH in peak positions of aliphatic CH stretching bands are shown in Figure 6.6.5. The 2973 (CH_3 asymmetirc stretch), 2940 (CH_2 asymmetirc stretch) and 2875 (CH_3 symmetirc stretch) cm^{-1} bands shift to higher wavenumber region (blue shift) for collagen. For keratin, the 2959 (CH_3 asymmetirc stretch), 2934 (CH_2 asymmetirc stretch) and 2874 (CH_3 symmetirc stretch) cm^{-1} bands slightly shift to higher wavenumber region (blue shift).

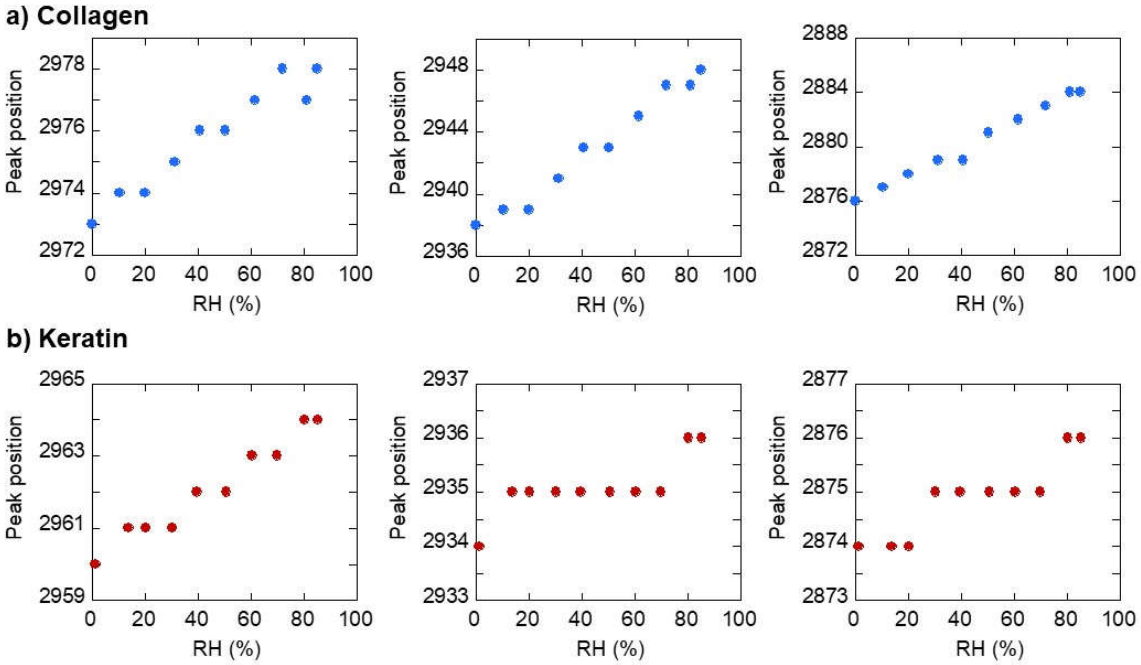

Figure 6.6.5. Peak positions of asymmetric stretching of CH_3 (2973 or 2959 cm^{-1}) and CH_2 (2940 or 2934 cm^{-1}), and symmetric stretching of CH_3 (2875 or 2874 cm^{-1}) for (a) collagen and (b) keratin as functions of RH.

6.6.6. CH Band Areas

Changes with RH in CH band areas are shown in Figure 6.6.6. They decrease quasi-linearly with increasing RH for keratin and collagen. The CH band area for ceramide decrease slightly with RH. The CH band area for lecithin show an upward convex trend with RH.

Combined with the CH band shifts in Figure 6.6.5, these data indicate interactions of water molecules with four biomaterials. The interaction appears to be significant for collagen with all the band shifts and band area decrease. For keratin, since the CH_3 band shift is major, the top of hydrophobic portion of keratin can be mainly interacted with water. Although no significant CH band shifts can be noticed for lecithin, the significant band decrease, especially at high RHs, indicate interactions of water with aliphatic chains of lecithin.

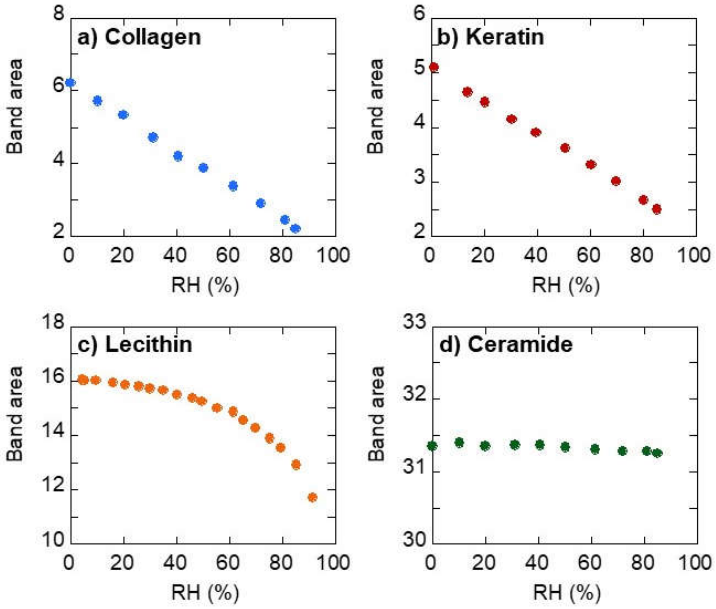

Figure 6.6.6. IR aliphatic CH band areas plotted against RH for (a) collagen, (b) keratin, (c) lecithin and (d) ceramide.

6.6.7. Finger Print Bands

Changes with RH in infrared bands in the finger print region (1800 − 1000 cm^{-1}) are shown in Figure 6.6.7. These band shapes are quite different for different biomaterials. Some band shifts can be recognized for amide III of collagen and keratin, C−O of ceramide and P−O, P−O−C and C=O of lecithin.

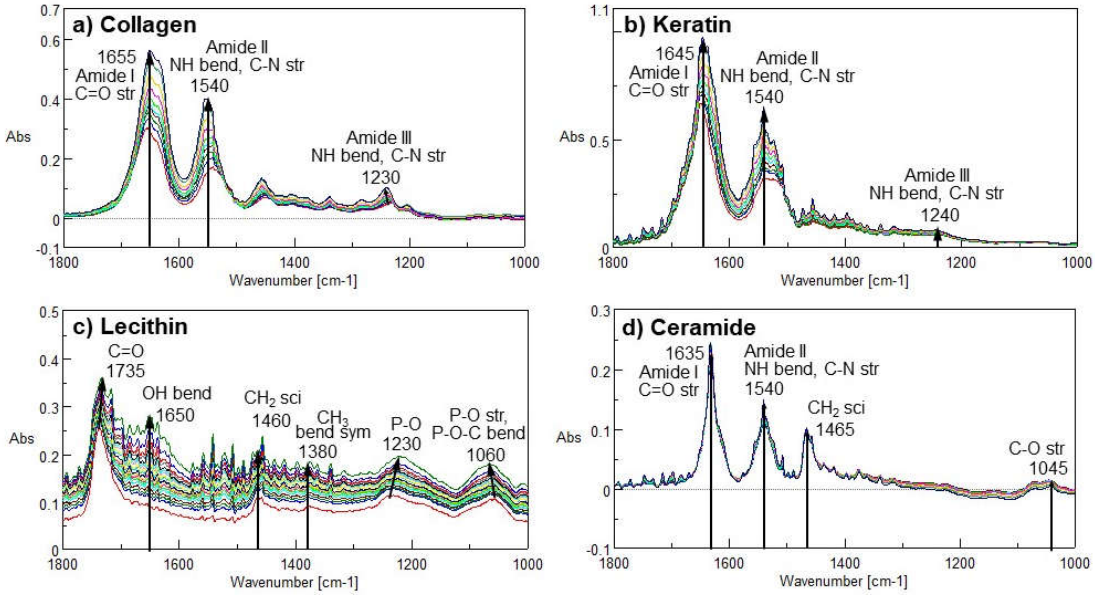

Figure 6.6.7. Infrared spectral changes of finger print regions (1800 − 1000 cm^{-1}) for (a) collagen, (b) keratin, (c) lecithin and (d) ceramide.

6.6.8. Finger Print Peak Positions

Changes with RH in peak positions of finger print bands are shown in Figure 6.6.8. The amide III bands of collagen shift to higher wave number region for all RHs (Figure 6.6.8a), suggesting overall adsorption of bound water to amide bonds. The amide III bands of keratin shift to higher wave number region at low RHs (Figure 6.6.8b), indicating water adsorption (bound water) to amide bonds at low RHs.

For lecithin, C=O, P−O stretching bands shift to a lower wavenumber region (red shift), while P−O−C bending bands shift to higher wavenumber region (blue shift) (Figure 6.6.8c − e). These observations indicate water adsorption to phosphate and carbonyl groups.

For ceramide, only C−O stretching bands show a shift at high RHs (Figure 6.6.8f), indicating bound water adsorption at high RHs.

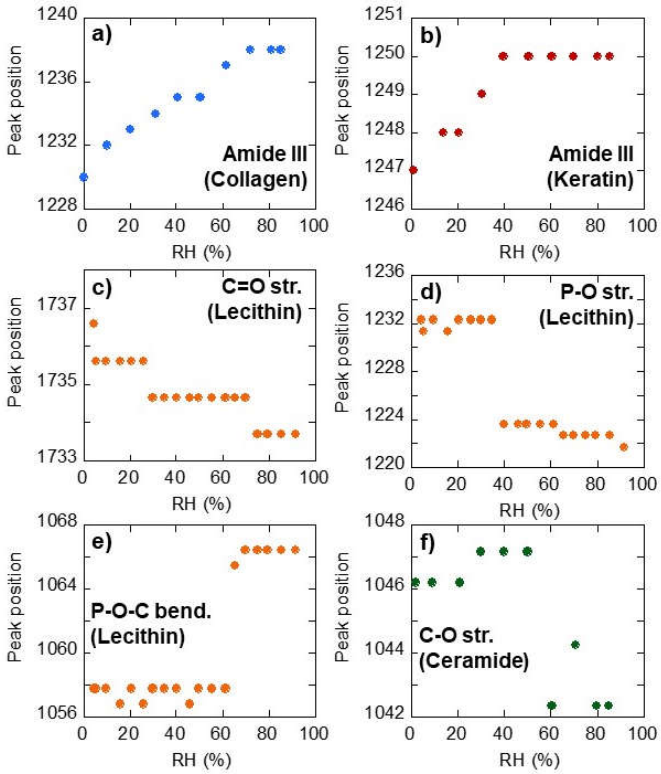

Figure 6.6.8. Changes with RH in peak positions of finger print bands. Amide III bands of (a) collagen and (b) keratin, (c) C=O, P−O stretching and P−O−C bending bands of lecithin and (d) C−O stretching band of ceramide.

6.6.9. Finger Print Band Areas

Changes with RH in the finger print band areas are shown in Figure 6.6.9. The amide II and III bands of collagen and keratin increase with RH (Figure 6.6.9a − d), indicating interactions with water.

For lecithin, band areas of P−O and C=O stretching and P−O−C bending increase with RH (Figure 6.6.9e − g), indicating water adsorption to phosphate and carbonyl groups.

For ceramide, C−O stretching band decrease with RHs showing an opposite trend to the above increasing trends (Figure 6.6.9h). Origins of these band increase / decreases are not yet well understood.

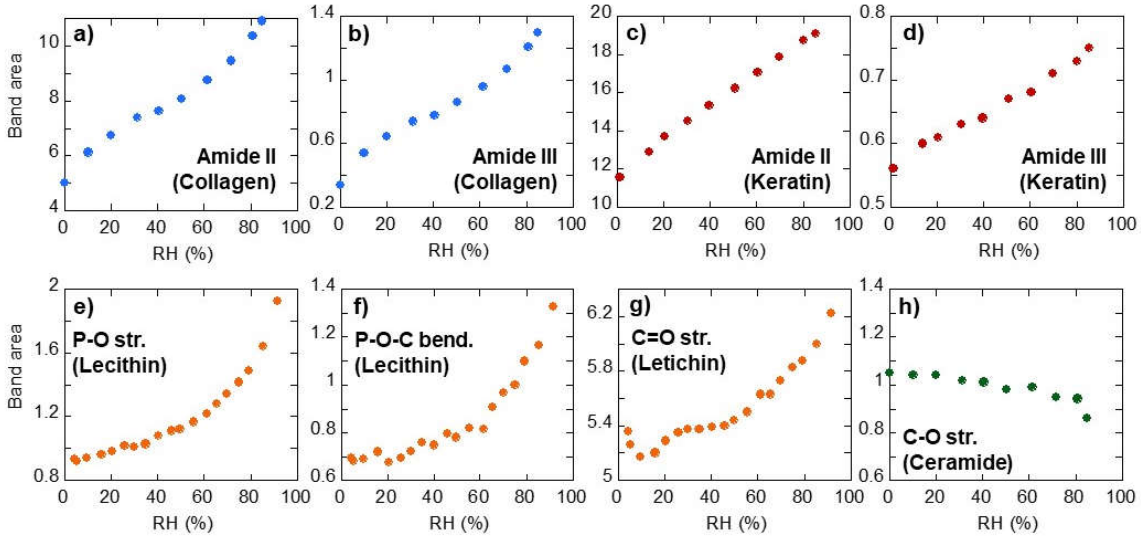

Figure 6.6.9. Changes with RH in finger print band areas. Amide II and III bands of (a) collagen and (b) keratin. (c) P−O and C=O stretching and P−O−C bending of lecithin and (d) C−O stretching band of ceramide.

6.6.10. Analyses of OH (+NH) Bands

The OH (+NH) stretching bands of biomaterials were fitted with two to four Gaussian components. The representative fitting results are shown in Figure 6.6.10. The bands for collagen, keratin and ceramide could be fitted by 4 Gaussian components: Free water (3440 − 3355 cm^{-1}), amide A (3330 − 3296 cm^{-1}), bound water (3210 − 3180 cm^{-1}) and amide B (3075 − 3065 cm^{-1}). For lecithin without amides, the OH band could be fitted by free water (3410 cm^{-1}) and bound water (3240 cm^{-1}).

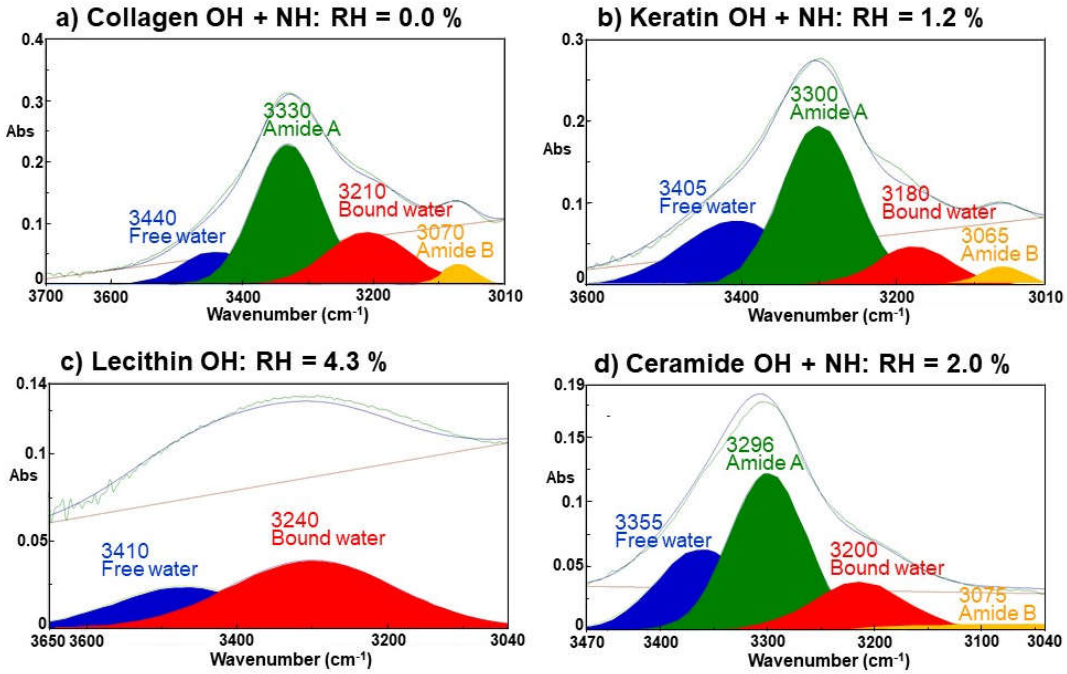

Figure 6.6.10. (a) Curve fitting of OH (+NH) stretching bands by four Gaussian components: free water (3440 − 3355 cm^{-1}), amide A (3330 − 3296 cm^{-1}), bound water (3210 − 3180 cm^{-1}), and amide B (3075 − 3065 cm^{-1}) for (a) collagen, (b) keratin and (d) ceramide and two Gaussian components: free water (3410 cm^{-1}) and bound water (3240 cm^{-1}) of (c) lecithin.

6.6.11. Band Areas of Gaussian Components in OH (+NH) Bands

Changes with RH in band areas of Gaussian components in OH (+NH) bands are shown in Figure 6.6.11. For collagen, band area of bound water is larger than that of free water at low RHs, but at higher RHs free water increases greatly (Figure 6.6.11a). For keratin, band area of free water always dominates (Figure 6.6.11b).

For lecithin, band area of bound water is larger than that of free water at low RHs, but at higher RHs that of free water becomes larger than that of bound water (Figure 6.6.11c). For ceramide, band area of free water is always larger than that of bound water (Figure 6.6.11d). The band area of bound water for ceramide increases at higher RHs.

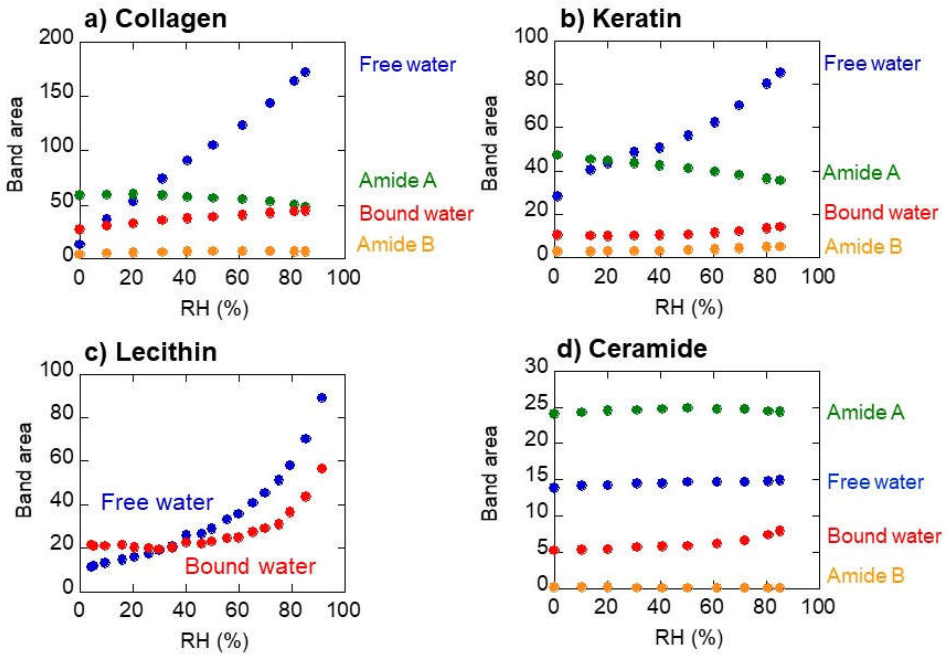

Figure 6.6.11. Changes with RH in band areas of OH (+NH) stretching bands for (a) collagen, (b) keratin, (c) lecithin and (d) ceramide.

6.6.12. Free and Bound Water Ratio

Band area ratios of free and bound water in the total band areas of water (free water + bound water) are shown in Figure 6.6.12. For collagen and lecithin, bound water ratio is larger than that of free water at low RHs, but at higher RHs free water dominates (Figure 6.6.12a, c). For keratin and ceramide, free water ratio always dominates (Figure 6.6.12b, d).

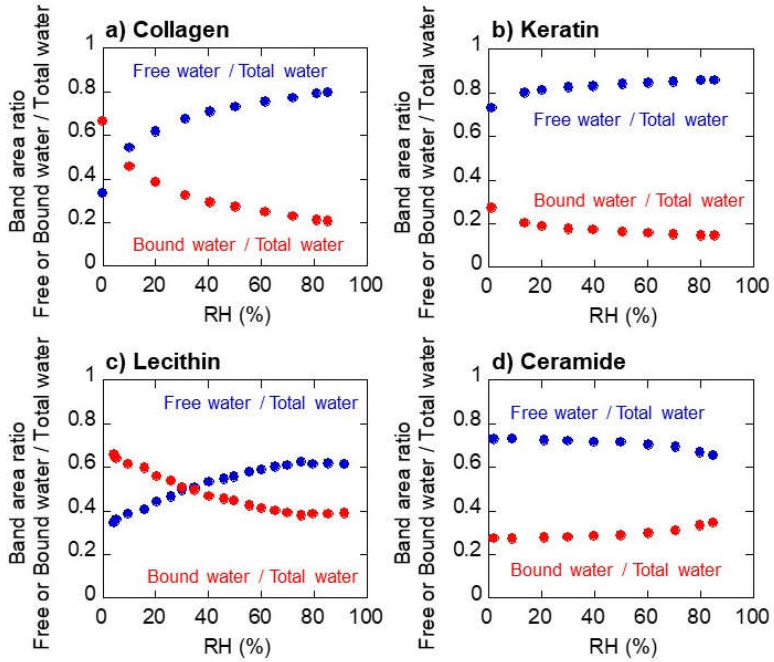

Figure 6.6.12. Changes with RH in factions of free and bound water in the total water for (a) collagen, (b) keratin, (c) lecithin and (d) ceramide.

6.6.13. Relations between Free / Bound Water and Functional Groups

Based on the above results, several functional groups of biomaterials have been suggested to interact with free and bound water. In order to examine further these interactions, relations between band areas of free / bound water and band areas of several functional groups were plotted in Figures 6.6.13 and 6.6.14.

For collagen, the band area of amide II (mainly C−N−H bending of peptide) shows positive relations with those of bound and free water (Figure 6.6.13a, b). On the other hand, the band area of CH shows a clear linear negative relation with that of free water (Figure 6.6.13c). Therefore, water molecules are adsorbed to peptide bonds and free water with longer H bonds are bound loosely to aliphatic CH groups cropping out on the triple helices.

For keratin, the band area of amide II (mainly C−N−H bending of peptide) shows positive relations first with that of bound water at low RHs (Figure 6.6.13d) and then correlates more with that of free water at higher RHs (Figure 6.6.13e). The band area of CH shows a negative

relation with that of free water (Figure 6.6.13f). Therefore, bound water is first adsorbed to peptide bonds followed by adsorption of free water and free water with longer H bonds are bound loosely to aliphatic CHs.

For lecithin, the band area of P−O shows positive relations with that of bound water, especially at low RHs (Figure 6.6.14a), while it is quasi-linearly correlated with that of free water at all RHs (Figure 6.6.14b). The band area of CH shows a linear negative relation with that of free water (Figure 6.6.14c). Therefore, bound water is first adsorbed to phosphates followed by adsorption of free water and free water with longer H bonds are bound loosely to aliphatic CHs.

For ceramide, the band area of C−O shows negative relations with that of bound water (Figure 6.6.14d), while it is correlated with that of free water at higher RHs (Figure 6.6.14e). The band area of CH shows a negative relation with that of free water at high RHs (Figure 6.6.14f). Therefore, bound water is first adsorbed to C−O bonds followed by adsorption of free water and free water with longer H bonds are bound loosely to aliphatic CHs.

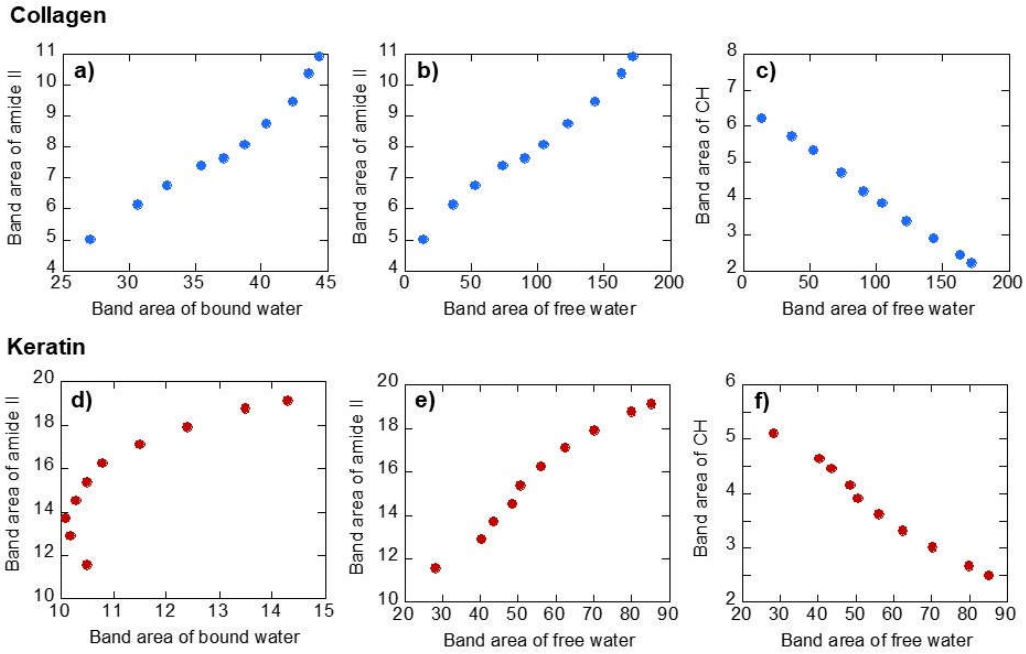

Figure 6.6.13. Band areas of amide II against band area of (a) bound water and (b) free water and (c) aliphatic CHs against band area of free water of collagen. Band areas of amide II against band area of (d) bound water and (e) free water and (f) aliphatic CHs against band area of free water of keratin.

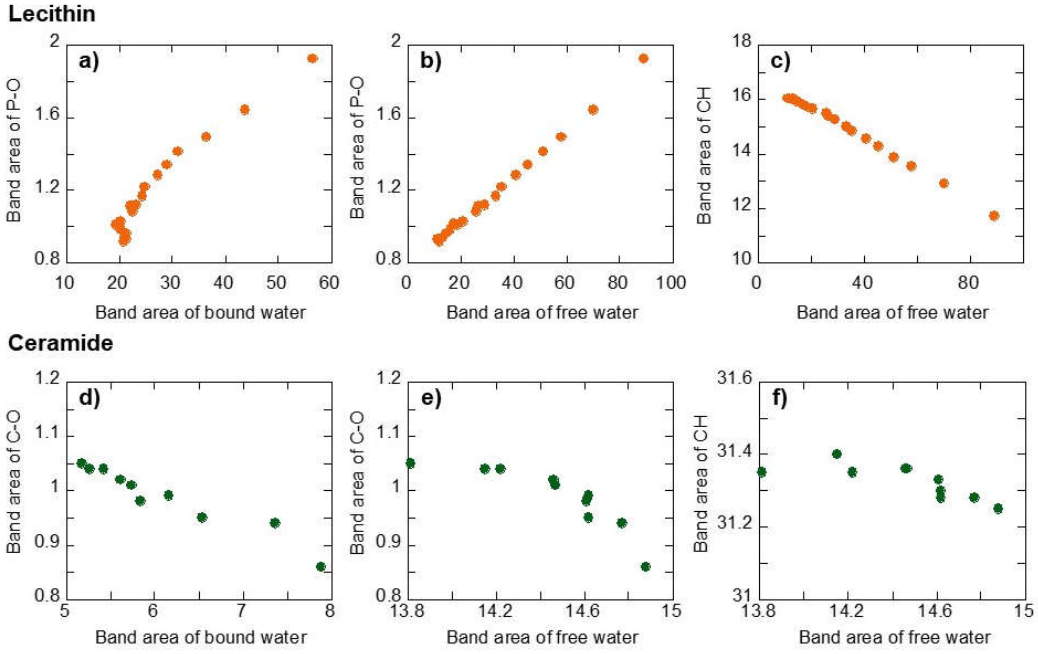

Figure 6.6.14. Band areas of P−O against band area of (a) bound water and (b) free water and (c) aliphatic CHs against band area of free water of lecithin. Band areas of C−O against band area of (d) bound water and (e) free water and (f) aliphatic CHs against band area of free water of ceramide.

6.6.14 Water Adsorption Models for Biomaterials

By using all the above results and discussion, the following working hypothesis for water adsorption to four biomaterials is proposed (Figures 6.6.15 and 6.6.16).

1) Collagen

For collagen, bound water with shorter H bonds and some of free water with longer H bonds are adsorbed first to peptide bonds inside the triple helices (Figure 6.6.15a). Further increasing water adsorption might occur for free water with longer H bonds bound loosely to aliphatic CH groups cropping out on the triple helices. These free water molecules might be incorporated among triple helix tubes in fibril structures.

(2) Keratin

For keratin, bound water with shorter H bonds and some of free water with longer H bonds are adsorbed first to peptide bonds inside the double helices (Figure 6.6.15b). Free

water with longer H bonds are bound loosely to aliphatic CHs, but restricted mainly to end CH_3 of aliphatic chains. These free water molecules might be bound among double helix tubes with hydrophobic surface in fibril structures.

(3) Lecithin

For lecithin, bound water with shorter H bonds adsorbed first to phosphate groups at low RHs (Figure 6.6.16a). Free water with longer H bonds is further adsorbed around phosphate groups. Free water molecules are also bound loosely to aliphatic CH chains.

(4) Ceramide

For ceramide, only C−O bonds can adsorb bound water (Figure 6.6.16b). At higher RHs, free water is further adsorbed around C−O (alcohol C−OH groups). Free water molecules are also bound loosely to aliphatic CH chains at higher RHs. However, amounts of water molecules adsorbed are very limited.

The present IR microspectroscopy combined with quartz crystal microbalance (QCM) and the relative humidity control system developed in this study can provide quantitative bases for amounts (wt%) and species (free and bound water) of water interacting with several functional groups (amides, phosphates, carbonyls, alcohols, aliphatic CHs) of biomaterials.

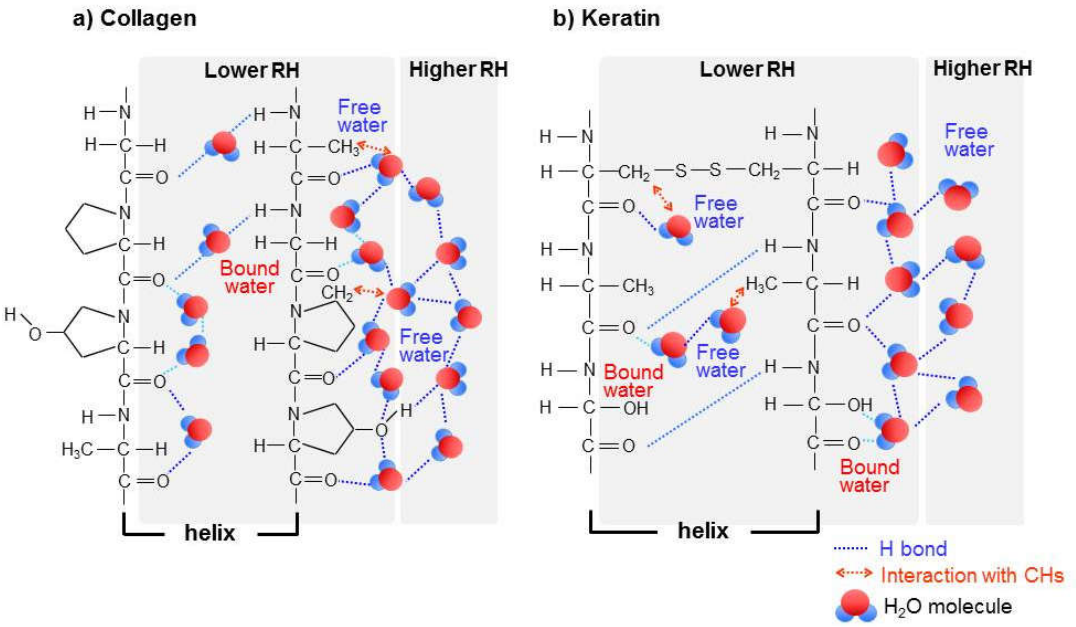

Figure 6.6.15. Water adsorption model for (a) collagen and (b) keratin.

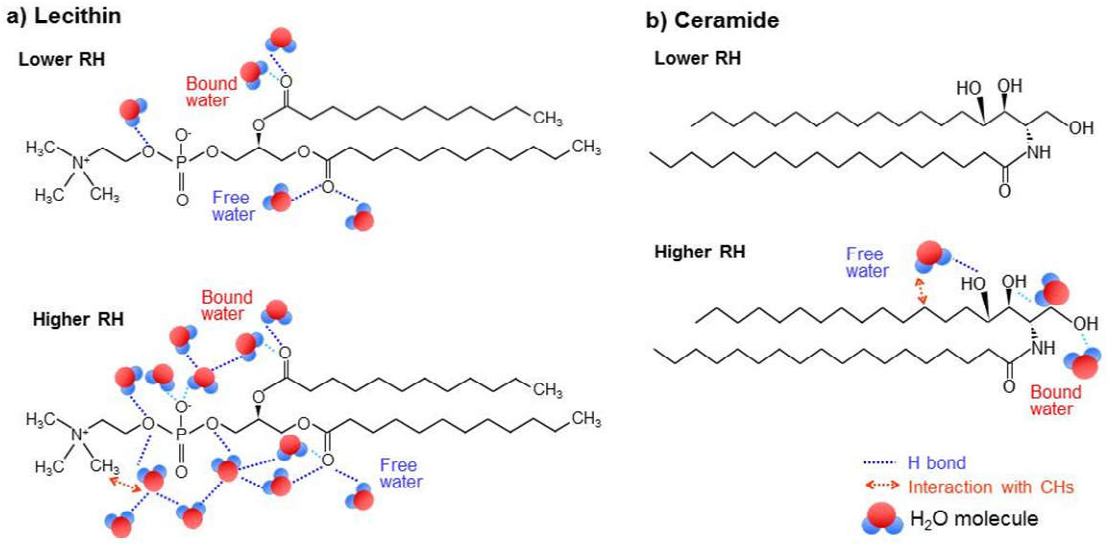

Figure 6.6.16. Water adsorption model for (a) lecithin and (b) ceramide.

6.7. Problems and Future Perspectives

By using the QCM method, weights of water adsorbed to biomaterials in small quantities could be determined in this study. Since one of the deficits of IR microspectroscopy was some lacks of quantitative estimates of concentrations of interested materials due to unknown absorption coefficients, the present method overcomes greatly this problem.

However, only total water contents could be determined in this study and contents of free and bound water could not be evaluated, because of the lack of molar absorption coefficients of free and bound water. It should be noted that the classification into free and bound water employed in this study is only an approximation assuming that water molecules can be roughly divided into longer and shorter H bond molecules. Therefore, further studies are needed to evaluate quantitatively different natures of water molecules.

The shifts of several IR bands are used here for showing interactions with water. For example, the lower wavenumber shift (red shift) of stretching vibration was taken in this study to show increasing hydrogen bonding with water molecules. Although this is true for O−H stretching bands, theoretical and/or experimental evidences for other bands are rare.

The higher wavenumber shift (blue shift) of bending vibrations was also taken in this study to show increasing hydrogen bonding with water molecules. However, this criterion has been based on our own experimental observation, firstly on collagen. Very few theoretical and/or experimental evidences are available for confirming this behavior.

In addition, increases and decreases of band areas employed in this study for suggesting interactions with water have almost never been reported in the literature. Although some experimental studies exist on band area changes upon structural changes (denaturation) of proteins, theoretical bases of band area changes remain mostly unknown.

It should be noted, however, a quasi-linear relation has been reported between integral absorption coefficients of OH stretching bands (band areas) of minerals and their frequencies (wavenumbers) (Libowitzky and Rossman, 1997). Based on this relation, lower wavenumber components with stronger H bonds have larger band areas and higher wavenumber components with weaker H bonds have smaller band areas. The analogies to this relation have been used to interpret changes in band positions and band areas in this study. However,

some opposite behaviors are already observed in the present study, which are in contradiction to the above criterion. Therefore, quantum mechanical and molecular dynamic calculations are necessary to understand these problems.

In this study, only four representative biomaterials (collagen, keratin, lecithin and ceramide) have been examined for their interactions with water under increasing relative humidity. However, they are only limited examples of diverse biomaterials present in our biological systems. Therefore, more examples should be investigated for obtaining more quantitative data sets leading to better understanding of interactions of water with biological systems.

References

Adhikari, A., Re, S., Nishima, W., Ahmed, M., Nihonyanagi, S., Klauda, J.B., Sugita, Y. and Tahara, T., 2016. "Water Orientation at Ceramide / Water Interfaces Studied by Heterodyne-Detected Vibrational Sum Frequency Generation Spectroscopy and Molecular Dynamics Simulation". *J. Phys. Chem.* 120: 23692−23697

Alipour, L., Hamamoto, M., Nakashima, S., Harui, R., Furiki, M. and Oku, O., 2016. "Infrared Microspectroscopy of Bionanomaterials (Diatoms) with Careful Evaluation of Void Effects". *Appl. Spectrosc.* 70(3): 427−442.

Atkins, P. and de Paula, J., 2012. "Physical Chemistry" 10th edn. Oxford, UK. Oxford University Press, 946−954.

Barba, C., Marti, M., Roddick-Lanzilotta, A., Manich, A., Carilla, J., Parra, J.L. and Coderch, L., 2011. "Water Sorption of Nails Treated with Wool Keratin Proteins and Peptides". *J. Therm. Anal. Calorim.* 104: 323−329.

Barel, A.O. and Clarys, P., 2014. "Skin Capacitance". In: Berardesca, E., Maibach, H. and Wilhelm, K., eds. Non Invasive Diagnostic Techniques in Clinical Dermatology. Berlin, Germany: Springer, 357−366.

Bassan, P., Lee, J., Sachdeva, A., Pissardini, J., Dorling, K.M., Fletcher, J.S., Henderson, A. and Gardner, P., 2013. "The Inherent Problem of Transflection-Mode Infrared Spectroscopic Microscopy and the Ramifications for Biomedical Single Point and Imaging Applications". *Analyst.* 138: 144−157.

Boryskina, O.P., Bolbukh, T.V., Semenov, M.A., Gasan, A.I. and Maleev, V.Y., 2007. "Energies of Peptide-Peptide and Peptide-Water Hydrogen Bonds in Collagen: Evidences from Infrared Spectroscopy, Quartz Piezogravimetry and Differential Scanning Calorimetry". *J. Mol. Struct.* 827(1−3): 1−10.

Bouwstra, J.A., Groenink, H.W.W. and Kempenaar, J.A., Romeijn, S.G. and Ponec, M., 2008. "Water Distribution and Natural Moisturizer Factor Content in Human Skin Equivalents are Regulated by Environmental Relative Humidity". *J Invest. Dermatol.* 128: 378−388.

Cameron, I.L., Haskin, C.L. and Fullerton, G.D., 2013. "Multiple Unfrozen Water Fractions in Biological Tissues: Freezing Point and Size". *Water.* 5: 45−56.

Cameron, I.L., Lanctot, A.C., Fullerton, G.D., 2011. "The Molecular Stoichiometric Hydration Model (SHM) as Applied to Tendon / Collagen, Globular Proteins and Cells". *Cell Biol. Int.* 35(12): 1205−1215.

Caspers, P.J., Lucassen, G.W., Bruining, H.A. and Puppels, G.J., 2000. "Automated Depth-Scanning Confocal Raman Microspectrometer for Rapid in vivo Determination of Water Concentration Profiles in Human Skin". *J. Raman Spectrosc.* 31: 813−818.

Doyle, B.B., Bendit, E.G. and Blout, E.R., 1975. "Infrared Spectroscopy of Collagen and Collagen-Like Polypeptides". *Biopolymers.* 14(5): 937−957.

Edwards, C. and Marks, R., 2005. "Hydration and Atopic Dermatitis". In: Fluhr, J., Elsner, P., Berardesca, E. and Maibach, H., eds. "Bioengineering of the Skin. Water and the Stratum Corneum". New York, NY: CRC Press; 2005: 323−333.

Egawa, M., Hirao, T. and Takahashi, M., 2007. "In vivo Estimation of Stratum Corneum Thickness from Water Concentration Profiles Obtained with Raman Spectroscopy". *Acta Derm. Venereol.* 87: 4−8.

Einhorn-Stoll, U., Hatakeyama, H. and Hatakeyama, T., 2012. "Influence of Pectin Modification on Water Binding Properties". *Food Hydrocolloids.* 27: 494−502.

Fabian, H. and Naumann, D., 2012. "Millisecond-to-Minute Protein Folding / Misfolding Events Monitored by FTIR Spectroscopy". In: Fabian H, Naumann D, eds. Protein Folding and Misfolding. Shining Light by Infrared Spectroscopy. Heidelberg, Germany: Springer: 54.

Frank, F., 2000. “Hydration and the Molecules of Life”. In: Water: A Matrix of Life, 2nd ed. Cambridge, UK: Royal Society of Chemistry, 2000, pp.118−151.

Garidel, P., Folting, B., Schaller, I. and Kerth, A., 2010. “The Microstructure of the Stratum Corneum Lipid Barrier: Mid-Infrared Spectroscopic Studies of Hydrated Ceramide: Palmitic Acid: Cholesterol Model Systems”. Biophysical Chemistry. 150: 144−156

Hamamoto, M., Katsura, M., Nishiyama, N., Tonoue, R. and Nakashima, S., 2015. “Transmission IR Micro-Spectroscopy of Interfacial Water between Colloidal Silica Particles”. *J. Surf. Sci. Nanotech.* 13: 301−306.

Hatch, C.D., Wiese, J.S., Crane, C.C., Harris, K.J., Kloss, H.G. and Baltrusaitis, J., 2012. “Water Adsorption on Clay Minerals as a Function of Relative Humidity: Application of BET and Freundlich Adsorption Models”. *Langmuir.* 28(3): 1790−1803.

Ikoma, T., Kobayashi, H., Tanaka, J., Walsh, D. and Mann, S., 2003. “Physical Properties of Type I Collagen Extracted from Fish Scales of Pagrus Major and Oreochromis Niloticas”. Int. *J. Biol. Macromol.* 32: 199−204.

Joseph, J. and Jemmis, E.D., 2007. “Red-, Blue-, or No-Shift in Hydrogen Bonds: A Unified Explanation”. *J. Am. Chem.* Soc. 129(15): 4620−4632.

Jung, S.M., Yoon, G.H., Lee, H.C., Jung, M.H., Yu, S.I., Yeon, S.J., Min S.K., Kwon Y.S., Hwang J.H. and Shin H.S., 2015. “Thermodynamic Insights and Conceptual Design of Skin-Sensitive Chitosan Coated Ceramide / PLGA Nanodrug for Regeneration of Stratum Corneum on Atopic Dermatitis”. *Nature.* DOI: 10.1038/srep18089

Kataoka, Y., Kitadai, N., Hisatomi, O. and Nakashima, S., 2011. “Nature of Hydrogen Bonding of Water Molecules in Aqueous Solutions of Glycerol by Attenuated Total Reflection (ATR) Infrared Spectroscopy”. *Appl. Spectrosc.* 65(4): 436−441.

Khazaka, G., 2005. “Assessment of Stratum Corneum Hydration: Corneometer CM825”. In: Fluhr, J., Elsner, P., Berardesca, E. and Maibach, H., eds. Bioengineering of the Skin. Water and the Stratum Corneum. New York, NY: CRC Press: 249−261.

Kitadai, N., Sawai, T., Tonoue, R., Nakashima, S., Katsura, M. and Fukushi, K., 2014. “Effects of Ions on the OH Stretching Band of Water as Revealed by ATR-IR Spectroscopy”. *J. Solution Chem.* 43(6): 1055−1077.

Kudo, S., Ogawa, H., Yamakita, E., Watanabe, S., Suzuki, T. and Nakashima, S., 2017. “Adsorption of Water to Collagen as Studied Using Infrared (IR) Microspectroscopy Combined with Relative Humidity Control System and Quartz Crystal Microbalance”. *Appl. Spectrosc.* 71(7): 1621−1632.

Kuligowski, J., Quintas, G., Garrigues, S. and De la Guardia, M., 2008. “Determination of Lecithin and Soybean Oil in Dietary Supplements using Partial Least Squares-Fourier Transform Infrared Spectroscopy”. *Talanta.* 77: 229

Leveque, J.L., 2005. “Water-Keratin Interactions”. In: Fluhr, J., Elsner, P., Berardesca, E. and Maibach, H., eds. Bioengineering of the Skin. Water and the Stratum Corneum. New York, NY: CRC Press: 15−26.

Li, X., Johnson, R. and Kasting, G.B., 2016. “On the Variation of Water Diffusion Coefficient in Stratum Corneum with Water Content”. *J Pharm. Sci.* 105: 1141−1147.

Libowitzky, E. and Rossman, R., 1997. “An IR Absorption Calibration for Water in Minerals”. *American Mineralogist.* 82: 1111−1115

Lucklum, R., Behling, C., Cernosek, R.W. and Martin, S.J., 1997. “Determination of Complex Shear Modulus with Thickness Shear Mode Resonators”. *J. Phys. D: Appl. Phys.* 30(3): 346−356.

Marechal, Y., 2007. “The Water Molecule in (Bio) Macromolecules”. In: The Hydrogen Bond and the Water Molecule: The Physics and Chemistry of Water, Aqueous and Bio-Media. Amsterdam, The Netherlands: Elsevier, pp.249−275.

Masuda, K., Haramaki, T., Nakashima, S., Habert, B., Martinez, I. and Kashiwabara, S., 2003. “Structural Change of Water with Solutes and Temperature up to 100°C in Aqueous Solutions as Revealed by Attenuated Total Reflectance Infrared Spectroscopy”. *Appl. Spectrosc.* 57(3): 274−281.

Masukawa, Y., Narita, H., Shimizu, E., Kondo, N. and Sugai, Y., 2008. “Characterization of Overall Ceramide Species in Human Stratum Corneum”. *J. Lipid Res.* 49: 1466−1476.

Mizuno, K., Ochi, T. and Shindo, Y., 1998. “Hydrophobic Hydration of Acetone Probed by Nuclear Magnetic Resonance and Infrared: Evidence for the Interaction C−H···OH_2”. *J. Chem. Phys.* 109(21): 9502−9507.

Nakamoto, K., Margoshes, M. and Rundle, R.E., 1955. “Stretching Frequencies as a Function of Distances in Hydrogen Bonds”. *J. Am. Chem.* Soc. 77(24): 6480−6488.

Nakamura, A., Arimoto, M., Takeuchi, K., 2002. “A Rapid Extraction Procedure of Human Hair Proteins and Identification of Phosphorylated Species”. *Biol. Pharm. Bull.* 25(5): 569−572.

Nomura, Y., Yamano, M. and Shirai, K., 1995. “Renaturation of a1 Chains from Shark Skin Collagen Type I”. *J. Food Sci.* 60(6): 1233−1236.

Olsztynska, S., Pietruszka, A., Kielbowicz, Z. and Czarnecki, M.A., 2018. “ATR-IR Study of Skin Components: Lipids, Proteins and Water. Part I: Temperature Effect”. *Spectrochim. Acta A Mol. Biomol. Spectrosc.* 188: 37−49.

Onga, C. and Nakashima, S., 2014. “Darkfield Reflection Visible Microspectroscopy Equipped with a Color Mapping System of a Brown Altered Granite”. *Appl. Spectrosc.* 68(7): 740−748.

Payne, K.J. and Veis, A., 1988. “Fourier Transform IR Spectroscopy of Collagen and Gelatin Solutions: Deconvolution of the Amide I Band for Conformational Studies”. *Biopolymers.* 27(11): 1749−1760.

Pohle, W., Gauger, D.R., Fritzsche, H., Rattay, B., Selle, C., Binder, H. and Bohlig, H., 2001. “FTIR-Spectroscopic Characterization of Phosphocholine-Headgroup Model Compounds”. *J. Mol. Struct.* 563−564: 463−467.

Raut, S.V., Nemade, L.S., Desai, M.T., Bonde, S.D. and Dongare, S.U., 2014. “Chemical Penetration Enhancers: for Transdermal Drug Delivery Systems”. *Int. J. Pharm. Sci. Rev. Res.* 4(1): 33−40.

Sauerbrey, G., 1959. “Verwendung von Schwingquarzen zur Wägung Dünner Schichten und zur Mikrowägung”. *Z.Phys.Chem.* 155(2): 206−222.

Scheiner, S., Kar, T., Gu, Y., 2001. “Strength of the CaH··O Hydrogen Bond of Amino Acid Residues”. *J. Biol. Chem.* 276(13): 9832−9837.

Schuttlefield, J.D., Cox, D. and Grassian, V.H., 2007. “An Investigation of Water Uptake on Clays Minerals using ATR-FTIR Spectroscopy Coupled with Quartz Crystal Microbalance Measurements”. *J. Geophys. Res.* 112: D21303.

Serup, J., 2005. “Hydration in Proriasis and Eczema”. In: Fluhr, J., Elsner, P., Berardesca, E. and Maibach, H., eds. Bioengineering of the Skin. Water and the Stratum Corneum. New York, NY: CRC Press, 351−358.

Shchipunov, Y.A. and Shumilina, E.V., 1995. “Lecithin Brindging by Hydrogen Bonds in the Organogel”. *Mat. Sci. Eng.* C3: 43

Shinshu Technology Licencing Organization. Home Page: http://www.shinshu-tlo.co.jp/official/ topics03.html, Accessed May 2, 2018.

Shoulders, M.D. and Raines, R.T., 2009. “Collagen Structure and Stability”. *Annu. Rev. Biochem.* 78: 929−958.

Siebert, F. and Hildebrandt, P., 2008. “Structural Studies”. Vibrational Spectroscopy In Life Science. Weinheim, Germany: Wiley-VCH, pp.156.

Sieg, A., 2014. “Raman Dpectroscopy”. In: Berardesca, E., Maibach, H. and Wilhelm, K., eds. Non Invasive Diagnostic Techniques in Clinical Dermatology. Berlin, Germany: Springer, 217−223.

Staroszczyk, H., Pielichowska, J., Sztuka, K., Stangret, J. and Kolodziejska, I., 2012. “Molecular and Structural Characteristics of Cod Gelatin Films Modified with EDC and TGase”. *Food Chem.* 130(2): 335−343.

Tagami, H., 2014. “Electrical Measurement of the Hydration State of the Skin Surface in vivo”. *Br. J. Dermatol.* 171: 29−33.

Tanaka, M., Okada, M., Zhen, Y.X., Inamura, N., Kitano, T., Shirai, S., Sakamoto, K., Inamura, T. and Tagami, H., 1998. “Decreased Hydration State of the Stratum Corneum and Reduced Amino Acid Content of the Skin Surface in Patients with Seasonal Allergic Rhinitis”. *Br J Dermatol.* 139: 618−621.

Tantipolphan, R., Rades, T., McQuillan, A.J. and Medlicott, N.J., 2007. “Adsorption of Bovine Serum Albumin (BSA) onto Lecithin Studied by Attenuated Total Reflectance Fourier Transform Infrared (ATR-FTIR) Spectroscopy”. *Int. J. Pharm*. 337(1): 40−47

Tonoue, R., Katsura, M., Hamamoto, M., Bessho, H. and Nakashima, S., 2014. “A Method to Obtain the Absorption Coefficient Spectrum of Single Grain Coal in the Aliphatic C−H Stretching Region Using Infrared Transflection Microspectroscopy”. *Appl. Spectrosc.* 68: 733−739.

Wang, B., Yang, W., McKittrick, J. and Meyers, M.A., 2016. “Keratin: Structure, Mechanical Properties, Occurrence in Biological Organisms, and Efforts at Bioinspiration”. *Mater. Sci.* 76: 229−318.

Xiao, X. and Hu, J., 2016. “Animal Hairs as Water-Stimulated Shape Memory Materials: Mechanism and Structural Networks in Molecular Assemblies”. *Sci. Rep.* 6: 26393.

Yoshida, S. and Koike, K., 2011. “Lipid and Membrane Dynamics in Biological Tissues-Infrared Spectroscopic Studies”. In: Iglič, A., ed. Advances in Planar Lipid Bilayers and Liposomes, Vol.13, Amsterdam, The Netherlands: Elsevier, 1−32

Zhang, O. Andrew Chan, K.L., Zhang, G., Gillece, T., Senak, L., Moore, D.J., Mendelsohn, R. and Flach, C.R., 2011. “Raman Microspectroscopic and Dynamic Vapor Sorption Characterization of Hydration in Collagen and Dermal Tissue”. *Biopolymers.* 95(9): 607−615.

List of Publications

Sachie Kudo, Hiromi Ogawa, Eri Yamakita, Shio Watanabe, Toshiyuki Suzuki and Satoru Nakashima.

"Adsorption of Water to Collagen as Studied Using Infrared (IR) Microspectroscopy Combined with Relative Humidity Control System and Quartz Crystal Microbalance"

Applied Spectroscopy, Vol. 71 (7), 1621-1632, 2017.

Sachie Kudo and Satoru Nakashima.

"Water adsorption with relative humidity changes for keratin and collagen as studied by infrared (IR) micro-spectroscopy"

Skin Research and Technology, Accepted on September 23, 2018 and published online on October, 2018.